

Study of a Glycine Hinge in ATP-sensitive Potassium Channels

by

Jeremy David Bushman

A DISSERTATION

Presented to the Neuroscience Graduate Program
and the Oregon Health & Science University
School of Medicine
in partial fulfillment of
the requirements for the degree of
Doctor of Philosophy

January 2012

School of Medicine
Oregon Health & Science University

CERTIFICATE OF APPROVAL

This is to certify that the Ph.D. dissertation of
JEREMY BUSHMAN
has been approved

Advisor, Show-Ling Shyng, PhD

Member and Chair, John Adelman, PhD

Member, Jeff Karpen, PhD

Member, Francis Valiyaveetil, PhD

Member, Michael Chapman, PhD

Dedication

To Thomas, Karen, Kathleen, and Martin, with my love;
and to my friends, who make it all worth it.

"Nothing in this world can take the place of persistence. Talent will not; nothing is more common than unsuccessful people with talent. Genius will not; unrewarded genius is almost a proverb. Education will not; the world is full of educated derelicts. Persistence and determination alone are omnipotent." -- Calvin Coolidge, 30th President of the United States

"Anything [biological] that happens fast, and is therefore interesting, involves an ion channel." --Anonymous

Table of Contents

Introduction.....	1
K _{ATP} Channels in Physiology and Disease.....	1
Composition and Structure.....	3
Trafficking and Regulation.....	5
K _{ATP} Gating as an Inward Rectifier.....	9
K _{ATP} Channel Intrinsic Gating.....	11
K _{ATP} Channel Inhibition by ATP.....	13
Location of K _{ATP} Channel Gates.....	16
Glycine Hinge Hypothesis.....	19
Scope of the Dissertation.....	20
Figure Legends.....	22
Chapter 1.....	32
Characterization and Functional Restoration of a Potassium Channel Kir6.2 Pore Mutation Identified in Congenital Hyperinsulinism	
Abstract.....	33
Introduction.....	34
Results.....	36
Discussion.....	44
Materials & Methods.....	50
Acknowledgements.....	55
Figure Legends.....	55
Chapter 2.....	70
K_{ATP} Channel Pore Mutant Inactivation Reveals Coupling between Transmembrane and Cytoplasmic Domains	
Abstract.....	71
Introduction.....	72
Results.....	75
Discussion.....	81
Materials & Methods.....	87
Figure Legends.....	89

Chapter 3.....	100
In Search of Flexibility in the TM2 Helices of Kir6.2	
Abstract.....	101
Introduction.....	103
Results.....	106
Discussion.....	111
Materials & Methods.....	115
Figure Legends.....	115
Conclusions and Future Directions.....	126
References.....	132

List of Figures and Tables

Introduction

Figure 1. Simple mechanism of glucose-dependent insulin secretion in β -cells.....	25
Figure 2. Structure of a Kir channel.....	26
Figure 3. SUR topology and the K_{ATP} octamer.....	27
Figure 4. Regulators of K_{ATP} channels and putative Kir6.2 binding sites.....	28
Figure 5. Mechanism of Inward rectification in Kir channels.....	29
Figure 6. K_{ATP} single channel currents and kinetic mechanisms.....	30
Figure 7. Gating conformations in the Kir pore.....	31

Chapter 1

Figure 1. Characterization of G156R mutant channels reconstituted in COS cells.....	61
Figure 2. Simulated heterozygous expression of G156R.....	62
Figure 3. Analysis of Kir6.2 tandem tetramers containing 0–4 G156R mutant subunits.....	63
Figure 4. Restoration of ion conduction in G156R or G156K mutant channels by a second site mutation N160D.....	64
Figure 5. The N160D mutation induces inward rectification on the WT- but not the G156R- or G156K-Kir6.2 background.....	65
Figure 6. Evidence suggests functionally relevant intersubunit interactions between G156D and N160R.....	66
Figure 7. Intra- and intersubunit interactions between G156R and N160D in the Kir6.2 tetramer.....	67
Figure 8. Nucleotide sensitivities of G156R/N160D charge-pair mutant channels.....	68
Table 1. Double mutant channel properties.....	69

Chapter 2

Figure 1. Inactivation of G156P Channels.....	93
Figure 2. Inward and outward currents inactivate at a similar rate.....	94
Figure 3. Varying ion concentrations or species does not change the inactivation rate.....	95
Figure 4. G156P inactivation rate is PIP2 sensitive.....	96
Figure 5. Increasing open-state stability	

eliminates inactivation.....	97
Figure 6. Cartoon Model of G156P inactivation.....	98
Supp Figure 1. Time-dependent recovery from inactivation.....	99

Chapter 3

Figure 1. Single channel bursts of G156R/N160D and G156R/N160E double mutant channels have altered intraburst kinetics.....	118
Figure 2. Partial proline scan of TM2 surrounding the two glycine residues show changes in sensitivity to channel regulators.....	119
Figure 3. Surface expression of TM2 proline mutations.....	120
Figure 4. Patch recordings and expression of G156 mutations.....	121
Figure 5. Single channel activity of WT and G156S from multi-channel patches.....	122
Figure 6. Mutations at the lower glycine position.....	123
Figure 7. Single G165P channels have reduced conductance and show nearly continuous bursting.....	124
Figure 8. Preliminary Two Hinge Model of Kir6.2 TM2 Gating.....	125

Abbreviations Used

ABC	ATP-binding cassette
ATP	Adenosine-5'-triphosphate
ADP	Adenosine-5'-diphosphate
BSA	bovine serum albumin
CHI	congenital hyperinsulinism
CTD	cytoplasmic domain
DEND	developmental delay, epilepsy, neonatal diabetes mellitus syndrome
DM	diabetes mellitus
EDTA	ethylenediaminetetraacetic acid
E_K	potassium equilibrium (reversal) potential
ER	endoplasmic reticulum
HEPES	4-(2-hydroxyethyl)-1-piperazineethanesulfonic acid
HBC	helix-bundle crossing
IC50	half maximal inhibitory concentration
K_{ATP}	ATP-sensitive potassium channel
KCO	potassium channel opener
KINT	intracellular potassium solution
Kir	inward rectifier potassium channel
L0	loop zero
LC-CoA	long-chain acyl co-enzyme A
MWC	Monod-Wyman-Changeux concerted model
NBF	nucleotide binding fold
PBS	phosphate-buffered saline
PIP2	phosphatidylinositol 4,5-bisphosphate
PNDM	permanent neonatal diabetes mellitus
P_o	open probability
SEM	standard error of the mean
STD	standard deviation
SUR	sulfonylurea receptor
TM	transmembrane
TMD	transmembrane domain
WT	wild type

Acknowledgements

First, I wish to thank my advisor Show-Ling. Your talents and versatility as a scientist, your patience, and your dedication to the success of those around you are the qualities of an exceptional mentor. You have challenged me to achieve and I am a better person because of it. The advice you have provided over the years has been invaluable to me and your counsel will always be welcome. Our long journeys breed success when accompanied by those who we respect in leadership and trust in guidance, and so I am fortunate that this journey was with you.

Thank you, members of the Shyng lab. Your good-natured attitudes and generosity have provided a convivial and productive atmosphere. Thanks especially to Emily Pratt, Joel Gay, Qing Zhou, and Paul Tewson for your camaraderie, collegial discussions and assistance with my work. Bright futures await all of you.

I wish to thank my wonderful parents, Tom and Karen Bushman, for their loving support. Ever since I was a young boy, you have instilled in me the value of hard work, dedication, and persistence; lessons that have helped me accomplish my dreams. The boundless faith you have in my abilities inspires me to do great things.

I also wish to thank Matt McGinley, Evan Vickers, and Nick Vyleta. Your friendships I will forever cherish, and the memories of our escapades will last a lifetime.

Abstract

The principal mediators of potassium conductance are potassium ion (K^+) channels, a superfamily of integral membrane proteins whose subunits assemble to form an aqueous pore. These pores utilize a filter to selectively permeate K^+ ions through passive diffusion down a concentration gradient across the plasma membrane of a cell. Potassium conductance dominates at the resting membrane potential of a cell, and shapes the waveform, duration, and strength of cell repolarization. In order to regulate ion conduction in response to various stimuli, K^+ channels open and close in a process called gating. Gating defines the kinetics of channel currents that determine K^+ flux and thus cell excitability. A major scientific research goal is to develop a complete picture of the motions that occur in the channel molecule during gating to better understand channel function.

A remarkable family of K^+ channels is the inward rectifiers (Kir). Their namesake property of rectification originates from block of the channel pore by multivalent cations in the cell cytosol. Kir channels possess the intrinsic capacity to rearrange the K^+ conduction pathway through interactions with phosphatidylinositol-4,5-bisphosphate (PIP_2) and other intracellular ligands that bias their gating conformation. Four transmembrane α -helix protein segments (TM2) line the conduction pathway, a single segment contributed from each of the K^+ channel subunits. Extensive scientific literature champions a model in which the TM2 helices partake in a bending motion critical to the gating mechanism. A hypothesis for channel gating was formed that a well-conserved glycine residue in the middle of each TM2 segment acts as a hinge to provide flexibility necessary for the helices to bend.

A disease mutation was identified in a patient with congenital hyperinsulinism (CHI). The mutation lies in the gene which encodes the pore subunits of the ATP-sensitive potassium (K_{ATP}) channel, and it replaces the glycine hinge with positively-charged arginine. K_{ATP} channels are a Kir family member that regulate K^+ conductance through interactions with intracellular nucleotides, coupling cellular metabolic state with excitability. They play a crucial role in glucose-dependent insulin secretion, and loss of channel function causes CHI.

Presented in this dissertation are studies using *in vitro* structure/function methods to understand the role of the TM2 glycine as a hinge in K_{ATP} channels. Chapter 1 studies the consequence of the glycine-to-arginine CHI mutation on channel function. Results show the positively-charged mutation eliminates ion conduction by altering the electrostatic environment of the pore. Channels incorporating mutant and wild-type subunits conduct potassium ions, consistent with the heterozygous patient phenotype and clinical outcome. K^+ currents were also recovered when a second negatively-charged mutation was placed in close proximity to stabilize the electrostatic environment in the pore. Position of the second mutation was ideal to establish a direct electrostatic interaction that restores ion conduction and gating. Nucleotide regulation in the double mutant channels was the same as WT, showing the glycine hinge is not essential for K_{ATP} channel gating. In Chapter 2, an attempt to reduce TM2 flexibility by mutating glycine to proline uncovered an unexpected phenotype called inactivation. Inactivation was defined as a severe reduction in spontaneous K_{ATP} channel activity. Many native K^+ channels exhibit C-type inactivation, a gating process that depends on permeating ions interacting with the selectivity filter. The glycine residue is in close proximity to the selectivity filter in Kir channels, and a glycine mutation could potentially stabilize a closed

filter conformation in K_{ATP} . However, current decay kinetics of G156P K_{ATP} channels did not change when ionic conditions were altered arguing against the mutation inducing C-type inactivation. An alternative hypothesis comes from previously identified inactivation mutations found in the cytoplasmic domain of K_{ATP} channels that disrupt intersubunit interactions. Cytoplasmic domains form the binding sites for regulatory molecules PIP_2 and ATP, and intersubunit interactions between cytoplasmic domains stabilize channel activation. G156P channel inactivation was sensitive to PIP_2 modulation and more significantly recovers from inactivation after channel inhibition by ATP, suggesting the mutation causes loss of coupling between the ligand-binding cytoplasmic domain and downstream gating apparatus in the transmembrane domain that is required to sustain channel activation. Chapter 3 summarizes additional mutagenesis study of the glycine hinge, and attempts to redress conceptual caveats of a hinge mechanism. The conclusions of this dissertation enhance our understanding of the transmembrane pore environment and its interaction with other channel domains, and they lay the groundwork for future considerations of the hinge hypothesis.

Background & Introduction

K_{ATP} channels in physiology and disease

ATP-sensitive potassium (K_{ATP}) channels are K^+ ion-selective pores in cell membranes that respond to changes in intracellular nucleotide concentrations. ATP-sensitive currents from K_{ATP} channels were first discovered in cardiac myocytes (Noma, 1983) and subsequently observed in numerous tissues where they play a variety of roles linking cell metabolism with K^+ permeation and cell excitability (for reviews see Hibino et al. 2010; Seino & Miki, 2003). In the heart, K_{ATP} channels are implicated in cardiac protection from ischemic events (Kane et al. 2005). They are present in various neural cell types where they are employed in many different functions including hormone secretion in the hypothalamus, dopamine outflow in the striatum, and more generally in neuroprotective effects by reducing neuronal firing rate and clearance of extracellular K^+ (Neusch et al., 2003). Neuroprotection from K_{ATP} may also be an important early effect of the ketogenic diet, which is commonly used to treat epilepsy (Ma et al., 2007). K_{ATP} channels are found in smooth muscle where they set vascular tone (Seino & Miki, 2003) and play a myoprotective role when skeletal muscle fatigues (Flagg et al., 2010). An ATP-sensitive current is also found in mitochondria (Inoue et al., 1991); however, its molecular identity is currently unclear.

Evidence for K_{ATP} channel presence and function in pancreatic β -cells (Cook and Hales, 1984; Ashcroft et al., 1984) offers perhaps the best example and clarified role of the channel in physiology, since channel regulation by nucleotides is critical to the process of glucose-dependent insulin secretion (Hiriart and Bryan, 2008; Figure 1A). The β -cell samples blood glucose levels with fast transport and metabolizes glucose to ATP. When increased ATP production raises the ratio of intracellular ATP concentrations relative to

ADP, K_{ATP} channels close causing membrane depolarization. This generates Ca^{2+} influx through voltage-gated calcium channels which triggers exocytosis of insulin containing granules. Conversely, when the ATP-to-ADP ratio declines under low glucose conditions, the K^+ conductance from K_{ATP} channels holds the membrane potential near the resting state and reduces insulin secretion.

A spectrum of congenital disorders due to dysregulation of insulin secretion underscores the importance of K_{ATP} channel involvement. K_{ATP} channels serve as a therapeutic target for sulphonylurea drugs and potassium channel openers to treat congenital disorders and other forms of diabetes (Ashcroft, 2005). Mutations in the genes that express K_{ATP} channel subunits lead to gain or loss of channel function. Gain-of-function mutations generally cause hypoinsulinemic disorders such as permanent neonatal diabetes mellitus (PNDM) and the more debilitating syndrome of development delay, epilepsy and neonatal diabetes (DEND), whereas loss-of-function mutations associate with congenital hyperinsulinism (CHI; Figure 1B). CHI inheritance and histopathology are quite heterogeneous, and symptoms can be severely detrimental to early stages of development. Molecular genetics investigations have vastly improved our knowledge for early recognition, correct diagnosis and treatment options, which are critical to a patient's outcome (Meissner & Mayatepek, 2002). In vitro study of disease mutations helps our understanding of the genotype-phenotype relationship in CHI and the mechanisms by which a mutation disrupts channel function (Shyng et al. 2012). Channel defects generally result from attenuated protein biogenesis, loss of trafficking of the channel to the surface and/or altered K_{ATP} gating. At the end of the introduction, we will discuss the clinical phenotype of a mutation found in patients with CHI.

Composition and Structure of K_{ATP} channels

K_{ATP} channels are well-defined as a hetero-octameric complex composed of two very dissimilar transmembrane proteins (Clement et al., 1997; Shyng and Nichols, 1997). The pore of the channel is a tetramer of inwardly-rectifying potassium channel subunits Kir6.x that co-assembles with four beta subunit sulphonyurea receptor subunits (SURx). The Kir channel family is a functionally diverse group of K^+ -selective pores with properties that will be thoroughly discussed. SUR is a member of the ATP-binding cassette (ABC) superfamily (Aguilar-Bryan et al. 1995), whose genes encode for one of the largest known families of transmembrane proteins. They bind and hydrolyze ATP to execute diverse cellular functions as pumps/transporters, channels, and modulatory subunits (Dean, 2002). Two genes KCNJ8 and KCNJ11 encode for subunits Kir6.1 and Kir6.2 respectively, and two genes ABCC8 and differentially spliced ABCC9 generate SUR1 and SUR2A/B subunits (Aguilar-Bryan et al., 1995; Inagaki et al., 1995; Inagaki et al., 1996; Chutkow et al., 1996). Subunit subtypes differ in tissue distribution providing a therapeutic opportunity for selectively targeting channel isoforms (Figure 1C). This thesis will focus on the brain and pancreatic isoform of Kir6.2/SUR1.

K^+ channel structural and functional information has revealed their molecular architecture, offering models for targeted study of protein regions important for channel function. Detailed information regarding K^+ channel regions was provided by atomic resolution crystal structures from several bacterial channel homologues including KcsA, MthK, and Kirbac1.1 (Doyle et al., 1998; Jiang et al., 2002; Kuo et al., 2003), of which KirBac1.1 shares the highest amino acid sequence homology with mammalian Kir channels (Durell et al., 2001). Single pore K^+ channels form a tetramer of subunits, and Figure 2 depicts the overall structure and the salient features of two opposing Kir subunits. Each subunit contains intracellular amino- and carboxy-termini, a signature

pore-loop located between two transmembrane spanning regions (TM1 and TM2), and an intracellular pre-M1 α -helix or slide helix. The pore-loops from the subunits narrow the extracellular mouth of the channel to ~ 2 angstroms, where a K^+ ion could efficiently substitute its hydration shell with main-chain carbonyl oxygens, giving this region the capacity to serve as the selectivity filter (Doyle et al., 1998; Zhou et al., 2001). Mutations in the pore-loop signature sequence abolish K^+ selectivity (Heginbotham et al., 1994). The pore-loop sequence is highly conserved between all K^+ channels, so it is assumed that the mechanism of selectivity and permeation is also conserved. Once past the filter, ions rehydrate and empty into a basin called the inner cavity, which in K_{ATP} channels may be as wide as 12 angstroms (Haider et al., 2007). Lining the walls of the inner cavity are the TM2 helices, their residues running the length of the membrane from the end of the pore helices to the intracellular side. The TM2 helices converge as they approach the intracellular space in the shape of an inverted teepee, forming the helix-bundle crossing (Doyle et al., 1998). Past the helix-bundle crossing, the Kir channel pore extends into the large C-terminal cytoplasmic domain through a narrowing called the G-loop and then widens into a large cytosolic vestibule (Kuo et al., 2003). Extension of the Kir structure into the cytoplasm provides a long pore that would create a dielectric environment for distant electrostatic effects on an ion moving along the conduction pathway (Robertson et al., 2008).

Atomic resolution structures are not yet available for either full length Kir6.x or SURx. Membrane topology and architecture of Kir6.2 is expected to be the classical potassium channel pore described above. The SUR1 topology is quite different; it consists of 17 transmembrane segments organized into three domains plus three intracellular loops, with the two large C-terminal loops containing consensus sequences for nucleotide binding folds (NBFs) (Figure 3). The ABC architectural core is composed in sequence of

TMD1, NBF1, TMD2, and NBF2. The NBFs contain conserved Walker motifs and a linker region that form binding sites for nucleotides with Mg^{2+} . Attached to the core through a structurally undetermined loop L0 is the unique TMD0. TMD0 is critical to the trafficking and function of Kir6.2 in the full K_{ATP} channel complex, and its association alone with truncated Kir6.2 modulates gating (Babenko and Bryan, 2003; Chan et al., 2003). A Kir-SUR tandem complex was weakly resolved (18 angstroms) with cryo-electron micrography and 3-D reconstruction (Mikhailov et al., 2005). The density would require tight packing of four Kir6.x subunits surrounded by four SURx subunits with TMD0 nestled in between TMD1, TMD2 and Kir6.2 (Figure 3). However, due to lack of a complete high resolution structure, identifying the nature of interactions in the tertiary and quaternary structure of the channel complex necessary for stable trafficking and function at the surface is a work in progress.

Trafficking and Regulation of K_{ATP} channels

Paramount to defining channel function is an understanding of the process of trafficking to the surface and the regulation of activity through ligand-dependent gating. A fully assembled octameric complex is required for the K_{ATP} channel to reach the plasma membrane (Zerangue et al., 1999; Neagoe & Schwappach, 2005). Both Kir6.2 and SUR1 subunits contain an endoplasmic reticulum retention motif RKR which must be mutually masked for channel progression to the Golgi. If the motif is mutated, both subunits can traffic to the surface alone (Zerangue et al., 1999). The RKR sequence in Kir6.2 locates within the last 25-36 amino acid residues at the C-terminus, and truncated Kir6.2 Δ C channels express functional K^+ channels at the plasma membrane alone (Tucker et al., 1997). This has been a useful alteration for isolating the Kir6.2 pore to study its specific properties in the absence of SUR. SUR subunits without Kir6.x

subunits have an intrinsic capacity to acquire their own structure, although it remains uncertain whether they independently form a functional entity (Aittoniemi et al. 2009).

A picture has slowly emerged of the complex nature of K_{ATP} as a ligand-gated channel. Nucleotide interactions are the key regulators of physiological K_{ATP} channel activity. Adenine nucleotides at Kir6.x and SURx have opposing effects: ATP binds to Kir6.2 to inhibit activity and MgATP and MgADP bind to SUR1 to activate the channel (Figure 4). Underlying this regulation is spontaneous channel activity. K_{ATP} channels in isolated membrane patches and a simple potassium solution are constitutively active in the absence of nucleotides; this is commonly referred to as intrinsic gating. Ensemble channel current then decreases with a variable time course, an observation called “rundown”. Rundown is principally due to loss of phosphatidylinositol bisphosphate (PIP_2) from the membrane patch (Ribalet et al., 2000). PIP_2 is a necessary cofactor for activity in Kir channels and it is required for channel activity in purified and reconstituted classical rectifiers Kir2.1 and Kir2.2 (Suh & Hille, 2008; D’Avanzo et al., 2010). PIP_2 stabilizes channel activation by directly interacting with Kir6.2 (Wang et al., 2002) to generate an intrinsic open probability (P_o ; probability of finding the channel in an open state) of ~ 0.5 in K_{ATP} channels. PIP_2 will be the primary phosphoinositide contributing to K_{ATP} channel intrinsic gating because channel sensitivity is higher than for most other phosphoinositides (Fan & Makielski, 1997). Importantly, PIP_2 membrane levels are unlikely to fluctuate quickly enough to be the primary determinant of cellular regulation of channels and will work as a cofactor rather than second messenger (Hilgemann 2007). A PIP_2 tone will set the basal channel activity for nucleotide modulation. However, PIP_2 and ATP exhibit a negative heterotropic interaction; PIP_2 antagonizes ATP inhibition of Kir6.2/SUR1 channel activity (Baukrowitz et al., 1998; Shyng and Nichols, 1998; Xie et

al., 1999; Nichols, 2006 review). This has broad implications for channel regulation when mutations or other factors influence the affinity and/or efficacy of PIP₂.

K_{ATP} channels also activate from binding the structurally similar molecule long chain acyl-Coenzyme A (LC-CoA), a derivative of fatty acids. Activation by LC-CoA is unique to K_{ATP} amongst Kir channels as all other subfamilies are inhibited by it (Rapedius et al., 2005). K_{ATP} molecular determinants for LC-CoA binding based on functional studies are similar to PIP₂ (Schulze et al., 2003; Fox et al., 2004). Of note, a fundamental difference in their chemistry is LC-CoA has much higher water solubility than PIP₂ and would not have the same diffusion constraints.

It is apparent that the binding sites for regulatory molecules involve residues in the tertiary structure that are far apart from each other in the primary sequence. A published structure of Kir2.2 with bound PIP₂ molecules indicates residues with basic side chains form a pocket in close proximity to the membrane within the C-terminal cytoplasmic domain (CTD) and a linker region spanning the CTD (Hansen et al., 2011). A single PIP₂ molecule spans the pocket to the bottom of TM2 and TM1. Previous functional studies suggest R54, R176, R177 and R206 form a PIP₂ binding site on Kir6.2, which are homologous to residues identified in the structural study with the exception of R54 (Baukrowitz et al., 1998; Shyng & Nichols, 1998; Shyng et al., 2000; Cukras et al., 2002a,b; Schulze et al., 2003). These positively-charged residues would be in close proximity to the cytoplasmic leaflet of the membrane where they could interact with the negatively-charged headgroup of phosphoinositides. If PIP₂ binding modulates channel sensitivity to ATP, how might one begin to functionally identify residues in an ATP binding site? It is possible to measure the channel's PIP₂ sensitivity using compounds like neomycin and poly-lysine, which screen PIP₂ molecules from their targets (Fan &

Makielski, 1997). Mutations can be grouped by their ability to decrease ATP sensitivity due to increased apparent PIP₂ affinity versus others that influence ATP alone. In addition, intrinsic open probability (Po) provides a measure of an allosteric PIP₂ effect. This won't necessarily delineate binding site residues from those that indirectly interfere with the binding site, but it gives a starting point for identifying relevant residues that could be mapped to homologous structural models of Kir6.2.

ATP likely binds to a site that is predominately if not exclusively on Kir6.2. It is important to emphasize that ATP binds to Kir6.2 independent of magnesium unlike its interaction with SUR. Characterization of disease mutations, selective mutagenesis studies, homology modeling and biochemical analysis give evidence toward a novel ATP binding site. The site locates at the interface of N- and C-terminal cytoplasmic domains between two adjacent Kir6.2 subunits (Antcliff et al., 2005; Figure 4). The Kir6.2 pore is a tetramer containing four ATP binding sites (Markworth et al. 2000). Based on functional studies, putative basic and uncharged residues in the binding site are R50 in the N-terminus and I182, K185, R201, and G334 in the C-terminus (Drain et al., 1998; Koster et al., 1999; Tucker et al., 1997; Li DP et al., 2000; Cukras et al., 2002a, 2002b). Photoaffinity labeling of R50 and K185 mutations using gamma-P32-labeled ATP further support their contribution (Tanabe et al., 1999). This places the ATP and PIP₂ binding sites in proximal if not over-lapping locations. Currently, it is uncertain whether the two molecules control channel gating by competing directly for the same site or through allostery. Homology modeling and kinetic study favor the explanation of an allosteric effect (Antcliff et al., 2005; Ribalet et al., 2005).

Mg²⁺ adenosine nucleotide binding to SUR is considered the principal mechanism of physiological K_{ATP} channel activation (Nichols et al. 1996; Proks et al. 2008). SUR NBF

motifs share good homology with ABC transporters and will presumably bind nucleotides similarly. Hydrolysis then may occur at two potential binding sites formed by an NBF dimer. Catalytic activity from hydrolyzing MgATP to MgADP was shown in SUR2 (Matsuo et al., 1999; Bienengraber et al. 2000). Energy obtained from the reaction would drive SUR conformational changes to transmit a signal to the pore. The necessity of catalytic activity to channel activation is unclear, since MgADP will bind as well to stimulate channels. Pharmacological openers (like diazoxide and other KCOs) and closers (sulphonylureas, glinides) also work through SUR1 to modulate gating of the Kir6.2 pore. **The focus of this thesis will be on ligand regulation and gating within the Kir6.2 pore domain of the channel.** We first consider the property of rectification.

K_{ATP} Gating as an Inward Rectifier (Kir) Channel

Kir channels have been found in a virtual ubiquity of cell types (for review see Hibino et al. 2010 p292). Their namesake property of inward rectification is an electrical term important for physiological activity. Currents carried by Kir channels do not behave according to Hodgkin & Huxley kinetics (1952) by varying with membrane potential alone; they depend on the electrochemical K⁺ gradient, the difference between membrane potential and the potassium reversal potential (E_K). Membrane potentials negative to E_K generate a large K⁺ current through Kir channels, whereas current at potentials positive to E_K is reduced, and the phenomenon can be readily seen in a graph of current-voltage relations (Figure 5). To state this simply, K⁺ ions flux through the channels into the cell more easily than out of the cell. This defining feature of Kir channels provides a cell the means to maintain the resting membrane potential using the K⁺ gradient and then shut off Kir conductance during membrane depolarization to prevent inadvertent short-circuiting of an action potential. Rectifiers regulate the resting membrane potential and firing threshold in neurons, and buffer extracellular K⁺ when

expressed in glia (Hille B, 2001; Newman EA et al., 1984). Unlike delayed-rectifier K^+ (Kv) channels and other voltage-gated channels that gate using a voltage sensor or region of protein which responds to changes in the membrane electric field, inward rectification is an extrinsic property of Kir channels in which the pore is “plugged” or blocked by multivalent cations (Hille, 2001). Mg^{2+} and polyamines penetrate deep into the pore when ions flow in the outward direction and block conduction (Fakler et al., 1994; Lu & Mackinnon, 1994).

Kir channels classify into two groups, either weak or strong rectifiers. The key structural difference between these two groups is an amino acid residue in the middle of TM2 of the channel known as the “rectification controller” (Wible et al., 1994; Figure 5). In K_{ATP} it is position N160, and since Kir channels are tetramers it places four residues in a symmetric position halfway through the membrane pointing a side chain directly into the channel lumen. Asparagine (single letter identifier N) has a polar side chain, so it will weakly interact with cations. In Kir2.1, the residue is aspartate (D) which places a side chain with a negative charge in the pore. The negative charge will have an electrostatic interaction with positively charged cations and stabilize a multivalent cation in the pore producing strong rectification (Lu & Mackinnon, 1994). N160D mutation in Kir6.2 converts the channel from a weak to strong rectifier. Additional polar and negatively-charged residues in the cytoplasmic domain make small contributions to rectification; their presence likely increases the local concentration of cations near the intracellular entrance of the pore by creating a favorable electrostatic environment (Nishida & MacKinnon, 2002). Rectification can also be used in functional studies to address properties of Kir channels; the N160D mutation in K_{ATP} is often utilized as a functional reporter of channel composition and environment in the pore.

K_{ATP} Channel Intrinsic Gating

How ion channels open and close is the subject of intense study because it will dictate the kinetics of many cellular processes. Development of the patch clamp technique (Hamill et al., 1981) allowed observation of single ion channel molecule fluctuations, and modeling channel state inter-conversions as a reaction mechanism provides a quantitative description of what physically happens during channel activation (Sivolotti, 2010). Implement the approach above to study K_{ATP} channels has been slow in part because their interactions with intracellular molecules are quite complex; the Kir6.2 pore will house four PIP₂ binding sites and four ATP binding sites, while SUR1 subunits contribute a possible eight Mg-nucleotide sites. The following sections will discuss what we currently understand about K_{ATP} channel gating in the pore, beginning with the spontaneous PIP₂-dependent activity known as intrinsic gating.

Single channel currents in the absence of nucleotides show bursts of activity containing a single open state (Figure 6A), interpreted from a single exponential fit to the open lifetime distribution, whereas multiple exponentials are fit to the closed time histogram (Enkvetchakul & Nichols, 2003). In between openings are “flickers,” or a short closed state (Hille, 2001); the short open and short closed components are termed “fast gating”. Bursts of openings are then separated by long periods of inactive or closed channels; the burst periods and interburst intervals are called “slow gating”. Burst length histograms are best fit with three or more exponentials. Increasing cofactor phosphoinositides in the inner membrane leaflet increases channel Po by increasing the mean open time, mean burst lengths and shortening interburst intervals (Fan & Makielski, 1999). Fast gating is voltage-dependent but ligand-independent, whereas ATP affects interburst transitions and burst lengths but has little effect on intraburst properties (Alekseev et al., 1998; Trapp et al., 1998; Fan & Makielski 1999; Li et al.,

2002). Recognition of two apparently distinct processes, the fast and slow gating events with only slow gating affected when ATP was present, led to the hypothesis that K_{ATP} channels possess at least two different locations in the structure that can close to physically restrict potassium permeation during intrinsic gating.

Structural requirements have also been identified in regions distant from the ion permeation pathway important for stabilizing intrinsic channel activation. In addition to residues considered important for PIP_2 binding, the cytoplasmic domains harbor residues that when mutated affect PIP_2 response or intrinsic gating. These residues include R192, E227, E229, V290, R301, and R314 (Lin et al 2003; Loechner et al., 2011). They generally map near the interface of adjacent Kir6.2 subunit N- and C-termini and are thought to maintain intersubunit cohesion, in several cases through direct interaction for example the salt bridge E229-R314 (Lin et al 2003). Mutant channels close with ATP usually with less sensitivity than WT channels; but upon ATP washout from an inside-out patch channel activity is substantially increased and then decays in a time-dependent manner. ATP binding to its site may reinitiate contacts between subunits that facilitate re-entry into the activated/open state. Additionally, exogenous PIP_2 application robustly activates mutant channels and will eliminate current decay if applied immediately following ATP removal. The time-dependent current decay was termed “inactivation”, although whether decay represents channel transitions to a new “inactivated” state or a channel state in the normal conformational pathway between PIP_2 binding and channel opening is unknown. That interpretation may depend on the optimal model that defines channel kinetics, which currently is actively debated (see Nichols 2006 and Proks & Ashcroft 2008; also see next section).

SUR also plays a role in ligand-independent gating. Truncated Kir6.2 Δ C channels have a low intrinsic open probability ($P_o \sim 0.1$) and a reduced ATP sensitivity ($\sim 100\mu\text{M}$, Tucker et al., 1997). SUR confers a higher P_o (~ 0.5) and ATP sensitivity ($10\text{-}20\mu\text{M}$) to WT channels, showing structural interactions between Kir6.x and SUR are critical for K_{ATP} intrinsic gating.

K_{ATP} Channel Inhibition by ATP

ATP alters single K_{ATP} channel gating kinetics by lengthening the long closed lifetimes and shortening the burst durations, without much effect on intraburst properties. From early structure/function studies using WT K_{ATP} single channel kinetics and concatenated channels, it was consistently argued that one ATP molecule which binds Kir6.2 was sufficient to close the channel (Qin et al., 1989; Nichols et al., 1991; Enkvetchakul et al., 2000; Markworth et al., 2000). Further single channel kinetic analysis support ATP closing a single inhibition gate (Drain et al., 2004). From modeling it was deduced that ATP can bind to both open and closed channel states, of which ATP has considerably greater affinity for the closed state (Enkvetchakul et al. 2001; Craig et al. 2008). As mentioned, PIP_2 stabilizes the open state of Kir channels, yet it is uncertain whether PIP_2 and ATP can simultaneously bind to the same Kir6.2 subunit or if a subunit is in an active state independent of PIP_2 to which ATP can bind.

How subunits cooperatively transition and how ligand binding brings about transitions can be predicted and tested from experimentally-derived mathematical gating models. Several kinetic models have been tested to explain how ATP binding leads to conformational changes in the channel complex. All models assume the channel has four homogenous ATP binding sites for inhibition. Established kinetic models fall

principally into two categories, independent and concerted, and the foremost candidate models are discussed here.

In the independent model (Figure 6B), subunits transition between active and relaxed conformations completely independent of one another and notably have no influence on changes in other subunits. When all four subunits simultaneously occupy the active conformation, the channel conducts ions. The model is similar to the one proposed by Hodgkin and Huxley (1952) for voltage-gated channels, and different from the classical Koshland Nemethy and Filmer (KNF) sequential model in which binding to one subunit makes subsequent conformational changes in other subunits more favorable. A time-homogenous Markov model that replicated the PIP_2 and ATP effects on single channel behavior was the tetrameric-allosteric gating model, an independent model that well predicts changes in P_o and macroscopic ATP IC_{50} concentration response caused by mutations and channel modulators (Enkvetchakul & Nichols, 2003; Nichols 2006). The tetrameric model contains an additional closed state (C_F in Figure 6) from the open-conducting state representing the fast intraburst transitions and separating it from ATP bound states. This is consistent with the existence of two independently-controlled gates in the structure with one dependent on ATP. A closed state (C_S in Figure 6) separates ATP bound closed states from the open state (Enkvetchakul et al., 2000). The model predicts that ATP predominately inhibits by “stabilizing closed states”, and that PIP_2 antagonizes the action of ATP allosterically by generating “open state stability”. Thus, the model infers that ATP and PIP_2 are not simultaneously bound.

In the concerted or Monod-Wyman-Changeux (MWC) model (Figure 6C), all four subunits are either active or relaxed and will undergo a simultaneous conformational change between states. ATP binding to a subunit exerts an additive effect on subunit

transitions. A prediction of the model was that subsequent reductions in free energy for transitions produce an exponential relationship between mean burst durations. Using mutated and truncated channels, Drain et al. (2004) showed the mean burst duration was exponentially dependent on the number of mutant subunits in heteromeric WT:mutant channels, arguing for cooperativity between subunits to reach the open state rather than independent subunits. Further study using tandem channels with a mutation in single subunits that could abolish ATP binding sites found the MWC model fit better to burst ratios than the independent model and others (Craig TJ et al. 2008). The model is principally emphasized because it incorporates ATP binding to the open state. If the open state is only achieved when PIP₂ is bound, the model easily accommodates simultaneously PIP₂ and ATP binding.

Independent and concerted models are currently debated and both have important caveats. The tetrameric model traditionally has not included an ATP-bound open state. More complex tetrameric schemes with the additional open state were attempted, but it was not evident that fitting burst durations using those models was tractable (Enkvetchakul & Nichols, 2003). In addition, certain truncated and mutant K_{ATP} channels which lengthened interburst closed intervals did not coincide with the independent model (Fang et al., 2006). In the other case, the current form of the MWC model does not reliably predict all of the macroscopic channel behavior caused by ATP inhibition (Proks & Ashcroft, 2008). Several experimental considerations cloud results from concerted model studies, such as unintended selection bias from heteromeric channel expression, restrictions caused by linker regions in concatenated channels, or using mutations with incomplete or misunderstood effects. Nonetheless, mechanistic single channel studies highlight interesting considerations for the K_{ATP} channel gating mechanism. They will help to identify physical interactions between functional units in the channel, to create

new models for simulating channel behavior, and to develop more complex quantitative cellular models to understand biological phenomenon.

Location of K_{ATP} Channel Gates

There is accumulating evidence that the selectivity filter and helix bundle crossing act as gates in K^+ channel pores. Gating was early considered a physical process distinct from ion permeation (Hille 2001), but as the molecular mechanisms of C-type inactivation were elucidated this view has slowly given way to one in which gating and permeation are coupled. A salient feature that links permeation with gating at the selectivity filter is the sensitivity of C-type inactivation to permeating ions (Hoshi et al., 1990; López-Barneo et al., 1993). Studies using ions that vary in permeability also show altered Kir single channel kinetics (Lu T et al., 2001b). Functional study in Kir channels demonstrates mutations at residues in or near the selectivity filter affect intraburst kinetics or “fast gating” (Lu T et al., 2001a; Proks et al., 2001). Other mutations have been found further out along the pore-loops in several Kir channels that affect gating (Chan et al., 1996; Guo & Kubo, 1998). Many of these residues are likely important for flexibility that affects the chemistry of the selectivity filter and vary efficiency to select and conduct ions (Noskov & Roux, 2006). Computer simulations of a K_{ATP} channel homology model using the Kirbac1.1 structure suggest there is flexibility near the filter and extracellular portion of the pore loops, and that distortions in the filter may result in channel gating (Capener et al., 2003; Domene et al., 2004). It is still unknown precisely which regions within K_{ATP} channels would affect flexibility that mediates gating near the selectivity filter.

The KcsA pore transmembrane domain can supplant a Kir channel pore and still confer Kir channel gating properties showing the conserved nature of the pore (Lu Z et al., 2001). Spectroscopy reveals two gates, one being the bundle crossing, in the KcsA

channel (Blunk et al., 2006). An early crystal structure of the bacterial homologue MthK channel was interpreted to be in the open state, as there is adequate space at the bundle crossing for a hydrated K^+ ion to pass through the opening (Jiang et al 2002a). In the bacterial homologue Kirbac1.1 structure, the space between helices at the bundle crossing is estimated to be 0.4-0.8 angstroms, suggesting it represents a closed state (Kuo et al., 2003). Larger diameters at the bundle crossing in recent eukaryotic Kir channel crystal structures might represent a partially open state (Hansen et al., 2011; Whorton & MacKinnon, 2011). The available structural data reveals potential gating conformations of the bundle crossing (Figure 7A). To support a bundle crossing gate hypothesis, structure/function studies have looked at residue content at the bundle crossing and accessibility to the inner cavity. Mutations of residue F168 that forms the narrowest point in the bundle crossing in K_{ATP} channels dramatically reduce ATP sensitivity and lengthen interburst closures, and analyses suggest this residue provides steric hindrance to block ion conduction (Rojas A et al., 2006). In addition, the mutation F168E can be titrated to increase channel bursting indicative of a gate forced open through electrostatic repulsion between negative charges (Khurana et al. 2011). The substituted cysteine accessibility method (SCAM) was used to test the accessibility of cysteines placed within the pore inner cavity by diffusing modifying reagents into the cytoplasmic end under conditions that bias channels in open or closed states. The pore of Kv channels appears to be gated by motions of the inner helices that open and close the helix bundle crossing, as cadmium (Cd^{2+}) and silver (Ag^+) accessibility to a cysteine in the inner cavity was reduced in the closed state (Liu et al., 1997; del Camino and Yellen, 2001). In constitutively active Kir2.1 channels, modification by small methanethiosulfonate compounds Cd^{2+} and Ag^+ is similar between open and apparent closed states suggesting the bundle crossing is not a gate (Xiao et al., 2003); however, Ag^+ also labeled non-pore facing TM1 substituted cysteines suggesting there was a

separate detour pathway for Ag^+ , and establishing a closed state will depend on the ability to manipulate PIP_2 levels in a cell-based system. A similar result was initially observed in K_{ATP} channels, but the ability of a closed pore to “trap” reagents with high diffusion/modification rates potentially obscured gated access (Phillips & Nichols, 2002; Phillips et al., 2003). In very high ATP (10mM) with an estimated $P_o < 0.01$, small charged cysteine-modifying reagents finally had slower modification rates compared with the open state (Phillips et al., 2003), indicating gated access for these compounds and a “leaky” helix bundle crossing gate in K_{ATP} channels in contrast to tight steric closure in Kv channels. The result also implicates ATP in controlling an intracellular gate to close the channel (Figure 7B). Bending motions proposed by the structural studies to open and close the bundle crossing gate will require flexibility in the TM2 helices.

A complication in the two gate hypothesis is structural evidence for a third gate. Pegan et al. (2005) crystallized the cytoplasmic domains from Kir2.1 and Kir3.1 and both show the location of a narrow girdle in the permeation pathway formed by the G-loop with small changes in the size of the opening. More recent full length Kir channel structures indicate larger differences in the diameter of the hole through the G-loop (Nishida et al., 2007; Whorton & Mackinnon, 2011). The residue I296 in the G-loop of K_{ATP} channels lines the pore, and its mutation produces a severe gain-of-function phenotype that causes a serious form of neonatal diabetes known as DEND syndrome (Proks et al., 2005). Whether the G-loop changes conformation in K_{ATP} channels or simply maintains a narrow and rigid entry point for K^+ ions into the intracellular end of the pore remains to be determined.

Glycine Hinge Hypothesis

The hinge hypothesis for a mechanism of K⁺ channel gating was put forward originally based on structural comparison of KcsA in the closed state and MthK channel in the open state (Jiang et al., 2002). It states the pore transmembrane helices bend at a glycine residue (central/upper glycine in Figure 7C) or a proline motif (PVP) to open the intracellular gate at the helix bundle crossing. Glycine adopts a wider range of dihedral angles than other amino acids, and proline residues break and kink the structure of a helix to provide “flexibility” to the helix and facilitate the bending motion. Mutagenesis studies in the voltage-gated Shaker channel and the voltage and Ca²⁺-gated BK channel confirmed the hypothesis and results were fairly conclusive; mutations reduced channel conductance in a graded manner (Magidovich & Yifrach, 2004; Ding et al., 2005). The central glycine was the most conserved residue (~70%) in TM2 for homologous K⁺ and cyclic nucleotide gated (CNG) channels (Jin et al., 2002). An initial analysis in Kir channels using Kir3.4 G-protein activated channels suggested the central glycine was crucial for G-protein gating (Jin et al., 2002).

Subsequent studies in Kir channels have generally led to adverse and more conservative interpretations that the upper glycine was unnecessary for gating. Re-analysis of Kir3.4 indicated a residue next to the upper glycine acts as the hinge point, with the glycine playing a secondary role to eliminate TM2 helix interactions with the selectivity filter (Rosenhouse-Dantsker & Logothetis, 2006). A threonine or serine at the same position in Kir4.1 and 5.1 respectively shows the central glycine position is not completely conserved in Kir channels. When the unconserved equivalents in Kir4.1/Kir5.1 heteromers were mutated to flexible glycine, they had reduced channel activity seen as decreased open probability; in other words, adding a flexible glycine had an adverse effect on the putative hinge position (Shang & Tucker, 2007). In addition, a

second completely conserved “lower” glycine in Kir channels is present in TM2 near the helix-bundle crossing, which could work in tandem with the upper glycine or compensate for its absence. In Kir1.1, mutation of both upper and lower glycines in the same channel decreased pH sensitivity but was not an absolute requirement for pH gating (Sackin et al., 2006). These studies generally dismiss the upper glycine as a hinge point with arguments against its necessity for flexibility.

Flexibility, i.e. the potential number of rotamers an amino acid can form, is a difficult parameter to isolate because the molecular environment around the amino acid has a significant contribution (Chakrabartty et al., 1991) and therefore in a 3-dimensional context may vary significantly between channel types. Interpretation of flexibility from functional data often requires the assumption that flexibility can be altered with single amino acid substitutions, i.e. by changing the sidechain. Most previous studies use open probability or current amplitude as a read-out of changes in flexibility to the intracellular gate; these parameters don't distinguish between an extracellular and intracellular gate. Absence of data for channel surface expression differences can negate or over-emphasize effects on macroscopic current amplitudes. Stable WT gating in Kir channels may also require dependency of or cooperativity between the two gates. Due to these complications, addressing the validity of the glycine hinge hypothesis remains an active research question.

Scope of this Dissertation

Hopefully this introduction offers a clear view of some of the principal ideas regarding the K_{ATP} channel and how we think about them in terms of physiology, composition, structure, regulation and gating. Its intent was to narrow our focus described in the abstract to the question examined by this work, specifically the role of the upper glycine

as a component of the gating mechanism of K_{ATP} channels. In Chapter 1, we will discuss the results from study of a disease mutation at the central glycine and consequences that arise from its presence in the pore.

In a collaborative publication from our lab (Pinney SE et al., 2008), a dominantly inherited mutation was found in the KCNJ11 gene in several patients with congenital hyperinsulinism from the same family. The parent was suspected hypoglycemic, although this diagnosis was not made until adulthood. One child from the pedigree was stillborn; a second was diagnosed hypoglycemic and a brief albeit possibly insufficient attempt at treatment using the K_{ATP} channel opener diazoxide failed, so an immediate pancreatectomy was performed. A third child was diagnosed hypoglycemic and responded well to diazoxide treatment. The mutation in KCNJ11 is in the protein coding region where the central glycine is replaced with arginine. Chapter 1 of this thesis characterizes the mechanism of channel defect caused by the mutation and further analysis allows an interpretation that reflects on the glycine hinge hypothesis. In using mutagenesis to study this glycine, an additional mutation generated an “inactivation” phenotype. Chapter 2 uses prior knowledge of channel inactivation to functionally assess this phenotype and describe how replacing the glycine in TM2 uncovers large domain interactions during K_{ATP} activation. Chapter 3 preliminary study takes a broader view of the flexibility in inner helix TM2 and suggests the lower glycine is not equivalent to the upper glycine and may be required for gating. A conclusion will summarize the studies and propose future approaches to understand the channel gating mechanism.

Figure Legends

Figure 1 – Simple mechanism of glucose-dependent insulin secretion in β -cells.

Cartoons depicting beta cell response to high and low glucose levels **(A)** under euglycemic and **(B)** under pathological conditions. The letter X indicates K_{ATP} channels contain a mutation. See text for detailed explanation. **(C)** Tissue distribution of subunit subtypes. Information collected from (Hibino et al., 2011).

Figure 2 – Kir Structure. Ribbon diagrams of the Kirbac1.1 crystal structure, depicted as the full tetramer **(A)** and two opposing subunits **(B)** showing the transmembrane domain and visible portion of the cytoplasmic N-terminus region (Protein databank ID 1P7B). Parts of interest are labeled and described in the text.

Figure 3 – SUR and hypothetical K_{ATP} octamer. **(A)** – Membrane topology of a sulphonylurea receptor subunit with labeled domains. **(B)** – Prediction of the assembled octameric complex structure using homology models inserted into cryo-electron micrograph density. Colors denote Kir6.2 (blue), TMD0 (yellow), and ABC transporter core domains (red). Images on the right are from (Mikhailov et al. 2005).

Figure 4 – Regulators of K_{ATP} channels and putative Kir6.2 binding sites. **(A)** – Chart of principal channel ligands colored by their effect on channel gating and listed below the subunit with which they interact. **(B)** – Space-filled model of binding sites for ATP (red) and PIP_2 (yellow) developed using homology model docking from (Haider et al., 2007).

Figure 5 – Inward rectification of Kir channels. (A) – Structural image of the ion permeation pathway formed by two opposing subunits. Labeled residues were shown to influence kinetics of rectification. Kir6.2 N160 is labeled for reference. Multivalent cations (images) diffuse into the pore to block ion conduction with membrane potentials depolarized from the potassium reversal potential (E_K). Image adapted from Bichet et al. 2003. (B) – Current-voltage relation for weak (blue) and strong (green) rectifier channels. Mutation of N160 to aspartate converts K_{ATP} channels from a weak to a strong rectifier.

Figure 6 – K_{ATP} single channel currents and kinetic mechanisms. (A) Traces from a single channel record at -80mV membrane potential in nucleotide-free solutions with no Mg^{2+} ions present. Current was sampled at 50kHz and filtered at 5kHz. Openings appear as downward deflections. Lower trace shown with increased time resolution to label dwell time parameters. (B) The independent (tetrameric) kinetic model. *Top*, diagrams show how individual subunits will transition between active (circle) and relaxed (square) states. K_o and K_c are ATP equilibrium binding constants, E_o is the equilibrium gating constant, and t (K_c/K_o) is a factor that changes with the equilibrium gating constant due to bound ATP. The right side shows the result of subunit transitions on the open/closed state of the pore tetramer. *Bottom*, the tetrameric model is represented as an abbreviated reaction scheme. C_s and C_f stand for slow and fast gating states, respectively. An additional subscript A is shown for ATP-bound states. States shown in brackets are for each individual subunit, and number of subunits indicated by the superscript four; the superscript four is NOT related to the transition rates. Rate constants are not shown. (C) The concerted MWC model. All four subunits are either active or relaxed. The factor t has exponential dependence depending on the number of ATP molecules bound. Reaction scheme is shown on the bottom. Images were adapted from Proks and Ashcroft, 2008.

Figure 7 – Gating conformations in the Kir pore. (A) View from the extracellular/inner cavity side looking down towards the helix-bundle crossing in closed and open configurations based on Kirbac1.1 and MthK structures (from Kuo et al., 2005). Depicted are TM2 (green), TM1 (purple), and the slide helix (red). **(B)** Hypothesized motions for transmembrane and cytoplasmic domains when PIP₂ and ATP bind to the channel. Image modified from Enkvetchakul et al., 2007, see below. **(C)** Ribbon depiction of a single Kirbac1.1 subunit (1p7b) with labeled regions that face the ion conduction pathway attributed to different structural gates and the locations of the central (upper) glycine and lower glycine.

Figure 3B image adapted by permission from Macmillan Publishers Ltd: The EMBO Journal, Mikhailov MV et al., copyright 2005.

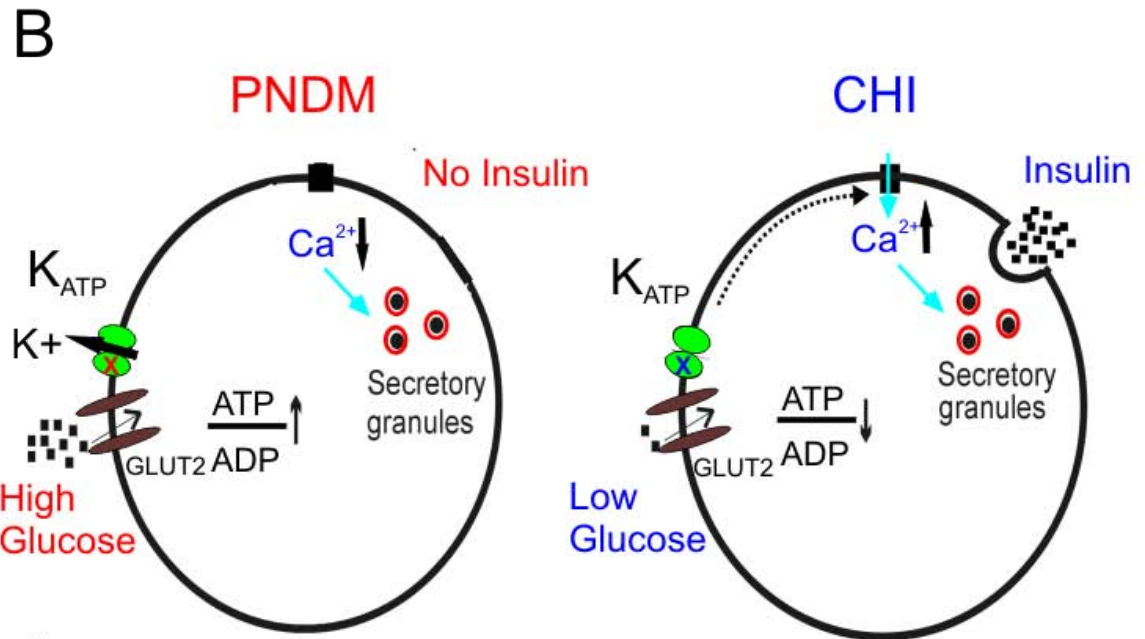
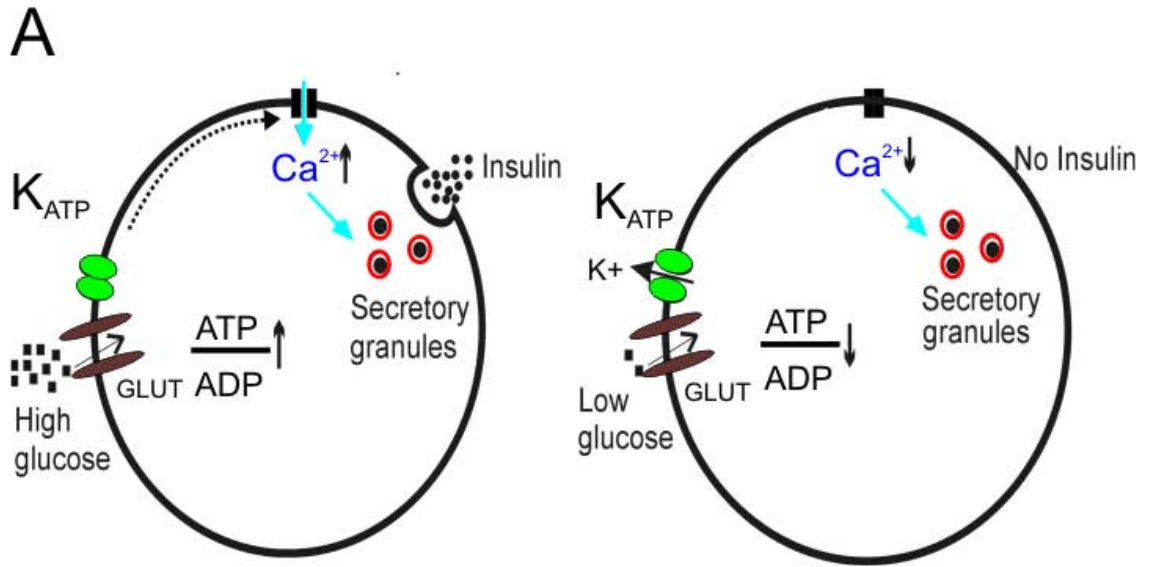
Figure 4B image adapted by permission from Macmillan Publishers, Ltd: The EMBO Journal, Haider S et al., copyright 2007.

Figure 5A image adapted by permission from Macmillan Publishers, Ltd: Nature Reviews Neuroscience, Bichet D et al., copyright 2003.

Figure 6B, C images reprinted from Proks & Ashcroft, Progress in Biophysics and Molecular Biology, 2008, with permission from Elsevier.

Figure 7A image reprinted from Kuo A et al., Structure, 2005 with permission from Elsevier.

Figure 7B image adapted from Enkvetchakul, D., I. Jeliaskova, J. Bhattacharyya, and C.G. Nichols. 2007. Control of inward rectifier K channel activity by lipid tethering of cytoplasmic domains. *J. Gen. Physiol.* 130:329-34.

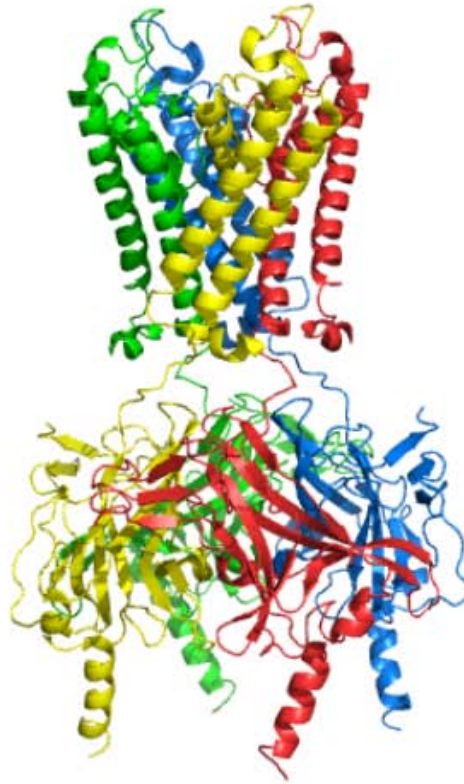


C

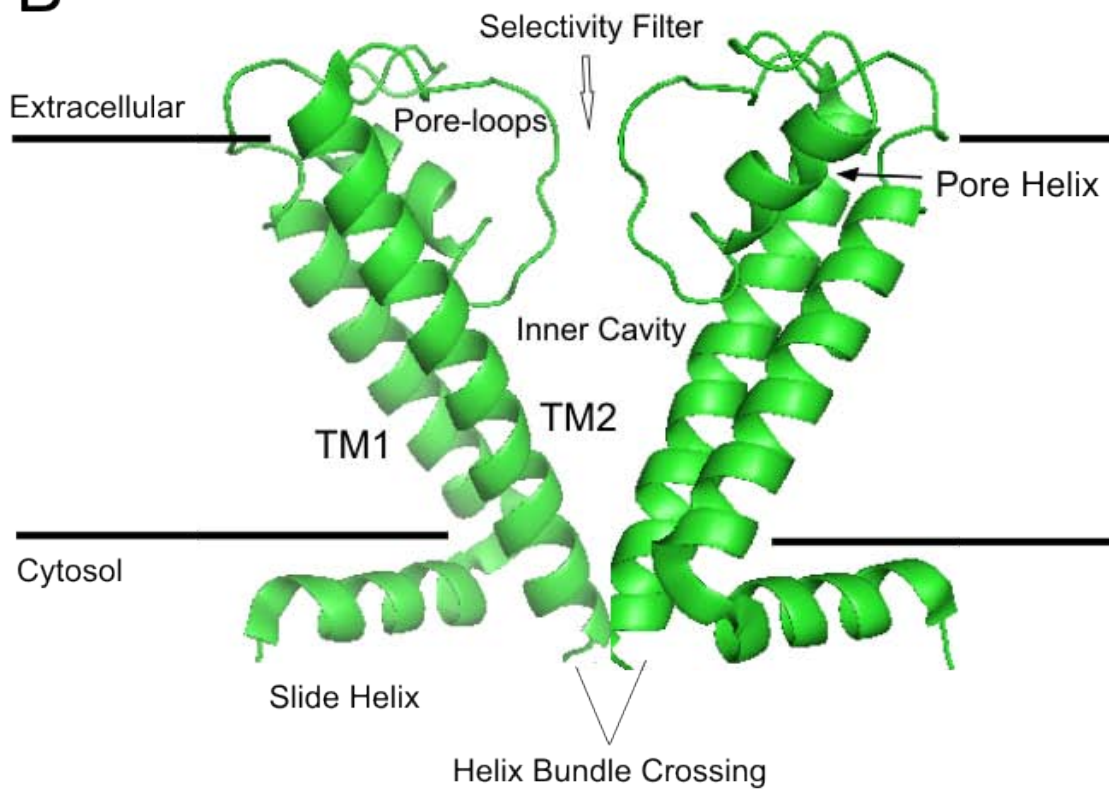
Kir6.1	Smooth muscle
Kir6.2	Pancreas, Heart
SUR1	Pancreas, Heart, Nervous (CNS/PNS)
SUR2A	Heart, Skeletal muscle
SUR2B	Brain, Liver, Skeletal muscle, Smooth muscle

JDB Intro Figure 1

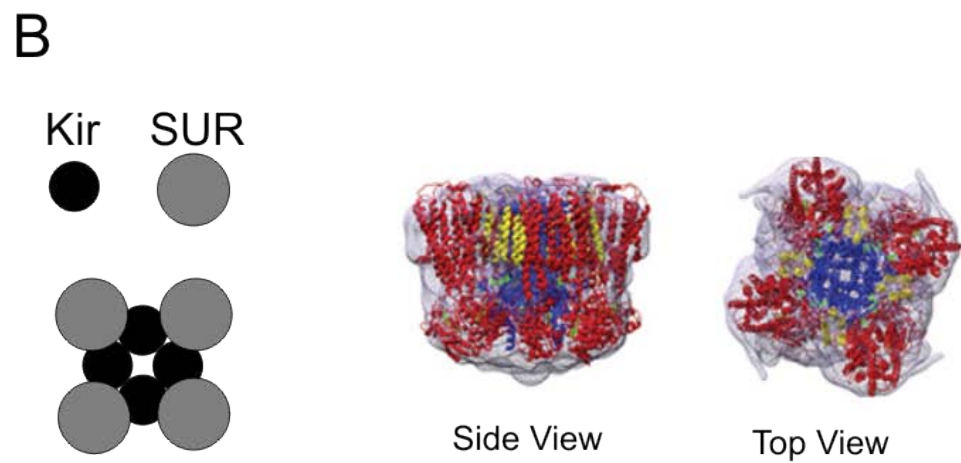
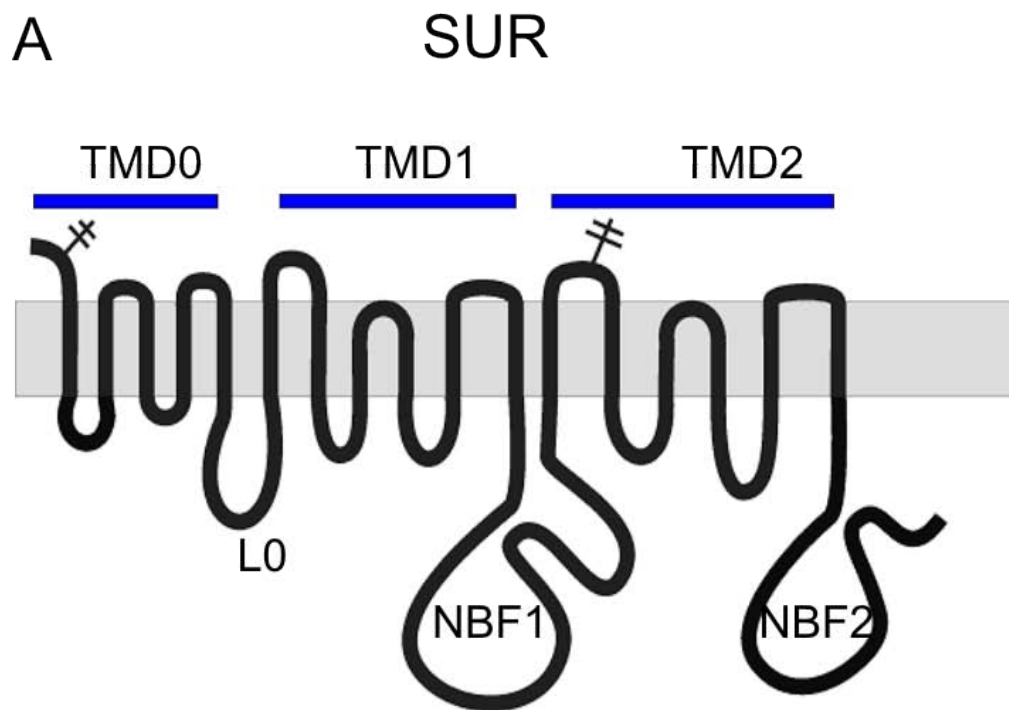
A



B



JDB Intro Figure 2

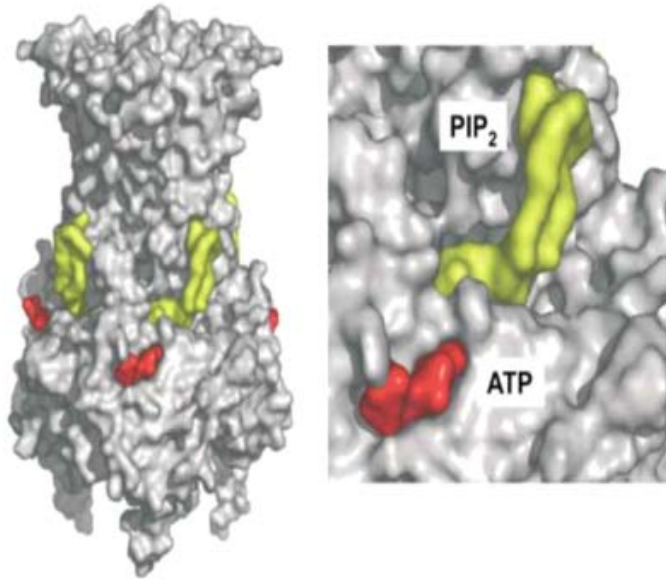


JDB Intro Figure 3

A

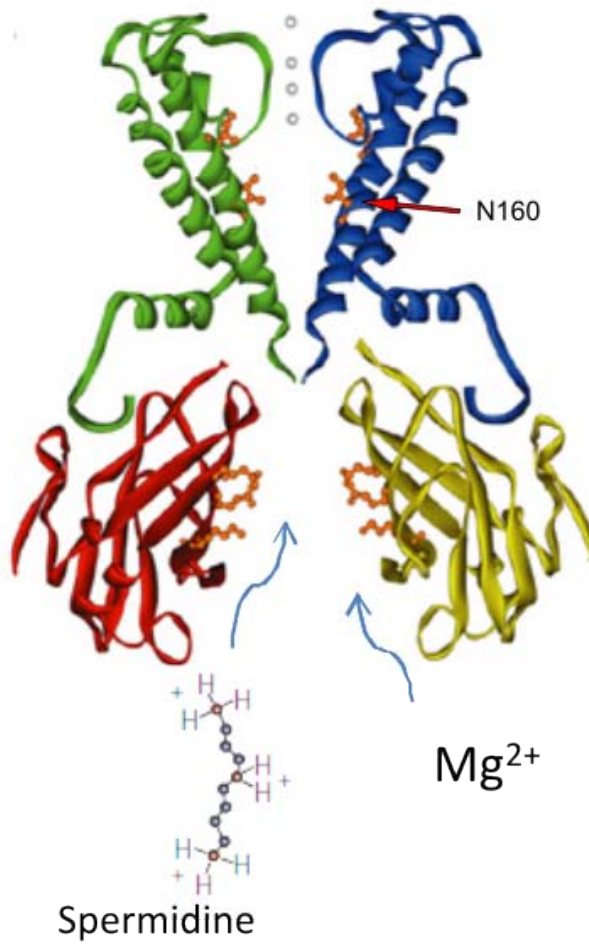
	Kir.x	SURx
Activators	PIP2 LC-CoA	MgADP MgATP KC openers
Inhibitors	ATP ADP	Sulphonylureas

B

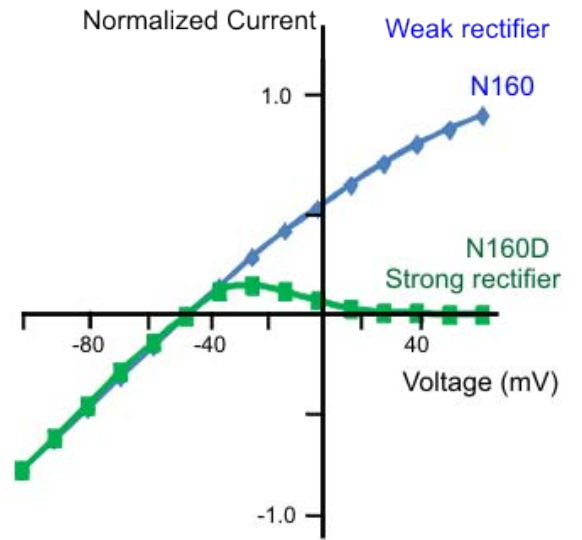


JDB Intro Figure 4

A

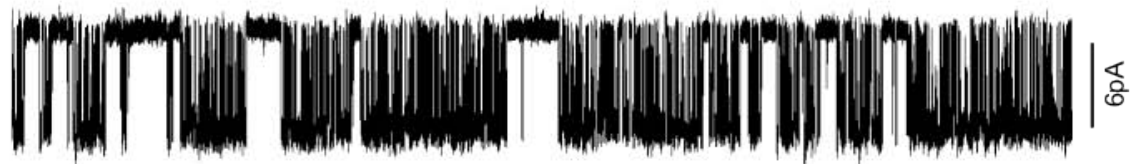


B

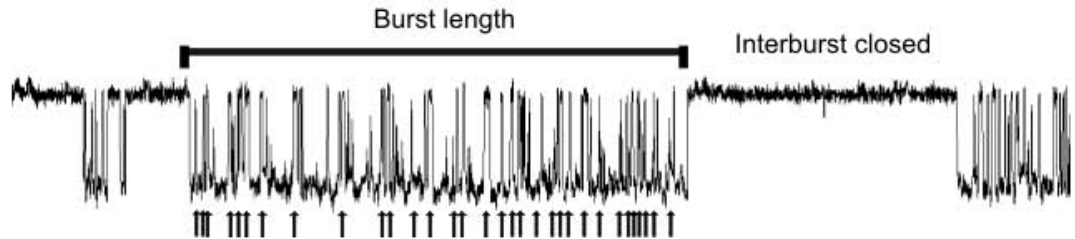


JDB Intro Figure 5

A Nucleotide-free



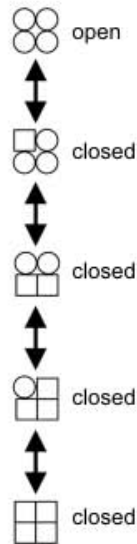
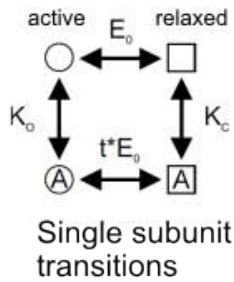
Total time 1.5s



Intraburst closures

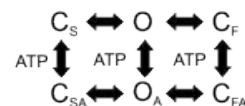
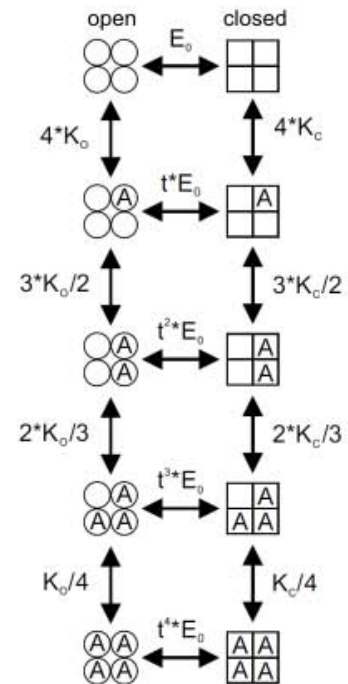
Total time 200ms

B



Independent Model

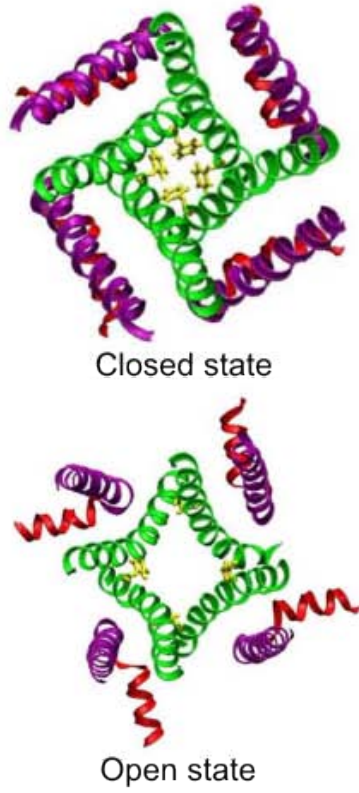
C



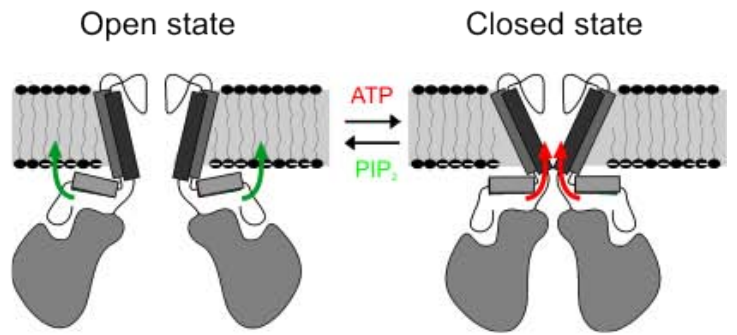
Concerted Model

JDB Intro Figure 6

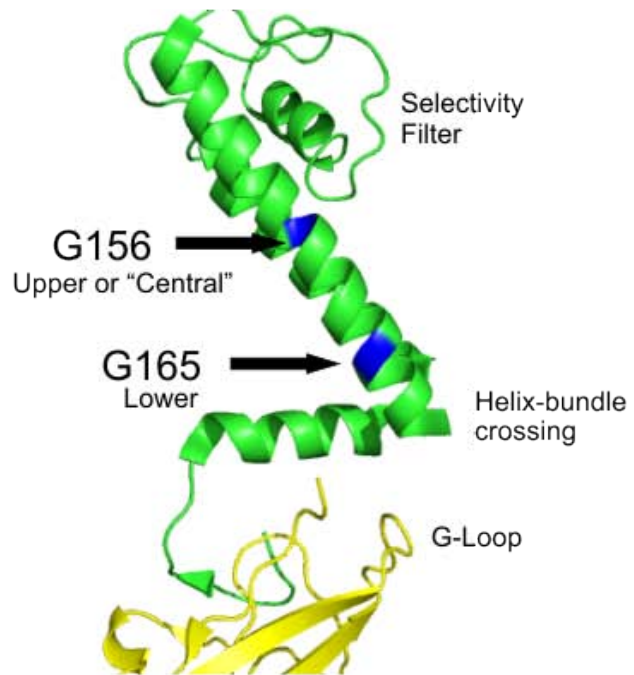
A



B



C



JDB Intro Figure 7

CHAPTER 1

Characterization and Functional Restoration of a Potassium Channel Kir6.2 Pore Mutation Identified in Congenital Hyperinsulinism

Jeremy D. Bushman[‡], Joel W. Gay[‡], Paul Tewson[‡], Charles A. Stanley[§], and Show-Ling Shyng[‡]

[‡]Center for Research on Occupational and Environmental Toxicology, Oregon Health & Science University

[§]Division of Endocrinology/Diabetes, The Children's Hospital of Philadelphia

Corresponding Author: Show-Ling Shyng

Chapter 1 is a manuscript published in:

Journal of Biological Chemistry, February 26, 2010, Volume 285, p. 6012-6023
© the American Society for Biochemistry and Molecular Biology.

In this chapter, JD Bushman performed molecular biology, experiments in Figures 1A-D, 2, 3D, 4, 5, 6, 7B-E, 8, and Table 1, and contributed to writing. J. Gay performed molecular biology and experiments in Figures 3A-C, and 7A-B. P. Tewson performed molecular biology. Further contributions mentioned in acknowledgements.

Abstract

The inwardly rectifying potassium channel Kir6.2 assembles with sulfonylurea receptor 1 to form the ATP-sensitive potassium (K_{ATP}) channels that regulate insulin secretion in pancreatic β -cells. Mutations in K_{ATP} channels underlie insulin secretion disease. Here, we report the characterization of a heterozygous missense Kir6.2 mutation, G156R, identified in congenital hyperinsulinism. Homomeric mutant channels reconstituted in COS cells show similar surface expression as wild-type channels but fail to conduct potassium currents. The mutated glycine is in the pore-lining transmembrane helix of Kir6.2; an equivalent glycine in other potassium channels has been proposed to serve as a hinge to allow helix bending during gating. We found that mutation of an adjacent asparagine, Asn-160, to aspartate, which converts the channel from a weak to a strong inward rectifier, on the G156R background restored ion conduction in the mutant channel. Unlike N160D channels, however, G156R/N160D channels are not blocked by intracellular polyamines at positive membrane potential and exhibit wild-type-like nucleotide sensitivities, suggesting the aspartate introduced at position 160 interacts with arginine at 156 to restore ion conduction and gating. Using tandem Kir6.2 tetramers containing G156R and/or N160D in designated positions, we show that one mutant subunit in the tetramer is insufficient to abolish conductance and that G156R and N160D can interact in the same or adjacent subunits to restore conduction. We conclude that the glycine at 156 is not essential for K_{ATP} channel gating and that the Kir6.2 gating defect caused by the G156R mutation could be rescued by manipulating chemical interactions between pore residues.

Introduction

Inwardly rectifying potassium (Kir) channels are expressed in a wide variety of cell types where they regulate membrane excitability in response to diverse signals (Nichols CG & Lopatin AN, 1997). They are characterized by two-transmembrane helices, TM1 and TM2, a re-entrant pore-helix, and cytoplasmic N and C termini. The structural mechanism by which Kir channels gate, a process that switches the channel between open and closed conformation, is not clearly understood. Collective structural and functional data from bacterial and mammalian Kir channels have led to a proposed gating model in which ligand binding to the cytoplasmic domains induces movement of an amphipathic helix called the slide helix along the lipid bilayer followed by lateral movement of the outer helix TM1. This then allows rotation and bending of the inner helix TM2 to open or close a lower gate located at the bundle crossing where the inner helices (TM2) of the four Kir subunits converge (Kuo A et al., 2005; Kuo A et al., 2003; Nishida & MacKinnon et al., 2002; Yi BA et al., 2001; Haider S et al., 2007). Within TM2, a central glycine that is conserved in most Kir channels was proposed in the bacterial MthK channel to serve as a hinge to allow the helix to bend during gating (Jiang Y et al., 2002). However, whether this glycine serves a similar role in Kir channels remains unresolved (Jin T et al., 2002; Rosenhouse-Dantsker & Logothetis, 2006, 2007; Shang & Tucker 2007; Kurata et al., 2004). Another important gating characteristic of Kir channels is that they conduct ions more readily in the inward rather than the outward direction because of blocking by intracellular Mg^{2+} and polyamines at positive membrane potentials (Hille, 2001; Lopatin et al., 1994). Although the inward rectification property is conferred by multiple structural features in the pore helix and the extended cytoplasmic pore of Kir channels, a residue in TM2 plays a critical role (Lopatin et al. 1994; Yang et al., 1995; Pegan et al., 2005). Thus, in weak inward rectifiers, such as in Kir1.1 and

Kir6.2, this residue is a neutral amino acid asparagine, whereas in strong inward rectifiers such as Kir2.1 and Kir3.1, the residue is a negatively charged aspartate (Lopatin et al., 1994).

Among Kir channels, Kir6.2 is unique in requiring co-assembly with the sulfonylurea receptor (SUR)2 for functional expression (Inagaki N et al., 1995). The channel complex formed by Kir6.2 and SUR is known as the ATP-sensitive potassium channel (Inagaki N et al., 1995, Aguilar-Bryan L et al., 1998). Kir6.2, being the pore subunit of the K_{ATP} channels, integrates signals from the regulatory subunit SUR1 and multiple ligands to control potassium ion conduction (Inagaki N et al., 1995; Ashcroft FM & Gribble FM, 1998; Nichols CG, 2006). Membrane phosphoinositides (such as phosphatidylinositol 4,5-bisphosphate) and long chain acyl-CoA (LC-CoA) activate the channel, whereas ATP inhibits the channel by direct interactions with Kir6.2. MgADP on the other hand stimulates channel activity by interacting with SUR1. Sensitivities of K_{ATP} channels to intracellular nucleotides ATP and MgADP enable the channels to couple cell metabolism to cell excitability (Nichols CG, 2006).

In pancreatic β -cells, the K_{ATP} channel composed of Kir6.2 and sulfonylurea receptor 1 (SUR1) is essential for triggering glucose-stimulated insulin secretion (Aguilar-Bryan et al., 1999; Ashcroft FM & Gribble, 1999). Upon glucose stimulation, the relative ATP to ADP concentrations in β -cells increase, driving K_{ATP} channel closure, membrane depolarization, Ca^{2+} influx, and insulin release. Mutations in Kir6.2 and SUR1 that lead to loss or gain of K_{ATP} channel function are well recognized as the major cause of congenital hyperinsulinism or neonatal diabetes, respectively (Huopio H et al., 2002; Aguilar-Bryan et al., 2001; Dunne MJ et al., 2004; Glaser et al., 2000). Functional analysis of mutant K_{ATP} channels has offered insight into not only disease mechanisms

but also the structure-function relationship of the channel (Huopio H et al., 2002; Aguilar-Bryan et al., 2001; Dunne MJ et al., 2004; Glaser et al., 2000). Here, we report functional characterization of a congenital hyperinsulinism-associated heterozygous Kir6.2 mutation of glycine 156 (the central glycine in TM2 hypothesized to serve as a gating hinge in potassium channels) to an arginine. Homomeric G156R mutant K_{ATP} channels are well expressed at the cell surface but do not give rise to potassium currents (Pinney et al., 2008). When co-expressed with WT Kir6.2 to simulate heterozygous expression, the mutant subunit was incorporated into the channel complex to alter channel function. We show that a second site mutation, N160D, which converts Kir6.2 from a weak inward rectifier to a strong inward rectifier in the WT background, restores ion conduction in the G156R channel. The G156R/N160D channel exhibits no voltage-dependent block by spermine, suggesting that electrostatic interactions of the two substituted amino acids underlie restoration of ion conduction. Interestingly, this interaction can occur both within the same subunit and between two neighboring subunits. Furthermore, G156R/N160D channels have single channel conductance and nucleotide sensitivities comparable to WT channels and are activated by metabolic inhibition in intact cells. These results indicate that the physical chemical property of the glycine residue at position 156 is not an absolute requirement for permeation and gating in Kir6.2; rather, appropriate interactions among the pore residues provide a structural environment conducive to permeation and gating.

RESULTS

The G156R Mutation Abolishes Channel Activity without Preventing Expression.

The G156R mutation in Kir6.2 was originally reported in a large scale study of dominant K_{ATP} channel mutation cases of congenital hyperinsulinism (Pinney et al., 2008). The

proband and her younger sister heterozygous for the G156R mutation presented with hypoglycemia in the newborn period. The younger sister responded to treatment with diazoxide. The proband received a pancreatectomy after treatment with diazoxide seemed ineffective, but the trial was likely too brief to judge its effectiveness. Initial *in vitro* reconstitution of the G156R mutant channel in COSm6 cells indicated relatively normal surface expression but no channel activity (Pinney et al., 2008). The biochemical and functional data characterizing this mutant phenotype are presented in Figure 1. Western blots of lysates from COSm6 cells transfected with G156R or WT channel cDNAs showed comparable SUR1 and Kir6.2 protein levels as well as a complex-glycosylated SUR1 band (upper) corresponding to SUR1 that has exited the endoplasmic reticulum and traversed medial Golgi (Figure 1A). Because SUR1 trafficking requires co-assembly with Kir6.2 into an octameric structure before endoplasmic reticulum export (Zerangue et al., 1999), the results indicate fully assembled G156R K_{ATP} channels reaching the cell surface. In agreement with the Western blot results, chemiluminescence measured from antibody-labeled G156R channels at the cell surface was ~80% of WT (Figure 1B).

Despite normal surface expression, channel activity was not observed in inside-out excised patches even after exposure to phosphatidylinositol 4,5-bisphosphate or LC-CoA (oleoyl-CoA was used throughout the study) which are both known to increase K_{ATP} channel open probability (Figure 1C). $^{86}\text{Rb}^+$ efflux experiments also showed no detectable mutant channel activity above background upon metabolic inhibition, in contrast to WT channels (Figure 1D). Moreover, channel current was not observed when other ions were substituted for K^+ , including Rb^+ , Na^+ , and Tl^+ ($n = 3$ each, not shown). The results indicate loss of channel function was due to the absence of measurable ion conduction.

Effect of Heterozygous Expression of G156R on Channel Conduction Properties.

G156R is identified as a dominant heterozygous mutation; we asked how co-expression of this mutant subunit with a WT-Kir6.2 subunit at a 1:1 cDNA ratio affects overall channel activity and whether the functional phenotype under this condition correlates with clinical phenotype seen in patients. Current amplitudes measured from excised patches of cells simulating heterozygous expression of G156R were reduced by ~60% compared with those from cells expressing pure WT channels (Figure 2A, n = 25 each, p < 0.001). The heterozygous channels exhibited a response to diazoxide stimulation similar to WT channels (Figure 2B). These results are consistent with the clinical phenotype in that channel function is reduced, but response to diazoxide remains.

Because homomeric G156R channels express at a comparable level to WT channels at the cell surface, it is reasonable to assume that in simulated heterozygosity studies both subunits are incorporated into the surface channel complex and contribute to channel activity. However, a possibility remains that the channel activity and diazoxide response in patients and in simulated heterozygous expression result from haplosufficiency, i.e. the WT Kir6.2 accounts for all the channel activity and diazoxide response observed. To directly test if G156R-Kir6.2 forms functional heteromeric channels with WT-Kir6.2, we asked whether Kir6.2 tetramers containing one or more G156R mutant subunits give rise to K_{ATP} currents. To control the number of mutant subunits, we constructed a series of concatenated Kir6.2 tandem tetramers with 0–4 G156R subunits. Subunits were separated with a 12-amino acid linkers (Figure 3A) spanning the C- to N- termini of adjacent subunits. This approach also allows us to assess the stoichiometry of G156R in blocking ion conduction in the Kir6.2 tetrameric pore. All tetrameric constructs produced proteins of the predicted size when transfected into COS cells, as shown by Western blots (Figure 3B). Chemiluminescence assays were used to measure surface expression

of the tandem channels in COS cells co-expressing SUR1 (Figure 3C). Although all tandem channels were expressed at the cell surface, their expression levels were considerably lower than channels formed by SUR1 and monomeric Kir6.2 subunits. Macroscopic inside-out patch recordings showed that tandem channels containing all four WT Kir6.2 generated substantial ATP-sensitive currents. Tandem channels containing one G156R subunit also generated detectable currents but at a much reduced level compare with WT-tandem channels (only ~10% of WT-tandem; Figure 3D). In tandem channels containing two G156R mutant subunits, the average current fell to about 1% that of WT tandem channels, and no activity was seen with tandem channels containing three or four mutant subunits. These results demonstrate that channels containing a single G156R subunit are still able to conduct potassium current; however, more than two mutant subunits in the tetramer eliminate channel activity. The results support the idea that mutant and WT Kir6.2 subunits can form heteromeric channels at the cell surface where G156R subunit-containing channels contribute to the overall currents.

Functional Rescue of the G156R Mutation. How does the G156R mutation affect ion conduction? One possibility is that this central glycine is essential for TM2 to undergo a bending conformational change to open the channel, as proposed for the bacterial potassium channel MthK (Jiang Y et al., 2002). Alternatively, a charged amino acid at this position may directly interfere with the permeation pathway either by altering the electrostatic profile of the pore or by restricting conformational movement involved in gating. Homology modeling of a closely related channel Kir3.4 has suggested that the equivalent glycine and an asparagine about one helical turn down TM2 both face the pore and that the side chains of amino acids placed in these two positions interact (Rosenhouse-Dantsker et al., 2006). We, therefore, tested if the mutation of the

equivalent asparagine at position 160 of Kir6.2 to a negatively charged aspartate (N160D) will alter manifestation of the G156R mutation effect on ion conduction. Charge pair mutant channels G156R/N160D had significantly reduced expression compared with the single mutation (Figure 4, A and B). However, these channels exhibited measurable ionic currents and efflux in response to metabolic inhibition (Figure 4, C and D). Channel activity in excised patches showed properties of K_{ATP} channels, with currents eliminated by 1 mM ATP and stimulated by 5 μ M LC-CoA. A similar loss of channel activity was observed when Gly-156 was mutated to a lysine; however, K_{ATP} currents were again recovered when the G156K mutation was combined with the N160D mutation (Figure 4, C and D). Moreover, replacing Asn-160 with glutamate (N160E) also restored ion conduction in the G156R or G156K background (Table 1). These results are consistent with the idea that the substituted amino acids at the 156 and 160 positions interact electrostatically to restore ion conduction. Charge reversal at the two positions (G156D/N160D or G156E/N160D) on the other hand did not yield functional channels (but see Figure 6), although surface expression of G156D/N160R was ~50% that of WT channels (Table 1). Furthermore, replacing the amino acid adjacent to Asn-160 or the amino acid predicted to be approximately one helical turn down from Asn-160 with an aspartate (A161D and L164D, respectively) failed to restore channel activity, suggesting that the orientation and distance of a negatively charged residue from G156R affects its ability to rescue the ion conduction defect caused by G156R (Table 1).

Mutation from asparagine to aspartate at the “rectification controller” position in Kir6.2 (N160D) converts K_{ATP} channels from weak to strong inward rectifiers. Prior studies have shown that under symmetrical K^+ solution conditions in inside-out patch recording, the N160D mutant exhibits a nearly linear current-voltage relationship from -100 to +100 mV in the absence of Mg^{2+} or polyamines similar to WT channels; however, in the

presence of Mg^{2+} or polyamines such as spermine, the outward currents at positive membrane potentials are diminished due to strong interaction between the aspartate residue and spermine, which blocks the pore (Lopatin et al., 1994; Shyng S et al., 1997). If functional rescue of the G156R mutant by N160D results from electrostatic interactions between the two substituted amino acids, one would predict that the aspartate will no longer contribute to inward rectification, as it will not be available to interact with the positively charged polyamines. Indeed, inside-out excised patches of G156R/N160D and G156K/N160D channels showed weak rectification at positive potentials when exposed to 20 μ M spermine (Figure 5), similar to WT channels but in contrast to N160D channels. As a control, in the absence of polyamines none of the channels exhibited strong rectification (Figure 5). Lack of rectification in the charge pair mutant channels indicates the positive charge of G156R or G156K prevents aspartate from stabilizing an interaction with a polyamine that enters the pore.

Both Intra- and Intersubunit Interactions between G156R and N160D Occur in the Kir6.2 Tetramer. In the G156R/N160D mutant channels, restoration of ion conduction could be due to charge interactions within a single subunit or between two adjacent subunits. In the process of screening various Kir6.2 mutants with single or double charge mutations, we have made the intriguing observation that although individual G156D or N160R mutant Kir6.2 failed to give rise to measurable currents in the presence of SUR1 ($n = 10-15$ each; data not shown), co-expressing G156D and N160R Kir6.2 at a 1:1 cDNA ratio in the presence of SUR1 generated potassium currents inhibited by ATP and stimulated by LC-CoA (Figure 6). The observation suggests G156D and N160R from different subunits could interact to restore channel function. To test this idea directly, we constructed a Kir6.2 tandem construct in which a G156R mutation or a N160D mutation was placed in the same subunit (G156R/N160D) or in adjacent subunits (G156R-

N160D). Expression of mutant tandem constructs was judged by Western blots and formation of channel complexes with SUR1 judged by chemiluminescence assays and patch clamp recording (Figure 7, A and B). Voltage-ramp experiments were again employed to assess spermine-induced inward rectification in these tandem mutant channels. Previous studies have shown that the extent of inward rectification in K_{ATP} channels becomes more pronounced as the number of N160D-containing subunits in the Kir6.2 tetramer increases (Shyng S & Nichols CG, 1997). Because only one N160D mutation is present in our mutant tandem channels, the positive membrane potentials were extended to +150 mV to observe spermine-induced block. Comparing the current-voltage relationship of WT \times 4, G156R-WT \times 3, N160D-WT \times 3, G156R/N160D-WT \times 3, and G156R-N160D-WT \times 2 tandem channels, it is apparent that the G156R and N160D arranged either in the same subunit or adjacent subunits exhibited less rectification than N160D-WT \times 3 channels at both 20 and 50 μ M spermine concentrations tested (Figure 7C). To better quantify the data, we calculated the current remaining in the presence of 50 μ M spermine as a fraction of the current observed in K-INT control solution at +150 mV. This analysis allows for correction of current deviation from WT \times 4 channels at positive potentials in K-INT control solution that are caused by the mutations themselves and not spermine (Figure 7D), as was observed previously by others (Lu & MacKinnon, 1995). This analysis revealed clearly that spermine-induced reduction in current is greater in N160D-WT \times 3 channels than in channels where G156R is present in the same or adjacent subunit (Figure 7E). These results led us to conclude that in the tetrameric Kir6.2 pore complex, G156R and N160D can form both intra- and intersubunit interactions to affect channel conduction.

Characterization of Gating Properties of Charge-pair Mutant Channels. Having observed restoration of potassium conduction in the charge-pair mutants

(G156R/N160D, G156R/N160E, G156K/N160D, and G156K/N160E) we sought to further characterize the gating properties of these channels. First, single channel recordings were made using symmetrical K-INT, 1 mM EDTA solution to assess single channel conductance. These experiments show that whereas the G156R/N160D mutant channels have single channel conductance (67 ± 1 picosiemens (pS)) close to WT channels (75 ± 2 pS), the G156K/N160D and G156K/N160E mutants have significantly reduced single channel conductance (18 ± 2 and 35 ± 3 pS, respectively; Table 1), suggesting the Lys-156 may interact with Asp-160 differently than Arg-156 to influence K^+ movement through the pore.

Next, we measured channel sensitivity to ATP. The ATP dose-response curves generated by fitting the data to a modified Hill equation (see the Figure 8 legend) gave IC_{50} values for WT (15.4 ± 2.5 μ M) and G156R/N160D (21.8 ± 4.3 μ M) that were not significantly different ($p > 0.05$; Figure 8A, Table 1). However, the G156K/N160D mutant did show significantly reduced ATP sensitivity with an IC_{50} of 47.7 ± 7.3 μ M ($p < 0.01$; Figure 8A), as did the N160D mutation alone ($IC_{50} = 102.0 \pm 17.1$ μ M, $p < 0.001$) as reported before (Shyng S et al., 1997). The ATP sensitivity of G156R/N160E and G156K/N160E was also measured, with IC_{50} values being 12.3 ± 1.7 and 7.2 ± 1.5 μ M, respectively; these values are close to the IC_{50} reported previously for N160E (17.7 μ M) (Shyng S et al., 1997). Because some G156R/N160D patches tend to run down quickly during exposure to different concentrations of ATP, quantification of the dose-response for this mutant is not as accurate as in WT. To circumvent this problem, we also compared the extent of channel inhibition at an ATP concentration close to the IC_{50} of the WT. In these experiments, inside-out patches were briefly exposed to 20 μ M ATP and a high concentration of ATP (1 mM) before the G156R/N160D mutant channels ran down significantly, and the residual activity during exposure was measured (Figure 8B).

G156R/N160D channels again showed similar levels of inhibition as WT, whereas G156K/N160D and N160D were both less inhibited. Finally, we examined the MgADP response of the G156R/N160D mutant channel, as this property is essential for physiological function of the channel in addition to proper conductance and ATP sensitivity (Nichols CG et al., 1996). The G156R/N160D mutant was stimulated to an extent comparable with WT channels (Figure 8C). These results show that the gating properties of G156R/N160D channels closely resemble those of WT channels and suggest they will sense metabolic changes similarly to WT channels.

DISCUSSION

Studies of K_{ATP} channel mutations identified in patients have significantly advanced our understanding of the structure-functional relationship of the channel and mechanisms by which mutations cause disease (Huopio et al., 2002; Ashcroft FM, 2005). In this work we have described the effect of a Kir6.2 mutation G156R on K_{ATP} channel function. We show that the mutation causes loss of channel function by eliminating K^+ conduction in homomeric mutant channels. Importantly, we demonstrate that the ion conduction defect caused by the G156R mutation can be suppressed by introducing a second mutation N160D at the inward-rectification controller site and that the resulting G156R/N160D channels exhibit nucleotide gating properties similar to WT channels. Moreover, using Kir6.2 tandem tetramer approach, we provide evidence that the interaction between G156R and N160D in the Kir6.2 tetramer can occur both within the same subunit and between two adjacent subunits. These findings have significant implications on not only the role of the Gly-156 residue in channel conduction and gating but also the spatial relationship of the inner pore helices. In addition, they illustrate how channel gating and

conduction properties can be manipulated by altering the chemical interactions of pore residues.

G156R as a Heterozygous Mutation and Implications for Disease Mechanism. In a previous large-scale study of heterozygous K_{ATP} channel mutations identified in congenital hyperinsulinism including G156R of Kir6.2, we have found that the mutant channel subunits tend to express well at the cell surface as homomeric channels (Pinney SE et al., 2008). It was suggested that these mutant channel subunits likely co-assemble with WT channel subunits to exert their gating effects in heterozygous patients. Our simulated heterozygosity and tandem tetramers studies provide evidence that this is indeed the case for G156R-Kir6.2. Under simulated heterozygous expression conditions, the activity of the ensemble heteromeric channels was significantly reduced (~40% of that observed in cells transfected with WT channel subunits only) but well above that expected if homomeric WT channels were the sole conducting species in the surface channel population (estimated to be ~6.25% assuming binomial distribution of heteromeric channels containing 0–4 WT subunits). We also showed that the ensemble heteromeric mutant channels exhibited a diazoxide response similar to WT channels. These observations are consistent with the clinical phenotype of the patients and provide a pathophysiological explanation for the G156R mutation where partial reduction of K_{ATP} channel activity would sustain a depolarized β -cell membrane potential base line compared with WT, leading to hyperinsulinemia and hypoglycemia. In addition, they suggest the G156R mutant subunit does not exert a complete dominant-negative effect in heteromeric channels, i.e. a single G156R in the Kir6.2 tetramer is insufficient to eliminate channel function, a notion directly supported by our result that concatenated Kir6.2 tetramer containing one G156R subunit forms ATP-sensitive potassium-conducting channels with SUR1. In tandem channels containing two G156R mutant

subunits, channel activity dropped precipitously to a negligible level, and in channels with more than two G156R subunits, ion conduction was completely absent. It should be acknowledged that although the tandem tetramer provides a useful tool to address the stoichiometric effect of the mutation on channel function, it does not completely recapitulate the behavior of channels formed by Kir6.2 monomers. For example, channels formed by SUR1 and the Kir6.2 tandem tetramer have overall reduced surface expression and reduced ATP sensitivity, as has been reported previously for channels formed by Kir6.2 tandem dimers or SUR1-Kir6.2 tandem heteromers (Shyng S et al., 1997; Clement JP et al., 1997; Lin YW et al., 2003). Thus, one cannot use the current amplitudes observed from the tandem tetramer constructs to predict the channel activity expected for simulated heterozygous expression of G156R.

Implication on the Structural Role of Gly-156 of Kir6.2 in K_{ATP} Channel Gating. The Gly-156 residue in Kir6.2 corresponds to a highly conserved central glycine found in most potassium-selective channels (Jiang Y et al., 2002, Rosenhouse-Dantsker & Logothetis, 2006). Based on comparison of crystal structures of bacterial potassium channels in the open or closed conformation, it has been proposed that the glycine provides a flexible hinge to allow TM2 to bend during gating (Jiang Y et al., 2002, Doyle DA et al., 1998). Although several subsequent structure-function studies seem to support this idea (Ding S et al., 2005; Jiang Y et al., 2003; Magidovich E & Yifrach O, 2004), it has become increasingly clear that such an interpretation might not apply to all potassium channels. Recent studies of a Kir3.4 channel have suggested that the corresponding central glycine does not play a hinge role in the pivoted bending of TM2 during gating; rather, the glycine residue, an amino acid lacking a side chain, appears necessary to prevent interactions with residues in its vicinity critical for gating (Rosenhouse-Dantsker & Logothetis, 2006, 2007). Our results that the functional defect

caused by the G156R mutation can be alleviated by a second site mutation, N160D, in the TM2 helix and that the resulting G156R/N160D channels show similar ligand-induced gating as WT are in agreement with the view that the central glycine does not play a necessary hinge role in K_{ATP} channel gating. In light of the findings presented here, an interesting and related question to address in the future is whether in Kir6.2 a lower glycine conserved in all Kir channels (G165 in Kir6.2) serves as a hinge as proposed by Kuo et al. (Kuo A et al., 2003) or the residue above the central glycine serves as the controller of TM2 bending as proposed for Kir3.4 (Rosenhouse-Dantsker & Logothetis, 2006).

Mechanisms by Which the N160D Mutation Restores Ion Conduction in G156R

Mutant Channels. Potassium channel pores conduct cations by stabilizing electrostatics in the low dielectric environment of the membrane (Roux & MacKinnon, 1999). Introducing fixed positive charges to the pore by G156R mutation in Kir6.2 would predictably destabilize cations within the central cavity. This could explain the complete absence of measurable conduction in G156R homomeric channels by cations with varying physical properties. On the other hand, introduction of a negatively charged side chain at a residue that faces the pore of Kir channels, for example N160D, can increase the binding rate and apparent affinity of oppositely charged molecules and ions; this is likely due to favorable electrostatics caused by an additional negative field that contributes greater positive charge stabilization (Kurata HT et al., 2004; Robertson JL et al., 2008). Such a stabilization effect could explain how N160D restores ion conduction and gating in the G156R background. In this case, the negatively charged side chain of aspartate at 160 helps stabilize the positively charged side chain of arginine at 156 to sequester the adverse effect G156R imposes on ion conduction. This interpretation is strongly supported by our results that inward rectification expected of the N160D

mutation is abrogated in the G156R/N160D mutant channels as one would predict if the negatively charged side chain of N160D is bound by the positively charged arginine to eliminate the strong binding site for spermine at positive potentials. That the G156R/N160E, G156K/N160D, and G156K/N160E charge pairs also yielded channels with measurable currents but attenuated inward rectification further support the idea that an electrostatic interaction occurs between the side chains of the substituted amino acids at these two positions. However, we note that rescue of channel function by introducing opposite charges into the K_{ATP} pore is position- and distance-dependent (Table 1); charge reversal at the two positions did not yield functional channels (but see discussion below), and substituting Ala-161 or the leucine one helical turn below Asn-160 with negatively charged amino acids failed to restore ion conduction in the G156R channel. Thus, it appears that the electrostatic environment immediately surrounding residue 156 would also affect the side chain orientation and its effect on ion conduction. Collectively, our data support the conclusion that a close electrostatic interaction between Arg-156 and Asp-160 is the mechanism underlying the restoration of ion conduction in the mutant channel. This mechanism is consistent with that proposed previously for a Kir3.4 channel in that the side chain of substituting amino acids at the equivalent central glycine can interact with residues in the vicinity, including those in the selectivity filter, the pore helix, and the TM2 helix (Rosenhouse-Dantsker & Logothetis, 2006, 2007). In particular, the side chain of a lysine at this position has been proposed to interact with a conserved threonine in the selectivity filter and an asparagine one helical turn down TM2. It would be interesting to determine in future studies if G156R in Kir6.2 also interacts with residues in the selectivity filter to interfere with channel function.

Somewhat surprisingly, we discovered that co-expression of two Kir6.2 mutants, G156D and N160R, which when individually expressed did not give rise to measurable currents,

recovered channel activity that was inhibited by ATP and stimulated by LC-CoA, characteristics of K_{ATP} channels (Figure 6). Because the two mutations are not in the same subunit, this observation indicates restoration of channel activity via intersubunit interactions between the two mutant residues. This conclusion is further substantiated by the tandem tetramer experiments in which spermine-induced inward rectification was used to probe the intra- versus intersubunit interaction between G156R and N160D. Our results that both G156R/N160D-WT \times 3 (same subunit) and G156R-N160D-WT \times 2 (neighboring subunits) tandem tetramer channels showed attenuated spermine-induced inward rectification compared with N160D-WT \times 3 channels support the notion that G156R and N160D can interact not only within the same subunit but also from adjacent subunits to affect channel behavior (Figure 7E). These results have the implications that the spatial arrangement of the inner pore helices must be such that the side chains of Arg-156 can form chemical interactions with Asp-160 in the same subunit as well as in the adjacent subunit. Curiously, the G156D/N160R combination in the same subunit did not restore channel activity (Table 1), suggesting that for this mutation pair, intersubunit interactions are favored. Future homology modeling and molecular dynamic simulation studies should take these implications into consideration.

Influence of the Chemical Environment of the Pore on Ligand-induced Gating.

Analysis of channel ATP sensitivity revealed subtle differences among the various charge-pair mutants. Although the G156R/N160D channels have ATP sensitivity very similar to WT channels, the G156K/N160D channels exhibit lower ATP sensitivity (IC_{50} ~3-fold higher than that of WT). The differences in gating between G156R/N160D and G156K/N160D suggest that although arginine and lysine share similar physical chemical properties, the structures of their side chains may impart differential interactions with aspartate. In this case, the arginine-aspartate interactions appear to suppress the effect

of individual mutations on gating more completely than the lysine-aspartate interactions, possibly because the arginine-aspartate pair interaction is more stable in the Kir6.2 TM2 structure. Variation in ATP sensitivity was further observed in the G156R/N160E and the G156K/N160E mutation combinations (Table 1). Although we do not yet have sufficient information to explain the gating property of the various mutants in molecular detail, the results from this study illustrate that gating properties of the channel are subject to changes in the chemical environment of the pore. From a medicinal chemistry point of view, our study leads us to speculate that it may be possible to manipulate the chemistry of a mutant Kir6.2 pore to restore channel gating by ATP and MgADP such that it will be physiologically functional, as we have shown for the G156R/N160D channels.

MATERIALS AND METHODS

Molecular Biology - Rat Kir6.2 cDNA is in pCDNA1/Amp vector and hamster SUR1 in pECE. Site-directed mutagenesis was carried out using the QuikChange site-directed mutagenesis kit (Stratagene), and the mutations were confirmed by sequencing. Mutant clones from two or more independent PCR reactions were analyzed to avoid false results caused by undesired mutations introduced by PCR.

Kir6.2 Tetramer Construction - The concatenated Kir6.2 tetramer design is shown in Figure 3A. A modified version of pCDNA1/Amp was generated by introducing a 5' Clal site into the multiple cloning sites of WT rat Kir6.2 pCDNA1/Amp using the QuikChange site-directed mutagenesis kit (Stratagene). This modified pCDNA1/Amp-Clal was used for the final subcloning to create the concatenated Kir6.2 tetramer and for expression in COSm6 cells. To generate individual subunits with appropriate linkers and 5' and 3' restriction sites for subcloning as shown in Figure 3A, the following PCR primer design

was employed. For subunit 1, a forward and reverse primer pair was used to generate a Clal site (underlined) at the 5' end and a 5xGln linker (parentheses) followed by a Nhel site (underlined) at the 3' end: forward (5'-TATAATCGATACTCTGCAATGAGGC-CCTAGGCCAAGCCAGTGTAGTGCC-3') and reverse (5'-ATATGCTAGC(CTGCTGCTGCTG)GGACAAGGAATCCGGAGAGATGC 3'). For subunit 2, a forward and reverse primer pair was used to generate an Nhel site (underlined) followed by a 5xGln linker (parentheses) at the 5' end and a 5xGln linker (parentheses) followed by a BamHI site (underlined) at the 3' end: forward (5'-TATAGCTAGC(CAGCAGCAGC-AGCAG)ATGCTGTCCCGAAAGGGCATTATCCC-3') and reverse (5'-ATATGGATCC(CTGCTGCTGCTGCTG)GGACAAGGAATCCGGAGAGATGC-3'). For subunit 3, a forward and reverse primer pair was used to generate a BamHI site (underlined) followed by a 5xGln linker (parentheses) at the 5' end, and a 5xGln linker (parentheses) followed by a Nhel site (underlined) at the 3' end: forward (5'-TATAGGATCC(CAGCAGCAGCAGCAG)ATGCTGTCCCGAAAGGGCATTATCCC-3 and reverse (5'-ATATGCTAGC(CTGCTGCTGCTGCTG)GGACAAGGAATCCGGAG-AGATGC-3'. For subunit 4, a forward and reverse primer pair was used to generate a Nhel site (underlined) followed by a 5xGln linker (parentheses) at the 5' end and an EcoRI site (underlined) at the 3' end: forward (5-TATAGCTAGC(CAGCAGCAGC-AGCAG)ATGCTGTCCCGAAAGGGCATTATCCC-3') and reverse (5'-ATATGAATTCCTGCAGCCCGACAAGTATCTTGTAACACCCCAGGCACACAGCGGC-3'.

PCR fragments were purified by gel extraction, digested with Clal and Nhel for subunit 1, Nhel and BamHI for subunit 2, BamHI and Nhel for subunit 3, and Nhel and EcoRI for subunit 4. Subunits 1 and 2 were ligated into an intermediate vector pJPA5, and subunits 3 and 4 were ligated into pJPA7 to generate dimers. Positive dimers were verified by sequencing and digested with Clal and BamHI for pJPA5 subunits 1 and 2 or

BamHI and EcoRI for pJPA7 subunits 3 and 4. The dimer fragments were then ligated into pCDNA1/Amp-ClaI to generate the final tetramer fusion constructs.

Western Blotting and Chemiluminescence Assay - Cell surface expression levels of mutant channels were assessed by Western blot and by a quantitative chemiluminescence assay using a SUR1 that was tagged with a FLAG epitope (DYKDDDDK) at the N terminus (fSUR1), as described previously (Taschenberger G et al., 2002). COSm6 cells grown in 35-mm dishes were transfected with 0.4 µg of rat Kir6.2 and 0.6 µg of fSUR1 using FuGENE 6® and lysed 48–72 h post-transfection in 20 mM HEPES, pH 7.0, 5 mM EDTA, 150 mM NaCl, 1% Nonidet P-40 with Complete Protease Inhibitors (Roche Applied Science). Proteins in the cell lysate were separated by 10% SDS-PAGE, transferred to nitrocellulose membranes, analyzed by incubation with appropriate primary antibodies followed by horseradish peroxidase-conjugated secondary antibodies (Amersham Biosciences), and visualized by enhanced chemiluminescence (Super Signal West Femto; Pierce). For chemiluminescence assay, cells were fixed with 2% paraformaldehyde for 30 min at 4 °C. Fixed cells were pre-blocked in phosphate-buffered saline (PBS) plus 0.1% bovine serum albumin (BSA) for 30 min, incubated in M2 mouse monoclonal anti-FLAG antibody for fSUR1 (10 µg/ml, Sigma) for 1 h, washed 4 × 30 min in PBS plus 0.1% BSA, incubated in horseradish peroxidase-conjugated anti-mouse secondary antibody (Jackson ImmunoResearch, Inc., 1:1000 dilution) for 20 min, and washed again 4 × 30 min in PBS plus 0.1% BSA. Chemiluminescence of each dish was quantified in a TD-20/20 luminometer (Turner Designs) after 10 s of incubation in Power Signal enzyme-linked immunosorbent assay luminol solution (Pierce). All steps after fixation were carried out at room temperature.

⁸⁶Rb⁺ Efflux Assay - COSm6 cells were plated onto 35-mm culture dishes and transfected with wild-type SUR1 and control or mutant rat Kir6.2 cDNA as described above. Cells were incubated for 24 h in culture medium containing ⁸⁶RbCl (1 μ Ci/ml) 2 days after transfection. Before measurement of ⁸⁶Rb⁺ efflux, cells were incubated for 30 min at room temperature in Krebs-Ringer solution with metabolic inhibitors (2.5 μ g/ml oligomycin and 1 mM 2-deoxy-d-glucose). At selected time points the solution was aspirated from the cells and replaced with fresh solution. At the end of a 40-min period, cells were lysed. The ⁸⁶Rb⁺ in the aspirated solution and the cell lysate was counted. The percentage efflux at each time point was calculated as the cumulative counts in the aspirated solution divided by the total counts from the solutions and the cell lysate (Dunne et al., 2004).

Electrophysiology - Patch clamp recordings were performed in the inside-out configuration as previously described (Lin YW et al., 2006). Briefly, COSm6 cells were transfected with cDNA encoding WT or mutant channel proteins as well as cDNA for the green fluorescent protein to help identify positively transfected cells. Patch clamp recordings were made 36-72 h post-transfection. Micropipettes were pulled from non-heparinized Kimble glass (Fisher) with resistance typically ~1-2 megaohms. The bath (intracellular) and pipette (extracellular) solution (K-INT) had the following composition: 140 mM KCl, 10 mM K-HEPES, 1 mM K-EGTA, pH 7.3. ATP and ADP were added as the potassium salt. For measuring ATP sensitivity, 1 mM EDTA was included in K-INT to prevent channel rundown (Shyng S et al., 1997). Unless specified, all currents were measured at a membrane potential of -50 mV (pipette voltage = +50 mV), and inward currents are shown as upward deflections. The MgADP or diazoxide response was calculated as the current in a K-INT solution containing either 0.1 mM ATP and 0.5 mM ADP or 0.1 mM ATP and 0.3 mM diazoxide (both with 1 mM free Mg²⁺) relative to that in

plain K-INT solution. When ATP sensitivity was reduced, base-line currents were obtained using 10 mM BaCl₂ block at +50 mV.

For spermine block measurements, holding potential was stepped from 0 to -100 mV (+100 mV membrane potential) for 30 ms, then ramped from -100 to +100 mV in 200 ms and stepped back to 0 mV for total recorded time of 1 s. In the tandem tetramer experiments shown in Figure 7, holding potential was stepped to -150 mV for 50 ms and ramped to 100 mV in 300 ms. Note in these experiments that control K-INT solution did not include EDTA.

To measure single channel conductance, currents were recorded using borosilicate glass (Sutter Instruments) electrodes coated with Sylgard and polished with a microforge (Narishige) to produce bath resistances of 8.0–12.0 megaohms. Currents were acquired at 100 kHz with an applied analog 4-pole Bessel filter with a cutoff frequency of 5-10 kHz. Recordings were filtered again offline using a gaussian or 8-pole Bessel filter with a cutoff of 2 kHz.

Data Analysis - Data were analyzed using pCLAMP software (Axon Instrument). Off-line analysis was performed using Microsoft Excel and Origin programs. Currents amplitudes in the voltage ramp experiments were averages of three consecutive voltage ramps and normalized to the most negative current amplitude (at -100 mV membrane potential). Statistical analysis was performed using the following. For current amplitudes, diazoxide and MgADP response, we used independent two-population two-tailed Student's t test; for ATP dose response and two-point estimation shown in Figure 8, A and B, we used one-way analysis of variance (ANOVA); for single channel conductance, we used both

one-way ANOVA and non-parametric Kruskal-Wallis tests (to test accuracy of significance with low data repetition).

Acknowledgments

We thank Dr. Yu-Wen Lin for data sharing, Dr. Thomas Baumann for use of glass electrode manufacturing equipment, and Dr. Qing Zhou and Emily Pratt for comments on the manuscript. We are grateful to the patients, the General Clinical Research Center staff, and the Children's Hospital of Philadelphia nurses.

Figure Legends

FIGURE 1. Characterization of G156R mutant channels reconstituted in COS cells.

A, shown are Western blots of SUR1 and Kir6.2 in cells transfected with cDNAs of fSUR1 (SUR1 that has been tagged with a FLAG epitope at the extracellular N terminus) and WT- or G156R-Kir6.2. fSUR1 was probed with anti-FLAG antibody, and Kir6.2 was probed with a rabbit antiserum raised against the C-terminal cytoplasmic domain of Kir6.2 (Lin YW et al., 2008). SUR1 was detected as a lower band (filled arrow), corresponding to the core-glycosylated form, and an upper band (open arrow), corresponding to the complex-glycosylated form. B, quantification is shown of cell surface expression of channel complexes using the chemiluminescence assay described under "Materials and Methods." The expression level of the mutant was shown as percent of that of WT channels. The error bar represents S.E. from four independent experiments. C, channel activity was assessed by inside-out patch clamp recordings. Top, the WT current trace shows the characteristic inhibition by ATP and activation by LC-CoA (oleoyl-CoA). Bottom, no currents were detected in cells expressing the G156R mutant. Recordings in this and the subsequent figures were made at -50mV, and inward

currents are shown as upward deflections. D, shown is a representative $^{86}\text{Rb}^+$ efflux experiment assessing K_{ATP} channel activity in untransfected cells or cells co-transfected with SUR1 and WT- or G156R-Kir6.2. Cells were treated for 30 min with metabolic inhibitors to activate K_{ATP} channels. Although WT channel activity was readily observed as $^{86}\text{Rb}^+$ efflux over time, the G156R mutant channels did not exhibit efflux above the background seen in untransfected cells.

FIGURE 2. Simulated heterozygous expression of G156R. COSm6 cells were transfected with G156R and WT Kir6.2 cDNA at a 1:1 cDNA ratio (denoted as WT:G156R) together with SUR1 cDNA to simulate heterozygous expression of the mutant Kir6.2 in patients. A, current density was estimated from isolated membrane patches using patch pipettes with closely matched sizes. Twenty-five patches each of WT- or WT:G156R-expressing cells from three-independent experiments were recorded. Top, shown are amplitude distributions of ATP-sensitive potassium currents (I). Bottom, shown is the averaged current amplitude normalized to that of WT-expressing cells. B, shown is a comparison of diazoxide response in channels recorded from WT- and WT:G156R-expressing cells. Top, representative current traces show the stimulatory effect of diazoxide. Patches were exposed to K-INT solutions containing differing concentrations of ATP or diazoxide, as indicated by the bars above the current traces. Free Mg^{2+} concentration in all solutions was ~ 1 mM. Bottom, shown is quantification of averaged diazoxide response. Channel activities observed in 0.1 mM ATP or 0.1 mM ATP + 0.3 mM diazoxide were expressed as the percent current of channel activity observed in K-INT solution (currents in 1 mM ATP were subtracted as background).

FIGURE 3. Analysis of Kir6.2 tandem tetramers containing 0–4 G156R mutant subunits. A, shown is a schematic of the concatenated Kir6.2 tetramer design (S1-4,

subunit 1-4; L1-3, linker 1-3). The detailed protocol for constructing the tetramer including primer information is provided under "Materials and Methods." B, shown is a Western blot of Kir6.2 monomer and various tandem tetramers expressed in COS cells. All cells were co-transfected with SUR1. Note in the Kir6.2 monomer lane that higher molecular weight bands likely representing oligomeric forms of Kir6.2 monomer are seen, as reported in previous studies (Lin CW et al., 2006). The tubulin blot was included as loading controls. C, chemiluminescence assays are shown comparing surface expression levels of channels formed in cells co-transfected with fSUR1 and Kir6.2 monomer or various Kir6.2 tandem tetramers (cDNA amount was adjusted to give an equal molar ratio for Kir6.2 monomer and tandem tetramers). D, shown is averaged patch current amplitude of the various Kir6.2 tandem tetramer channels expressed in COS cells. Each bar represents the mean \pm S.E. of 5-13 patches (as shown above the bar).

FIGURE 4. Restoration of ion conduction in G156R or G156K mutant channels by a second site mutation N160D. A, shown are Western blots of SUR1 and Kir6.2 in COSm6 cells co-transfected with cDNAs for fSUR1 and one of the following Kir6.2s: WT, G156R/N160D, G156K, or G156K/N160D. B, surface expression of various channels was quantified using the chemiluminescence assay described under "Materials and Methods." C, representative traces are shown of inside-out patch clamp recordings from cells expressing different mutant channels. In contrast to the G156R mutant shown in Figure 1C, ATP-sensitive currents were readily detected from cells expressing the G156R/N160D mutant. Some activation by LC-CoA was also apparent based on the slow inhibition by ATP after LC-CoA exposure. The G156K mutation also abolished channel activity, and this defect was similarly overcome by introducing the second mutation N160D. D, $^{86}\text{Rb}^+$ efflux assays show activation of the G156R/N160D and

G156K/N160D mutant channels by metabolic inhibition as seen for WT channels, albeit to a lesser extent likely due to differences in expression levels and gating properties (see also Figure 8 for ATP and MgADP responses). In contrast, no channel activity was detected for the G156K mutant, as with the G156R mutant shown in Figure 1.

FIGURE 5. The N160D mutation induces inward rectification on the WT- but not the G156R- or G156K-Kir6.2 background. COSm6 cells were transfected with cDNAs of SUR1 and one of the following Kir6.2s: WT, N160D, G156R/N160D, or G156K/N160D. Inside-out patches were subjected to a voltage-ramp protocol (membrane potential +100 to -100mV) in control K-INT solution or K-INT solution containing 20 μ M spermine. The pipette solution was K-INT. Representative experiments for each channel type are shown. Currents were normalized (Irel) to that seen at -100mV. Although currents from N160D channels were completely blocked by spermine at positive membrane potentials, little block was observed for WT, G156R/N160D, or G156K/N160D channels. Similar results were obtained from four experiments.

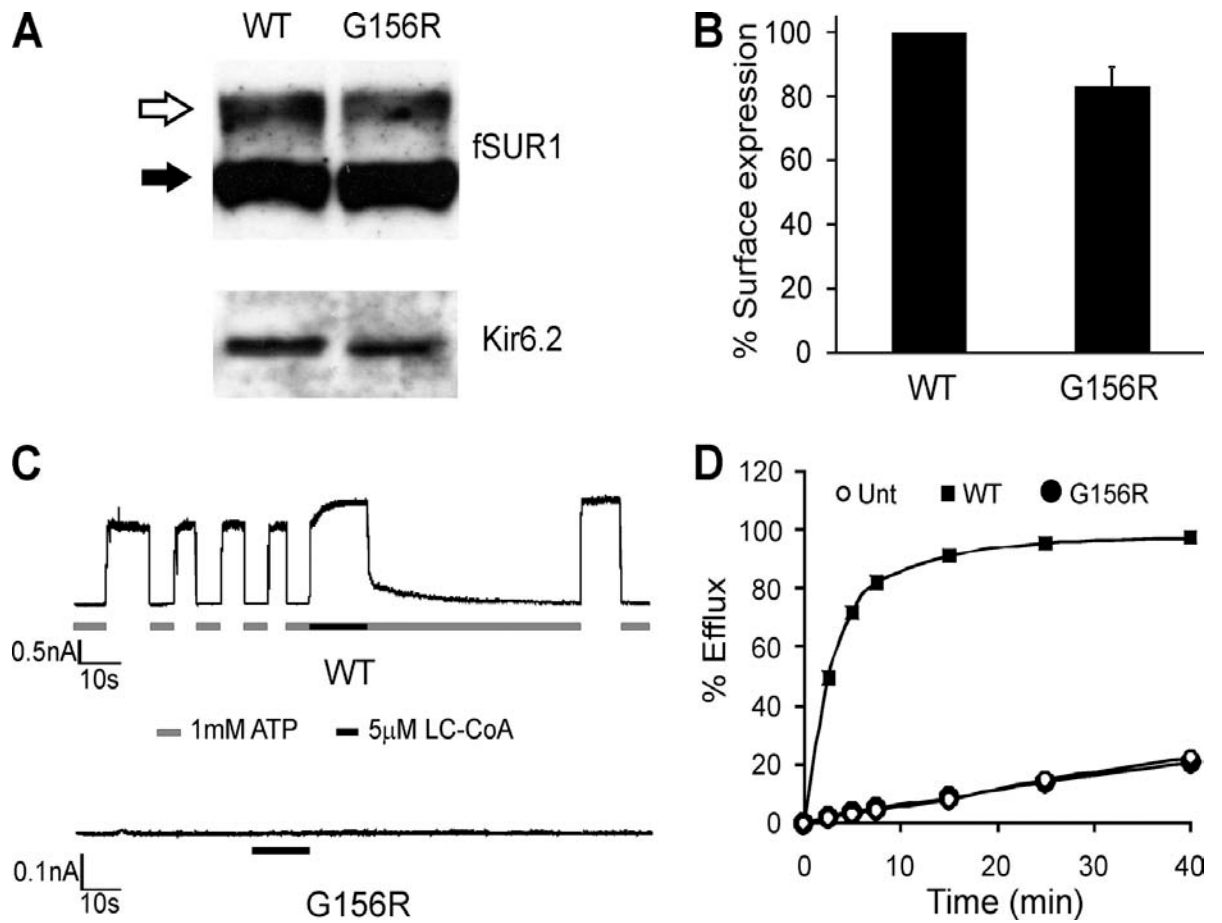
FIGURE 6. Evidence suggests functionally relevant intersubunit interactions between G156D and N160R. Shown is a representative inside-out patch clamp recording from COSm6 cells transfected with cDNA of SUR1 and a mixture of G156D Kir6.2 and N160R Kir6.2 at equal molar ratio. Patch was exposed to 1 mM ATP or 5 μ M oleoyl-CoA as indicated. Of note, neither G156D Kir6.2 nor N160R Kir6.2 alone generated measurable currents when co-expressed with SUR1 (n = 10-15; not shown) (Shyng S et al., 1997). Also, placing G156D and N160R in the same subunit failed to generate potassium currents upon co-expression with SUR1 (Table 1).

FIGURE 7. Intra- and intersubunit interactions between G156R and N160D in the Kir6.2 tetramer. A, shown is a Western blot of Kir6.2 monomer and various tandem tetramers expressed in COS cells. All cells were co-transfected with SUR1, and the tubulin blot was shown as the loading controls. B, chemiluminescence assay results show surface expression of the various mutant tandem tetramer channels, although at a much reduced level compared with channels formed by co-expressing SUR1 and Kir6.2 monomer. Note in this figure that GR denotes G156R, and ND denotes N160D. *GR/ND* refers to G156R and N160D in the same subunit, and *GR-ND* refers to G156R and N160D in adjacent subunits in the Kir6.2 tandem tetramer. C, inside-out patches containing various tandem tetramer channels were subjected to a voltage-ramp protocol (+150 to -100 mV) in control K-INT solution or K-INT solution containing 20 or 50 μ M spermine. Averaged current-voltage profiles of the channels (from four-six patches) are shown. Currents were normalized (*Irel*) to that seen at -100 mV. D, current of the various mutants at +150 mV in K-INT control solution was normalized to that of WT tandem tetramer (denoted as WT \times 4) at -100 mV in K-INT to show the spermine-independent difference caused by the mutations. E, Current observed at +150 mV in the presence of 50 μ M spermine for each channel was shown as the fraction of current observed at the same membrane potential in K-INT solution for the respective channel.

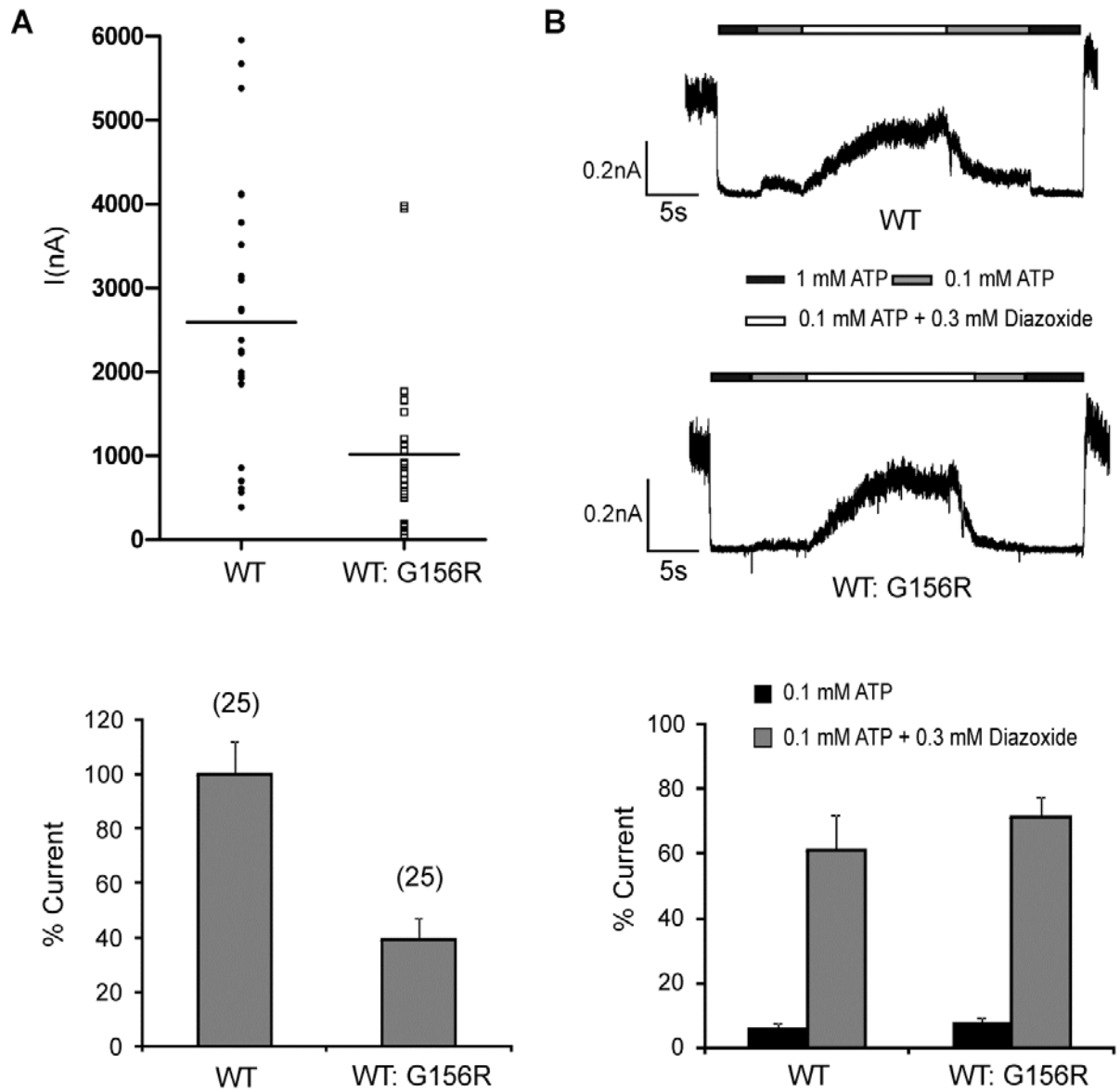
FIGURE 8. Nucleotide sensitivities of G156R/N160D charge-pair mutant channels.

A, ATP dose-response curves obtained by fitting the data points to the modified Hill equation ($I_{rel} = 1/(1 + ([ATP]/IC_{50})^H)$), where *Irel* is the current relative to that seen in the absence of ATP, *IC*₅₀ is [ATP] necessary for half-maximal inhibition of channel activity, and *H* the Hill coefficient. Recordings were made in K-INT/1 mM EDTA solution to minimize rundown (Lin YW et al., 2003). Error bars represent S.E. of 5–6 patches. The *IC*₅₀ values are as shown in Table 1. The *H* values are WT = 1.2 \pm 0.2, G156R/N160D =

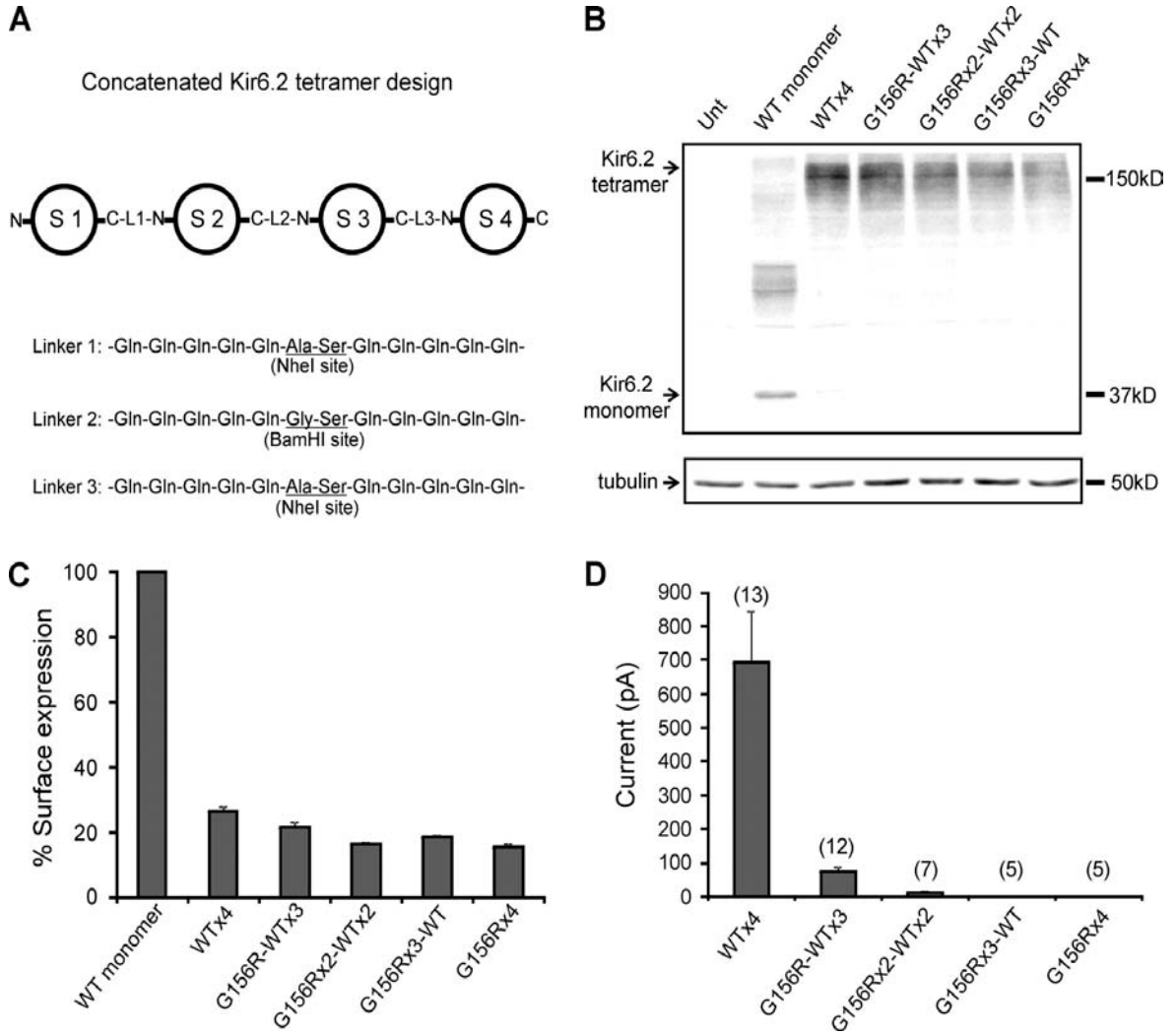
0.8 ± 0.2 , G156K/N160D = 1.2 ± 0.5 , and N160D = 1.4 ± 0.2 . B, ATP sensitivity was also assessed by comparing channel activity at 20 μ M ATP. The number of patches for each channel type is shown above the bars. There was no significant difference between WT and G156R/N160D ($p > 0.05$), but a significant difference was observed between WT and G156K/N160D or N160D ($p < 0.01$). C, left, representative traces of WT and G156R/N160D channels show channel response to MgADP. Patches were exposed to various concentrations of ATP and ADP as indicated by the bars above the recordings. Free $[Mg^{2+}]$ was 1 mM in all solutions. Right, quantification is shown of channel response to ATP and MgADP. Currents in 0.1 mM ATP or 0.1 mM ATP plus 0.5 mM ADP were normalized to currents in nucleotide-free solution. Again, there is no significant difference (6–7 patches) in MgADP response between WT and G156R/N160D ($p > 0.05$).



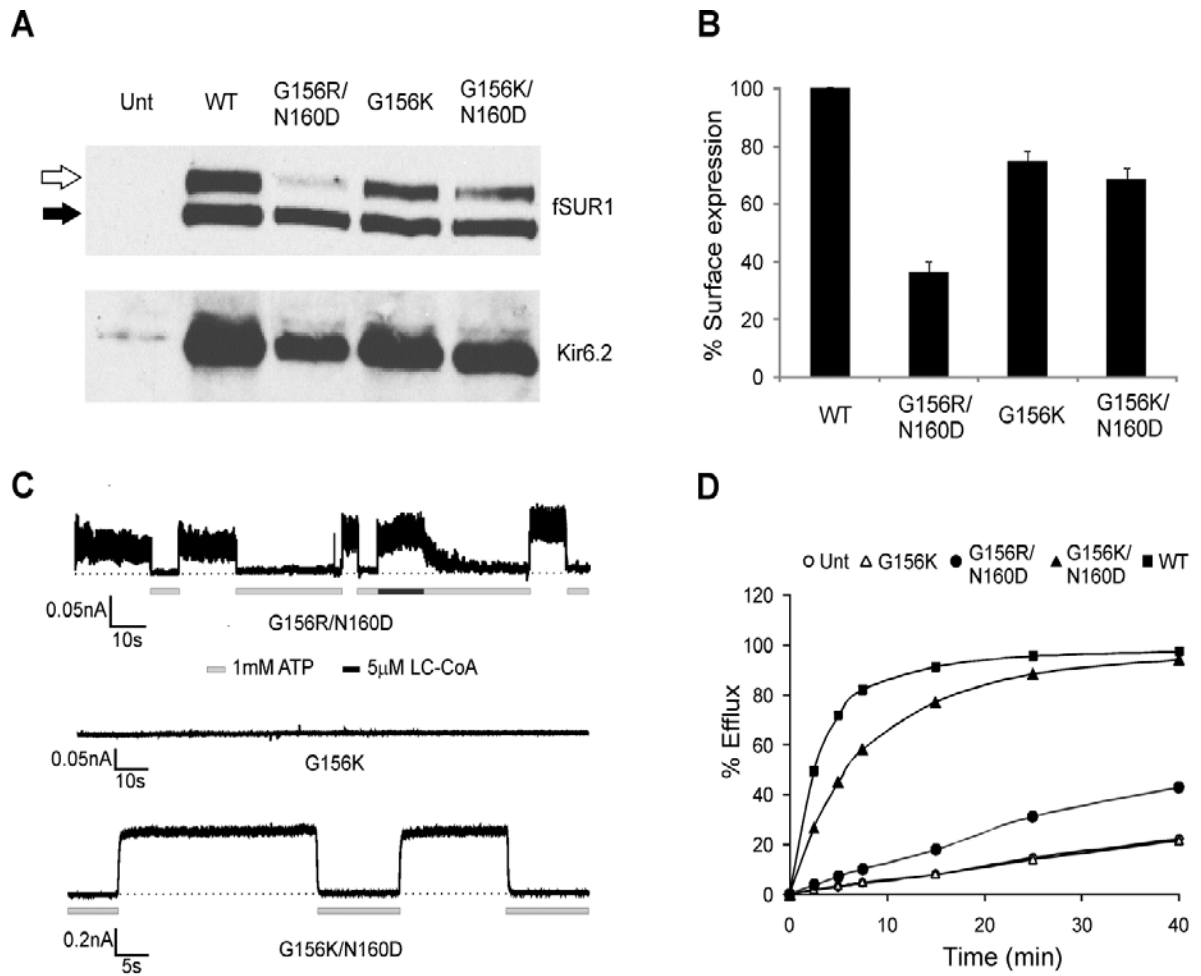
Chapter 1 Figure 1



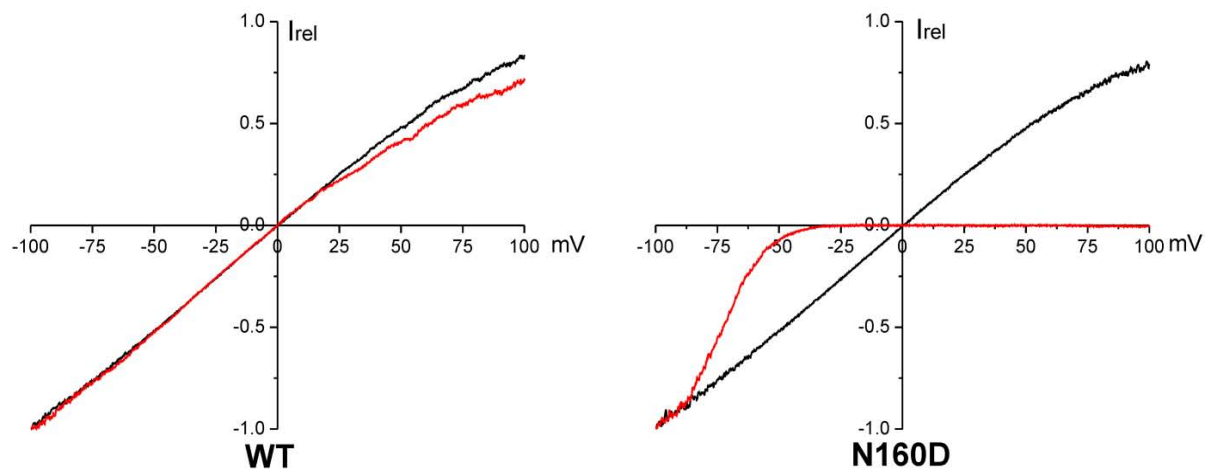
Chapter 1 Figure 2



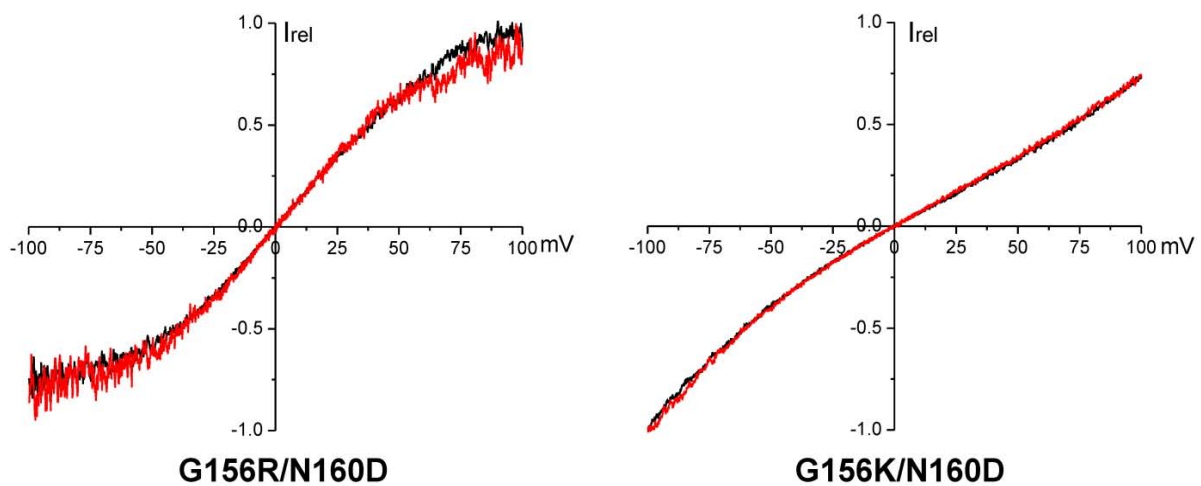
Chapter 1 Figure 3



Chapter 1 Figure 4

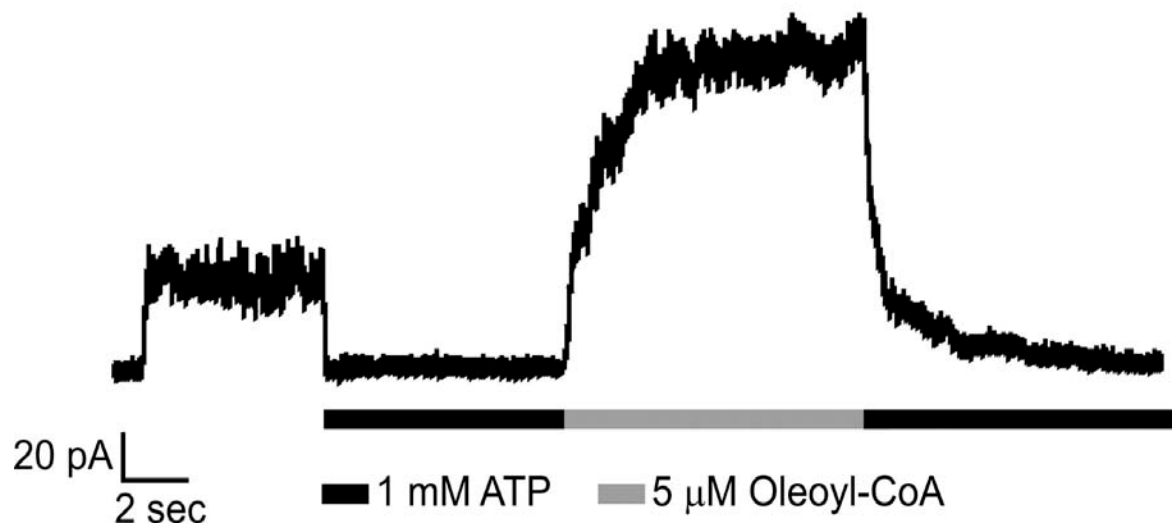


— Control
 — 20 μ M Spermine

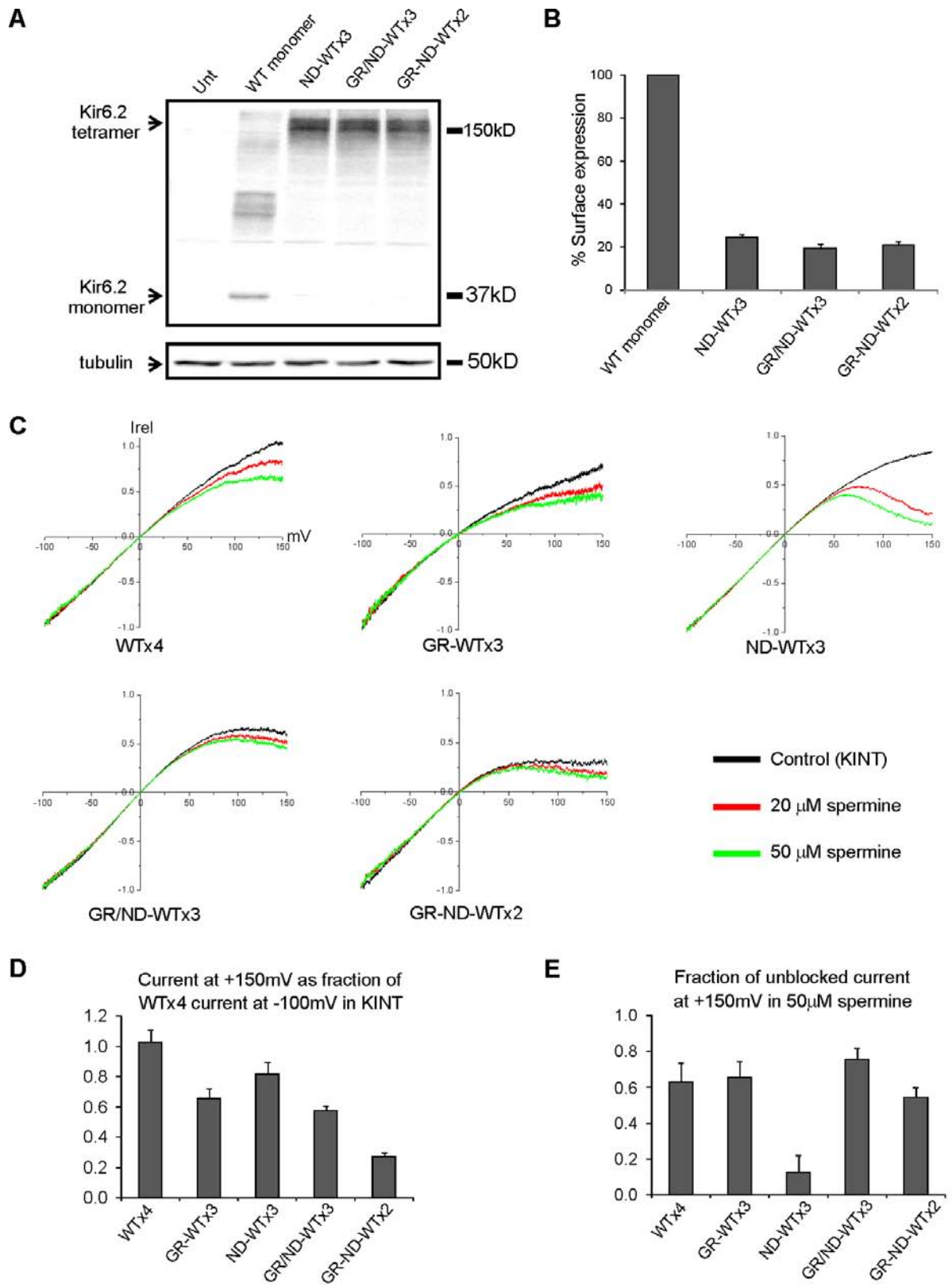


Chapter 1 Figure 5

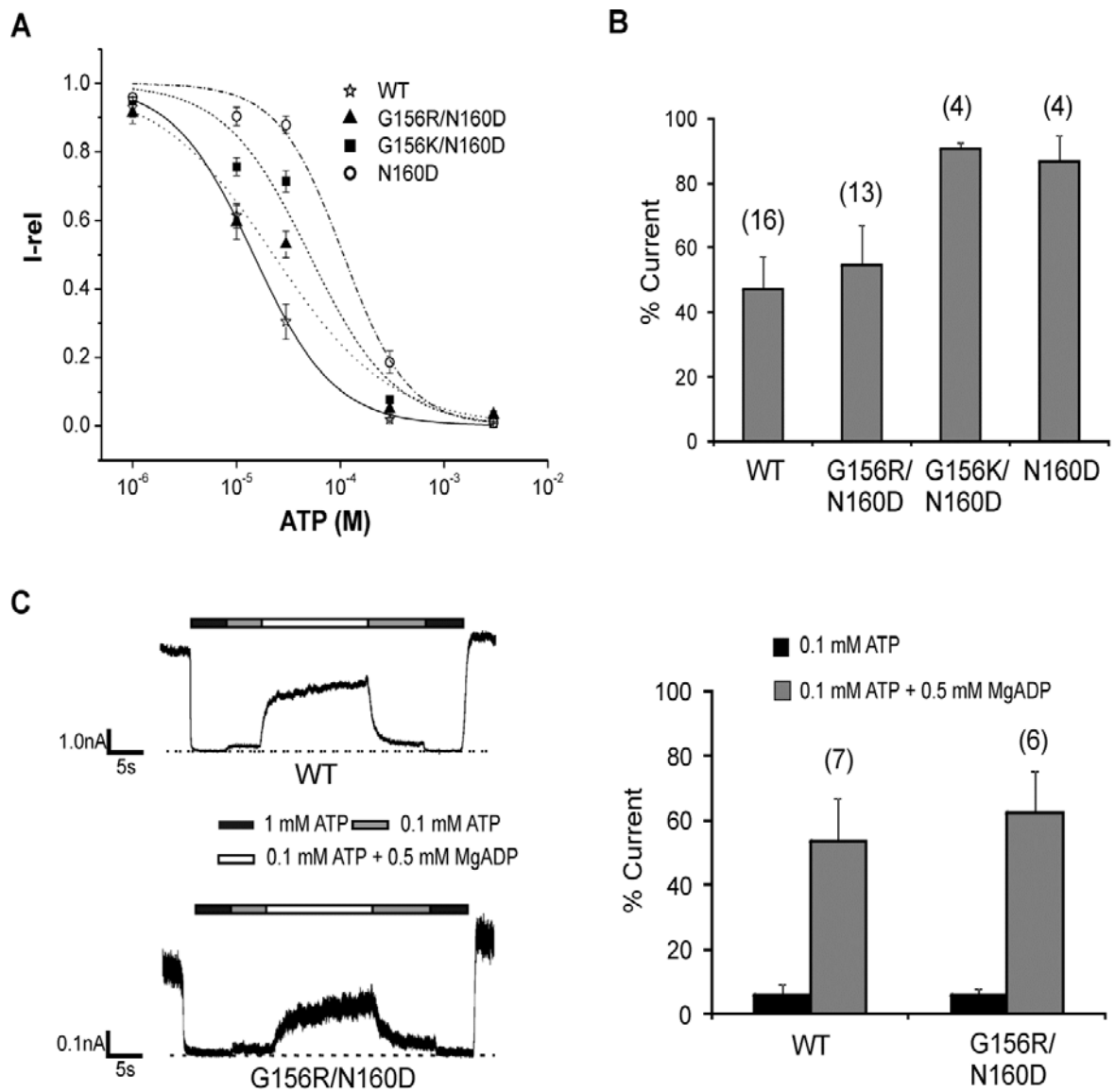
G156D Kir6.2 +N160R Kir6.2 at 1:1 cDNA ratio



Chapter 1 Figure 6



Chapter 1 Figure 7



Chapter 1 Figure 8

Chapter 1 Table 1

Mutant channel properties

Channel	Surface expression ^a %	Patch activity	ATP sensitivity (IC ₅₀) ^b μM	Single channel conductance ^c Picosiemens
WT	100	Yes	15.4 ± 2.5	75 ± 2
N160D	N.D. ^d	Yes	102.0 ± 17.1	~75 ^e
G156R/N160D	37 ± 4	Yes	21.8 ± 4.3	67 ± 1
G156R/N160E	29 ± 2	Yes	12.3 ± 1.7	76 ± 2
G156K/N160D	69 ± 4	Yes	47.7 ± 7.3	18 ± 2
G156K/N160E	38 ± 3	Yes	7.2 ± 1.5	35 ± 3
G156D/N160R	56 ± 8	No ^f		
G156D/N160K	ND	No		
G156E/N160R	ND	No		
G156E/N160D	ND	No		
G156R/A161D	ND	No		
G156R/L164D	ND	No		

^a The value represents the means ± S.E. of 4–10 chemiluminescence experiments.

^b ATP sensitivity was determined in K-INT solution containing 1 mM EDTA to minimize rundown; the IC₅₀ values, therefore, tend to be higher than in those reported in studies by others where no EDTA was included in the K-INT solution. The value represents the mean ± S.E. of 4–6 patches.

^c Values represent the averaged data of three recordings; error is S.E.

^d ND, values not determined.

^e Single channel conductance for N160D is from Shyng *et al.* (31).

^f From three-seven patches.

Chapter 2

K_{ATP} Channel Pore Mutant Inactivation Reveals Coupling between Transmembrane and Cytoplasmic Domains

Jeremy D. Bushman and Show-Ling Shyng

Chapter 2 is a manuscript in preparation. JD Bushman performed all of the experiments and authored the manuscript. JW Gay and E Olsen assisted with molecular biology.

Abstract

Spontaneous phosphatidylinositol-4, 5-bisphosphate (PIP₂)-dependent activity of ATP-sensitive potassium (K_{ATP}) channels underlies channel regulation by adenine nucleotides. Previous studies show interactions in the cytoplasmic domain of the channel are required to facilitate and maintain channel activation, and selective mutagenesis and disease mutations in this domain result in time-dependent channel inactivation. We report mutation of the central glycine in the pore-lining second transmembrane segment (TM2) to proline in K_{ATP} channels produces channel inactivation. Bath application and removal of Mg²⁺-free ATP, which binds the cytoplasmic domain of Kir6.2 and closes the channel, recover G156P channel activity. Unlike C-type inactivation, a consequence of selectivity filter closure in many K⁺ channels, the rate of inactivation in G156P channels was insensitive to changes in extracellular ion concentration or ion species fluxing through the pore. Instead, the rate of inactivation decreased with exogenous application of PIP₂ and increased when PIP₂-channel interaction was inhibited with neomycin. These findings are consistent with the mutation reducing the ability of PIP₂ to stabilize the open state of K_{ATP} channels, similar to mutations in the cytoplasmic domain that produce inactivation. When open state stability was increased by addition of a 2nd gain-of-function mutation, G156P inactivation was abolished. Uncovering inactivation by mutation of the transmembrane helices highlights a requirement for coupling between the Kir6.2 transmembrane and cytoplasmic domains that stabilizes the activated channel.

Introduction

Regulation of Kir channel activity by intracellular factors is of major physiological significance. K_{ATP} channels are members of the Kir channel family, and the pancreatic isoform contains four pore-forming Kir6.2 subunits surrounded by four modulatory sulfonylurea receptor (SUR) 1 subunits (Inagaki et al., 1995; Aguilar-Bryan L et al., 1995; Shyng S et al., 1998). K_{ATP} channels couple metabolic signals to potassium flux across cell membranes through their interactions with intracellular nucleotides. The dynamic motions that occur in K_{ATP} channels from ligand-binding during transitions between open and close states remain unclear. A novel yeast assay to identify gain-of-function mutations in the homologous G-protein coupled Kir (GIRK) channel found a proline mutation, S176P, adjacent to the central glycine in TM2 that produced constitutively open channels (Sadja et al., 2001). Prolines cause kinks in alpha helices adding anisotropic flexibility that could bias directionality of helix motions. A proline scan along TM2 of a G-protein-independent spontaneously-active form of GIRK channels led to alpha-helical periodicity in gain/loss-of-function effects above the HBC and complete loss of function below the HBC, in support of the HBC as gate regulated by the motions of TM2 (Jin et al., 2002). The reasoning was that increasing the size of the HBC with a proline kink increases channel activity, while narrowing the HBC reduces activity.

In Chapter 1, we examined the glycine hinge hypothesis and found that the TM2 helices do not require the central glycine for WT channel regulation by intracellular nucleotides. Potentially, TM2 could bend at several positions along the helix in order to open the helix bundle crossing (HBC) in K_{ATP} . To probe the nature of TM2 flexibility, we used prolines to scan regions of TM2 in Kir6.2 of K_{ATP} channels. In our initial test, the central glycine in Kir6.2 was replaced with proline and spontaneous activity was reduced similar to the

GIRK study. The standard method of excised inside-out patch electrophysiology used to measure spontaneous activity of K_{ATP} channels found a surprising effect in G156P channels caused by ATP. When patches were excised and mutant K_{ATP} channels were moved from the high intracellular nucleotide environment of the cell into bath nucleotide-free solutions, spontaneous ensemble channel currents increased and peaked followed by a time-dependent decay to low steady-state amplitudes. When patches were re-exposed to ATP followed by ATP removal, channel currents recovered and activated again near peak amplitudes demonstrating spontaneous G156P channel currents are no longer stable, and suggesting the channel inactivates.

Ion channel inactivation is a process in which the channel cannot achieve or sustain the open conducting state resulting in a closed channel pore for extended periods. Several mechanisms for inactivation in K^+ channels describe movement of channel structural elements that close the pore. In N-type inactivation, a ball-and-chain model proposes the intracellular polypeptide N-terminus of channel subunits enters and occludes the intracellular end of the pore blocking K^+ entry (Hoshi et al., 1990). Removal of the N-terminal fragment eliminates N-type inactivation. Another form called C-type inactivation involves closure of the extracellular region containing the selectivity filter. C-type inactivation is a time-dependent process that decreases channel currents due to stable closure of the selectivity filter, and its rate is modulated by altering interactions in the filter with mutation, by external ions, and in some cases by membrane potential (Kurata & Fedida, 2006). Permeant ions bind to the selectivity filter and influence conformational changes that lead to inactivation (Choi et al., 1991; Kiss et al., 1999; Cuello LG et al., 2010a). Ions that bind more tightly than K^+ with some K^+ channel filters, such as Rb^+ , slow channel closure and reduce inactivation rates (Swenson & Armstrong, 1984; Demo SD & Yellen G, 1992). A form of inactivation caused by mutations was previously

described in K_{ATP} channels. Residues such as E227, R301 and R314 in the C-terminal cytoplasmic domains important for Kir6.2 inter-subunit interactions reduce intrinsic PIP_2 -dependent channel activity when mutated (Lin YW et al., 2003; Lin YW et al., 2008). R301 is a disease mutation, and inactivation was sufficient to cause loss of function that would lead to the CHI clinical phenotype (Lin YW et al., 2008). In addition, the mutation E128W in the C-terminus of TMD0 domain in SUR1 also lead to channel inactivation, possibly through interference with PIP_2 -channel interactions (Pratt et al., 2011). Collectively, study of inactivation mutations suggest a model in which the Kir6.2 pore requires inter-subunit interactions at the interface of Kir6.2 and Kir6.2-SUR1 cytoplasmic domains to sustain its high spontaneous P_o . ATP binding to its site at the Kir6.2 subunit interfaces can recover interactions in the pore that facilitates re-entry into the conducting state. However, the structural mechanism by which the pore closes in K_{ATP} during inactivation is currently unknown.

A severe structural limitation placed upon the central glycine may limit dynamic TM2 movements in the Kir channel pore crucial to global conformational changes. As described in the thesis introduction, both the selectivity filter and HBC are putative gates in the transmembrane domain of Kir6.2 and either gate could be influenced by mutation of the glycine. What mechanism for G156P channel inactivation fits with the K_{ATP} channel gating model? Here we report characterization of the G156P inactivation phenotype. Inactivation was intrinsic to the Kir6.2 pore-forming subunits, and recovered with ATP exposure when SUR1 was present. The close proximity of the central glycine to the selectivity filter raises the possibility that the mutation interferes with selectivity filter gating and induces C-type inactivation. In contrast with a salient feature of C-type inactivation, the rate of diminishing current was not sensitive to the extracellular ion concentration or ion species conducting through the pore. Rather, the rate G156P

inactivation changed by manipulating channel interactions with PIP₂ and stabilizing the channel open state. Together, these observations show that mutation of the central glycine in TM2 causes loss of open state stability by disrupting K_{ATP} gating connected allosterically to ligand binding in the cytoplasmic domains of the channel. We interpret our findings in light of recent structural evidence towards a gating model that requires coupling between the transmembrane and cytoplasmic domains that facilitates stable K_{ATP} channel activation.

Results

Central glycine mutation in Kir6.2 inactivates K_{ATP} channels. In K⁺ solution conditions that abrogate channel current rundown, wild-type (WT) K_{ATP} channels produce relatively stable spontaneous current amplitudes reflecting an ensemble intrinsic channel Po of ~0.5 in an excised inside-out patch in the absence of nucleotides (Fig 1A). Previous reports identified K_{ATP} channel mutations that cause inactivation; upon channel activation by patch excision or removal of bath-applied ATP, currents decay in a time-dependent manner (Shyng et al., 2000; Lin et al, 2003, 2008; Loechner et al., 2011). Currents were recovered when the patch was exposed to ATP for periods between tens of seconds and minutes and then removed. We found that mutation of the central glycine in TM2 to proline (G156P) produces a similar rapid decrease in channel activity that re-activated with inhibition by ATP (Fig 1A). Reactivation shows that ATP binding to the cytoplasmic domain of the channel induces a conformational change that recovers the altered pore domain from the inactivated state. It is possible that mutation of glycine to proline produces an aberrant global Kir6.2 structure that disrupts interactions with SUR1. SUR1 elevates the Kir6.2 Po from ~0.1 to ~0.5, and interfering with Kir6.2-SUR1 coupling could lead to inactivation, as observed in E128W SUR1

mutant channels (Pratt et al., 2010). Kir6.2 cannot express at the cell surface without SUR1 shielding an ER retention signal (Zerangue et al., 1999). Truncated forms of Kir6.2 in the absence of SUR1 are able to traffic independently and form functional channels (Tucker et al., 1997). When transfected as the truncated form Kir6.2 Δ 36C G156P alone, patch excision of G156P Kir6.2 Δ 36C channels produced measurable current followed by inactivation (Fig 1B), evidence that the Kir6.2 pore is sufficient to produce inactivation. These currents were not recoverable with subsequent exposure to ATP, suggesting SUR1 is involved in mediating the ATP reactivation effect possibly by increasing the P_o and/or ATP sensitivity of the channel pore (Tucker et al., 1997). When Kir6.2 Δ 36C was co-expressed with SUR1, inactivated mutant channels were again re-activated.

The steady-state intrinsic activity of G156P channels was low; excised patches with seemingly small numbers of channels produced infrequent openings separated by long-lived periods of inactivity, although sparse bursts of activity were observed (Fig 1C). Single channel conductance estimated from patches containing multiple single channel amplitudes was \sim 74 pS, a value similar to our previous report for WT channels using identical conditions (Bushman et al. 2010), demonstrating the G156P mutation does not affect K^+ flux through the pore. Despite increased amounts of transfectant (see methods), current amplitudes in G156P channel patches were lower on average compared to WT channels and amplitudes measured from previous inactivation mutations (Fig 1A example; averaged data not shown). To determine if current amplitudes were due to reduced mutant channel surface expression, WT and G156P channels were transfected with equal amounts and labeled with a FLAG antibody that recognizes a FLAG-epitope tagged SUR1. SUR1 requires assembly with Kir6.2 into an octameric complex for export from the endoplasmic reticulum and trafficking to the

surface (Zerangue et al., 1999). Luminescence measured from immuno-labeled surface G156P channels was similar to WT (Fig 1D). Thus, reduced ensemble current amplitudes were not due to changes in conductance or channel expression, and may be a result of channel inactivation.

G156P inactivation does not exhibit properties of C-type inactivation. Mutation of glycine to proline is a severe change in the physical-chemical amino acid properties at that position. Substitutions at the central glycine of Kir channels are in close enough proximity to interact with the selectivity filter. Assuming the selectivity filter functions as a gate, we reasoned that the G156P inactivation phenotype may be a result of a stably closed selectivity filter, analogous to the mechanism of C-type inactivation. Although current mechanisms that describe C-type inactivation require specific interactions near the selectivity filter to stabilize a closed state (Raja, 2011), it is not untenable that changing the structure near the filter of K_{ATP} channels could disrupt a stable open and K^+ -conducting filter. For instance, Kir1.1b inactivation in low extracellular K^+ has increased sensitivity to the K^+ concentration when intersubunit salt bridges near the selectivity filter were mutated (Sackin H et al., 2009). A functional strategy could be utilized to probe inactivation in the absence of a detailed molecular picture of the Kir6.2 pore domain. We tested the salient C-type inactivation feature that the rate of current decay of inactivating channels depends on the conducting ion species and the external K^+ concentration.

To verify G156P channel currents consistently reach peak amplitudes that reproduce a similar inactivation rate, we first examined reactivation by ATP using a paired pulse protocol to verify the exposure time between activations could fully recover the prior current amplitude (Supplementary Fig 1A). Solutions were exchanged across the inside-

out patch using rapid perfusion (see Methods). G156P had a remarkably short reactivation time course, requiring only a 2 second exposure to ATP. All subsequent data presented used a > 5 second ATP exposure time. G156P recovery time course was markedly faster than cytoplasmic domain mutations recovery, which required much longer ATP exposure times (Supplementary Fig 1B; see Discussion for explanation). To coincide with previous studies which measured the inactivation rate during outward K^+ flux, we measured the time course of inactivation for several mutations using different command potentials in the same patch in equimolar potassium solution. Currents decayed to an initial plateau along a single exponential time course (Fig 2A). We note that in many cases the plateau steady-state currents continued to decrease or occasionally increase but rarely reached baseline, and optimal curve fits were obtained when the current initially plateaued. Using this fitting rationale, no significant difference was observed in the decay time constant between different membrane potentials for any of the inactivation mutations tested (Fig 2B). We also note that upon patch excision, current amplitudes started either at a low value that increased with subsequent exposures to ATP (Fig 4B top trace), or at a larger value that slowly ran down over time. ATP-recovered amplitudes were measured several times to verify the amplitude was reproducible.

We then measured the inactivation current decay of G156P channels under different ionic conditions and tested a second inactivation mutant channel, cytoplasmic Kir6.2 R314A. R314 forms a salt bridge between adjacent Kir6.2 cytoplasmic domains with E229 (Lin et al., 2003). Outward (+80 mV) current decay for both mutations did not vary under low or high K^+ conditions, or when K^+ was replaced with rubidium (Fig 3). Rubidium has decreased single channel conductance in WT channels, probably from binding more tightly than K^+ to the filter and should slow the C-type inactivation rate. The

results indicate G156P channels do not exhibit inactivation analogous to C-type inactivation, and may share a common mechanism with other K_{ATP} inactivation mutations.

G156P inactivation rate depends on PIP_2 -channel interaction. Phosphoinositides, in particular PIP_2 , are necessary for the intrinsic activity of Kir channels (Suh & Hille, 2008). If G156P mutation disrupts PIP_2 open state stability, then exogenous PIP_2 should enhance intrinsic activity after exposure to ATP. We exposed excised patches containing G156P channels to PIP_2 and the channel activator oleoyl co-enzyme A (LC-CoA). We found that both PIP_2 and LC-CoA stabilized channel activity, i.e. reduced or eliminated current decay, and increased peak current amplitudes during application after exposure to ATP (Fig 4A & B), in agreement with previous studies of K_{ATP} mutant inactivation (Lin et al., 2003). When membrane patches were excised, initial channel current varied in its amplitude. For example, in Figure 4A, patch excision led to an immediate increase in current amplitude indicating these channels were in a closed state ready for activation. In the top trace of Figure 4B, patch excision produced small current amplitudes that increased from several re-exposures to ATP, suggesting most of the channels initially occupied an inactivated state. Current amplitudes initially observed reflect the intracellular environment and current state the channels occupy at the outset of the experiment, and application of channel activators exposed to the patch push channel equilibrium from whatever initial conformational state channels occupy towards the open state. Upon washout, LC-CoA diffuses from the patch due to its higher water solubility compared with PIP_2 , resulting in an apparent decrease in peak amplitude and increase in inactivation rate. In addition, stable channel activation was frequently not sustained over longer exposures to LC-CoA (Fig 4B), and channel current increased little during LC-CoA application when channel currents inactivated to a steady-state level

(not shown). This is in marked contrast to other inactivating mutations, such as the intracellular domain mutation R192E, which activates to previous peak responses with applied LC-CoA after inactivation current decay plateaued (Fig 4B). G156P channels appear to have a severely reduced sensitivity to channel activators PIP₂ and LC-CoA.

If G156P channel inactivation is a consequence of decreased open state stability, and an increased membrane pool of PIP₂ favors the channel toward the open state, then inhibiting PIP₂ from binding with the channel would predictably decrease peak activation amplitudes and accelerate inactivation. To test this hypothesis, we perfused WT and inactivation mutant channel patches with neomycin, which reversibly inhibits PIP₂-protein interactions. Application of 5 μM and 20 μM neomycin increased inactivation in a dose-dependent manner, quantified as an increase in the normalized decay constant of a mono-exponential fit to the current decay (Fig 4C). R314A channel inactivation also increased with 20 μM neomycin (data not shown). Increased rates in the presence of neomycin suggest that channel closure caused by inactivation increases as a result of reduced apparent PIP₂ affinity. Collectively, the PIP₂ and neomycin results show that mutant channel sensitivity to PIP₂ determines the time-course of inactivation.

Gain-of-Function mutations stabilize inactivation. Numerous gain-of-function mutations in Kir6.2 and SUR1 cause neonatal diabetes (Hattersley & Ashcroft 2005). We tried to stabilize the inactivating channel in the open state by introducing transmembrane and cytoplasmic domain mutations shown to cause overactive K_{ATP} channels by increasing the open probability of the channel. Mutations from Kir6.2 N-terminal cytoplasmic domain (V59G), the second transmembrane lining segment (N160D, L164P, C166S), G-loop in the C-terminal cytoplasmic domain (I296L), and TMD0 of SUR1 (F132L) were placed in a Kir6.2 G156P background (Fig 5B). Inside-out

excised patch recordings at +50mV membrane potential produced stable outward currents that were blocked completely with 10mM BaCl₂ for most mutations (Fig 5A). Currents were blocked by 10mM ATP similarly to channels that only contain gain-of-function mutation; low channel current amplitudes (Figure 5A) could be due in part to reduced surface expression of the second mutation. These results show that inactivation is overcome by shifting the closed-to-open equilibrium dramatically towards the open state, much like the effect of increasing membrane PIP₂ concentrations. However, the double mutations Kir6.2 G156P/N160D and Kir6.2 G156P + SUR1 F132L still inactivated with a rate similar to G156P alone (data not shown). Exceptions to rescue by mutations were explained by considering the reduced ATP sensitivity of the mutation, which is an indirect effect of increased channel P_o (Figure 5C). Gain-of-function mutations with higher ATP sensitivity were not able to rescue the inactivation, reflecting a lower degree of enhancement in open state stability.

Discussion

K⁺ channel inactivation results in closure of the ion conduction pathway during channel activation. The pore may close at a narrow location that acts as a gate, for example during C-type inactivation at the selectivity filter. TM2 lines the transmembrane permeation pathway of K⁺ channels and several K⁺ channel gating models propose the TM2 segments function as the activation gate by opening and closing the bundle crossing (Doyle et al., 1998; Perozo et al., 1999; Jiang et al., 2002; Kuo et al., 2003; Kuo et al., 2005; Ader et al., 2008). It has also been proposed, and discussed in the thesis introduction, that the bundle crossing is the “ligand-sensitive” gate in K_{ATP}, responding to signals from ATP and PIP₂ binding (reviewed in Nichols, 2006). PIP₂ binds with the Kir6.2 cytoplasmic domains to stabilize channel gating in the open conducting state.

ATP binds to the same domains to stabilize the closed non-conducting conformation. Thus, intracellular ligands binding to the cytoplasmic domain induce a conformational change that leads to propagation of an activation or inhibition signal to the channel pore TMs. Our data show inactivation induced by mutation of TM2 was strongly dependent on PIP₂-channel interactions suggesting the mutation disrupts allosteric crosstalk between the CTDs and TMs (Figure 4). Taken together, our findings provide functional evidence supporting K_{ATP} gating models of a conformational pathway linking the TM and CTD interface critical for maintaining stable channel activation.

Absence of C-type Inactivation. Voltage-gated potassium (Kv) channels and the prokaryotic KcsA channel also contain two gates at the bundle crossing and filter, and both channel types exhibit C-type inactivation. Structural changes in the selectivity filter during C-type inactivation affect its relationship with permeant ions (Choi et al., 1991; Kiss et al., 1999; Cuello LG et al., 2010a). The model for C-type inactivation is a rearrangement of local interactions within and in close proximity to the selectivity filter leading to a non-conducting filter conformation. The inactivation process in KcsA is thought to be directly coupled to the opening of the activation gate at the bundle crossing (Cuello LG et al., 2010a), and mutations near the filter in the transmembrane lining helices can influence selectivity filter closure (Cuello LG et al., 2010b). Our observations that the G156P inactivation rate did not change when voltage, extracellular and permeating ionic conditions were varied (Figures 2 & 3) suggest that current models of C-type inactivation do not explain the inactivation observed in mutant K_{ATP} channels. Our conclusion is consistent with specific interactions in the extracellular pore-loop and between the pore-loop and TMs maintaining the stability in the filter. Stability in the selectivity filter in Kir channels may persist from a combination of local interactions and concerted global motions in the TMs that maintain the conductive filter conformation

during the activation process. In agreement with an intact TM architecture, K⁺ single channel conductance was the same in G156P channels and WT channels (Figure 1C), arguing flux along the length of the ion conducting pathway is unchanged. In addition, trafficking of G156P channels to the surface was also like WT as expected if folding and biogenesis were unaffected by physical association of subunits (Figure 1D).

Inactivation corresponds to recovery of PIP₂ interactions by an ATP-induced conformational change. Ligand binding-to-channel gating transduction is a reversible process, and mutations altering any component of binding/transduction/gating would affect the entire allosteric pathway. If TM2 moves dynamically to open and close the bundle crossing in response to PIP₂, it would be expected that mutations which inhibit TM2 movements also affect PIP₂ sensitivity. Proline mutation of the glycine likely kinks the helix in a direction unfavorable for TM2 bending into the open state, consistent with previous study of GIRK channels (Jin et al., 2002). The inactivation phenotype emerges by shifting channel equilibrium away from the PIP₂-bound open state towards the closed/inactivated state. G156P mutation destabilizes the open state and/or enhances stability of a long-lived inactivation state. G156P channels often produced small current amplitudes at excision and amplitudes grew in response to subsequent ATP exposures (Figure 4B Top), suggesting that these channels predominately occupied the inactivated state at patch excision. Membrane PIP₂ and cytosolic ATP concentrations will vary from cell to cell, and even small differences could lead to large variation in the initial state channels observe when a patch was excised depending on the sensitivity of inactivation to different channel ligands. LC-CoA reduced G156P channel inactivation after recovery by ATP but generally did not eliminate it or increase channel currents, also consistent with inactivation that had weaker sensitivity to stimulation compared to cytoplasmic domain mutant channels (Figure 4B). The strength of inactivation and its effect on

ligand sensitivity would depend on how the mutation disrupts components that stabilize the activation pathway. Cytoplasmic domain mutations might only interfere with the intersubunit interactions they specifically form, whereas distortion of the TM2 helix could compromise multiple locations of the structure involved in the activation pathway. Nevertheless, gain-of-function mutations that enhance open state stability abolish G156P inactivation regardless of the region in the structure we placed the mutation (Fig 5). Many of these mutations were previously shown to increase apparent PIP₂ affinity, and the degree to which the mutation biases the channel equilibrium in favor of the open state indicated indirectly by channel sensitivity to ATP determines whether the channel inactivates.

ATP binding to the mutant inactivating channel recovers closed channels into a state that will access the open state before inactivating. The effect of ATP on G156P channel recovery may be a consequence of biasing the channels into conformations that readily transition to the open channel state. Through mass action ATP would pool channels into ATP-bound closed states away from the inactivated state; thus when ATP is removed, channels could transition through the unbound closed state to briefly occupy the open state. ATP is normally quite high in the cell (mM range), and channels would predominately occupy ATP-bound closed states facilitating channel activation upon patch excision. An inactivation mutation that alters the CTDs directly might affect the ATP binding site and would likely slow down recovery of channels from inactivation. The ATP binding site located further away from the conduction pathway would be largely intact in G156P channels. Recovery could involve small movements between TM and CTD domains when ATP acts to close the channel, producing a faster recovery time than mutations required to stabilize the CTDs or Kir-SUR interactions. This prediction was consistent with the faster kinetics of G156P channel recovery from inactivation with

ATP compared to other CTD mutations that produce inactivation (Supplemental Fig 1). Considering the expected structural location of ligand binding sites, we acknowledge an alternative possibility that the close proximity of PIP₂ and ATP sites could cause ATP binding to rearrange the CTDs and the PIP₂ binding site. ATP binding would reset misalignment of TM and CTD residues that interact with PIP₂ by a global rearrangement into a favorable conformation for PIP₂ to rebind upon removal of ATP.

G156P Inactivation Model: disrupting functional link between TMs and CTDs.

What specific conformation of the channel might the inactivated state in the quantitative model represent? Large conformational changes in the cytoplasmic domain observed in recent Kir channel structures suggest the inactivated state may involve the CTDs. Direct physical interactions between the N- and C-terminal cytoplasmic domains of Kir6.2 subunits are important for channel gating (Jones et al., 2001). CTD interactions also appear to be important in other Kir channels; intersubunit interactions that regulate pH-dependent gating were found in Kir1.1 and Kir4.1/5.1 channels (Casamassima et al., 2003; Leng et al., 2006). A slew of crystal structures of the bacterial homologues Kirbac1.1 and 3.1 identify a large scale rotation in the CTDs relative to the TMDs (Clarke et al., 2010). Surface contacts that form salt bridges between C-terminal CTDs in a “latched” state reorganize to form new interactions that stabilize an “unlatched” state. Reconfiguring interactions will contribute to the free energy of the closed-to-open allosteric transition if these states are involved in channel activation. If latched or unlatched states are inherently unstable, perhaps due to local distortions at the CTD interface, the channel would briefly trap into a local minimum along the energy landscape of the transition. The hypothesis is supported by the fact that most inactivating mutations previously identified locate in the CTDs; inactivating mutations R314 and E229 appear to form a salt bridge, and charge reversal or crosslinking

stabilizes channel activation (Lin et al., 2003). The Clarke study saw an additional conformational state in which the N-terminal cytoplasmic “slide helix” moves to interact with the C-terminal CTDs and form a new “twist” state. Intriguingly, in these structures the density in the selectivity filter was reduced suggesting the filter exhibits a non-conductive configuration. The structural bridge formed between the slide helix attached to TM1 and the adjacent subunit’s C-terminal CTD links the CTDs to the TMDs. In summary, the structures suggest CTD domains undergo significant changes in conformation that are correlated with changes in the TM domain, specifically the selectivity filter. Previous functional studies suggest a mechanism for K_{ATP} channel inactivation where mutations disrupt contacts between adjacent subunit CTDs of the Kir6.2 tetramer or with companion SUR1 (Lin et al., 2003; Lin et al., 2008; Pratt et al., 2011). Since the ATP binding pocket locates at the interface of CTDs, ATP binding could induce a conformational change that re-engages subunit contacts or reprimed the CTDs into a conformation ready for activation. Thus, the collective structural and functional evidence implies a model in which the CTDs have dynamic properties important for ligand-sensitive gating.

We summarize G156P inactivation with the model illustrated in Figure 6, where transduction forces which open the gate propagate through a conformational pathway at the TM and CTD interface, rather than isolated to the TMs or CTDs. Conformational restriction placed on TM2 attenuates coupling between the TM and CTD domains and leads to channel inactivation. PIP_2 binding or gain of function mutations stabilize the channel in the open state to prevent inactivation, and ATP binding induces conformational changes in the CTDs that transiently recover the functional link between Kir6.2 TM-CTD domains priming channels for activation. Although TM2 and the C-terminal domain are a continuous polypeptide, the region in red indicated in the model

denotes a hypothetical coupling “linker” between the two domains. Further study will be necessary to identify protein regions at the TM-CTD interface important for the coupling interaction.

Materials and Methods

Molecular Biology—Rat Kir6.2 and hamster SUR1 cDNAs were in pUNIV vector to enhance surface expression (Venkatachalan et al., 2007). Mutagenesis was performed using QuikChange site-directed mutagenesis kit (Stratagene), and mutations confirmed by sequencing. Mutant clones from two or more independent PCR reactions were analyzed to avoid false results caused by undesired mutations from PCR.

Chemiluminescence Assay—Cell surface expression levels of WT and mutant channels were assessed by a quantitative chemiluminescence assay using a SUR1 that was tagged with a FLAG epitope (DYKDDDDK) at the N-terminus (fSUR1), as described previously (29). Cells were fixed with 2% paraformaldehyde for 20 min at 4°C. Fixed cells were pre-blocked in phosphate-buffered saline (PBS) plus 0.1% bovine serum albumin (BSA) for 30 min, incubated in M2 mouse monoclonal anti-FLAG antibody for fSUR1 (10 µg/ml, Sigma) for 1 h, washed 3 x 20 min in PBS plus 0.1% BSA, incubated in horseradish peroxidase-conjugated anti-mouse secondary antibody (Jackson ImmunoResearch, Inc., 1:1000 dilution) for 25 min, and washed again 4 x 30 min in PBS plus 0.1% BSA. Chemiluminescence of each dish was quantified in a TD-20/20 luminometer (Turner Designs) after 10 s of incubation in Power Signal enzyme-linked immunosorbent assay luminol solution (Pierce). All steps after fixation were carried out at room temperature. Signal-to-noise averaged ~9 : 1 for WT channels : background.

Electrophysiology—Patch clamp recordings were performed in the inside-out configuration. COSm6 cells were transfected with cDNA encoding WT or mutant channel proteins as well as cDNA for the green fluorescent protein to help identify positively transfected cells. Patch clamp recordings were made 36–72 h post-transfection. Micropipettes were pulled from non-heparinized Kimble glass (Fisher) with resistance 0.5–2 megaohms. The bath (intracellular) and pipette (extracellular) solution K-INT had the following composition: 140 mM KCl, 10 mM K-HEPES, 1 mM K-EGTA, 1 mM K-EDTA, pH 7.3. EDTA was included in all solutions to prevent channel rundown. ATP was added as the potassium salt (Sigma-Aldrich). For ion substitution experiments, KCl was replaced with either 5mM KCl 135mM NMDG, 300mM KCl, or 150mM RbCl. Command potentials varied and are stated in the figure legends as membrane potential (negative of command potential in inside-out patch). When ATP sensitivity was reduced, base-line currents were obtained using 10 mM BaCl₂ block at +50 mV membrane potential. To achieve rapid perfusion, a home-made piezo-driven device was used to move a theta pipette flowing KINT and KINT + ATP solutions on an excised patch. Open-tip current response 10-90% rise times to high versus low K⁺ solutions was less than 5 ms, whereas WT and mutant K_{ATP} channel patch current rise times were typically 50-100 ms (data not shown), consistent with previous rapid perfusion measurements (Baukrowitz T et al., 1998). Slow-to-form membrane patch seals with >200 ms rise times coincided with observing highly variable inactivation rates within the same patch, and these data were discarded. Some patches (for all of the mutations tested) never consistently re-activated with ATP, with peak currents decreasing by >95% within 1 minute. This phenomenon is likely due to channel rundown that was not prevented by solution conditions, which occasionally was observed in WT channels as well, and these patches were also discarded from analysis. To measure single channel conductance, currents were recorded using borosilicate glass (Sutter Instruments) electrodes coated

with Sylgard and polished with a microforge (Narishige) to produce bath resistances of 8.0–12.0 megaohms. Currents were acquired at 50 kHz with an applied analog 4-pole Bessel filter with a cutoff frequency of 5–10 kHz. Recordings were filtered again offline using an 8-pole Bessel filter with a cutoff of 2 kHz prior to analysis and presentation.

Data Analysis—Data were analyzed and displayed using pCLAMP software (Axon Instruments), Microsoft Excel and Origin programs. For Supplementary Figure 1, 2-3 trials for each interval in the same patch were tested. To account for rundown observed in patches despite presence of EDTA due to the long ATP exposures needed to re-activate several mutant channels, the plotted values were calculated as (Peak amplitude of 2nd activation) / ((Peak of 1st activation within trial + Peak of 1st activation from next trial) / 2). Statistical analysis was performed using the following: for current amplitudes, we used independent two population two-tailed Student's t test; for ion substitution and neomycin sensitivity comparisons, we used one-way analysis of variance (ANOVA) with Tukey posthoc test.

Figure Legends

Figure 1. Inactivation Phenotype of G156P Channels. (A) Sample traces of voltage clamp inside-out patch recordings containing Kir6.2 WT or G156P mutant channels. Dashed lines show current baseline. (B) Sample traces of Kir6.2 G156PΔ36C alone or co-expressed with SUR1 (n=4 and 5 patches, respectively). In A and B, membrane potential was -50mV. (C) Sample traces of inside-out recordings at -80mV from one (WT) or several (G156P) channels. Dark gray bar denotes region displayed with increased time resolution. On the right, a representative current-voltage relation for G156P single channel amplitudes. Values are the mean of gaussian fits to identifiable

peaks in an amplitude histogram for a given potential ($n = 7$ patches). Conductance is measured from slope of the line. (D) Surface expression measured from quantitative chemiluminescence assay; see methods for details.

Figure 2. Inward and outward currents inactivate at a similar rate. (A) G156P channels were re-activated in an inside-out patch switching from KINT with 3 mM ATP to KINT alone at different membrane potentials. Current traces from the same patch were fit with a mono-exponential decay function (gray line). (B) Summary graph of mean lifetime of current decay fits ($\tau \pm$ SD) for different inactivation mutations. Previously characterized mutations R192E (Lin et al., 2003), R301C (Lin et al., 2008), and R314A (Lin et al., 2003) are located in the cytoplasmic domain (each mutation $n = 5-10$ patches).

Figure 3. Varying ion concentrations or species does not change the inactivation rate. *Top*, sample traces from different G156P and R314A channel inside-out patches using symmetrical 150mM K^+ , 5mM extracellular/150mM intracellular K^+ , or symmetrical 150mM Rb^+ ion conditions. *Middle*, plot of current decay time course under different conditions normalized to the peak currents. *Bottom*, Summary bar plot of mean lifetime $\tau \pm$ SD for different ion conditions tested (quantities are mM concentration). Pipette solution is the extracellular solution. Currents recorded at a +80mV membrane potential. Number of patches for each condition is shown above bar in brackets.

Figure 4. G156P inactivation rate is PIP_2 sensitive. (A) Sample trace of G156P channels reactivated by 5 mM ATP into KINT or KINT with 5 μ M PIP_2 . (B) Sample traces of G156P or R192E channels exposed to ATP to recover activity followed by either KINT or KINT with 5 μ M oleoyl co-enzyme A. G156P channel current decayed in

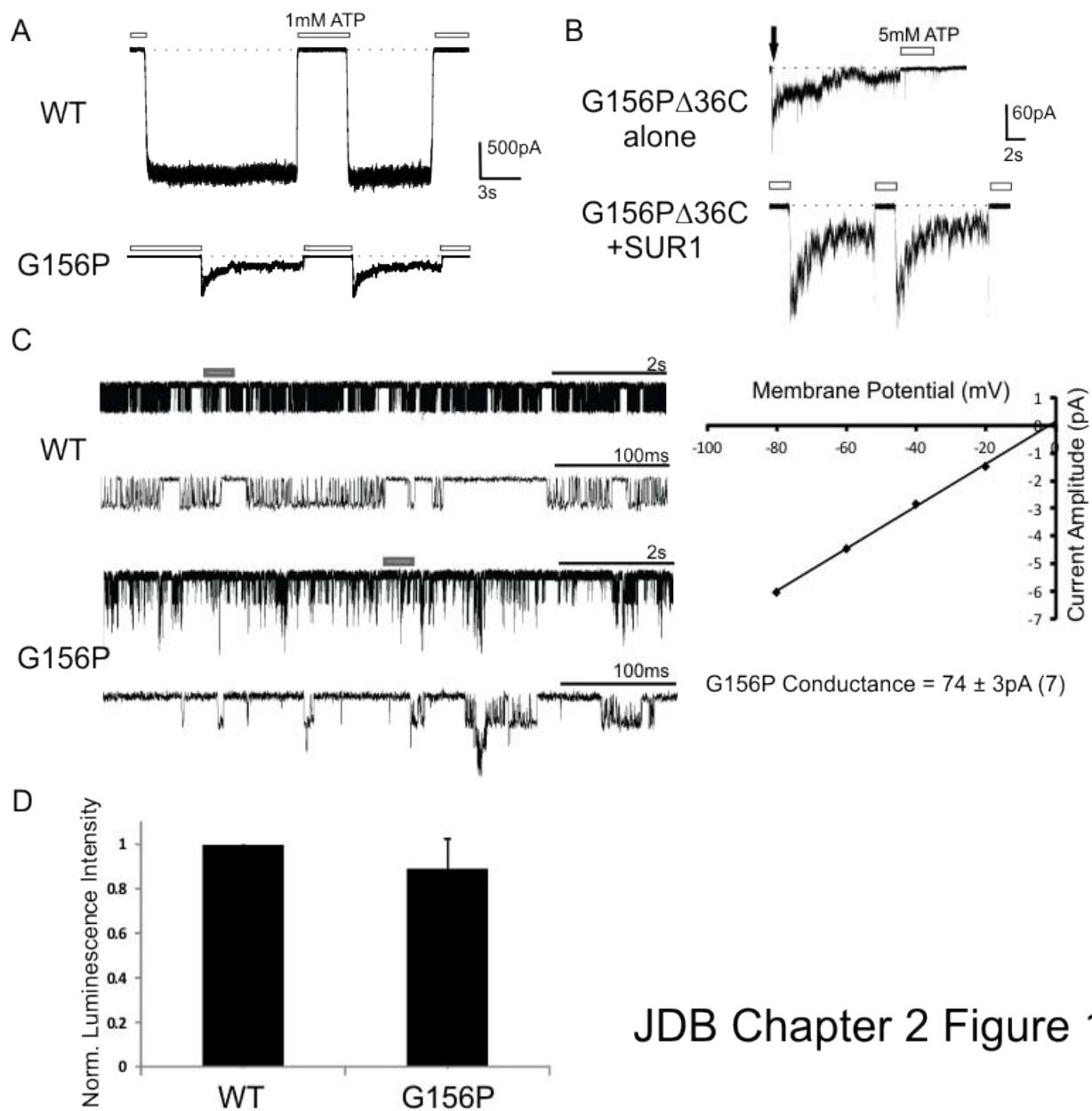
presence of LC-CoA; R192E activity was recovered by LC-CoA without ATP exposure. Note effect of LC-CoA was reversible. (C) *Left*, example traces of G156P channels exposed to KINT or KINT with 5 μ M neomycin upon ATP recovery of channels. *Right*, summary bar plot of normalized mean decay constant \pm SD (units: 1/s / 1/s_{1st Kint}) for a mono-exponential function fit to decay currents. Normalization was to the fit of the first KINT exposure (to a value of 1).

Figure 5. Increasing open-state stability eliminates inactivation. (A) Sample traces from double mutant channels containing G156P and a second disease gain-of-function mutation previously reported. Outward currents were recorded at +50mV. BaCl₂ blocked K_{ATP} currents to establish baseline. (B) Image of potassium channel Kirbac1.1 crystal structure with residues labeled where mutations were made. (C) Plot of WT and each gain-of-function mutations' IC50 values taken from previous reports: Kir6.2 V59G (Proks et al., 2004), N160D (Shyng SL et al., 1997), L164P (Tammara P et al., 2008), C166S (Tsuboi et al., 2004), I296L (Proks et al., 2005), and SUR F132L (Proks et al., 2007). All IC50s were for ATP in the presence of EDTA. Dotted line arbitrarily drawn to distinguish constructs that eliminated (black dot) or failed to eliminate (grey dot) inactivation.

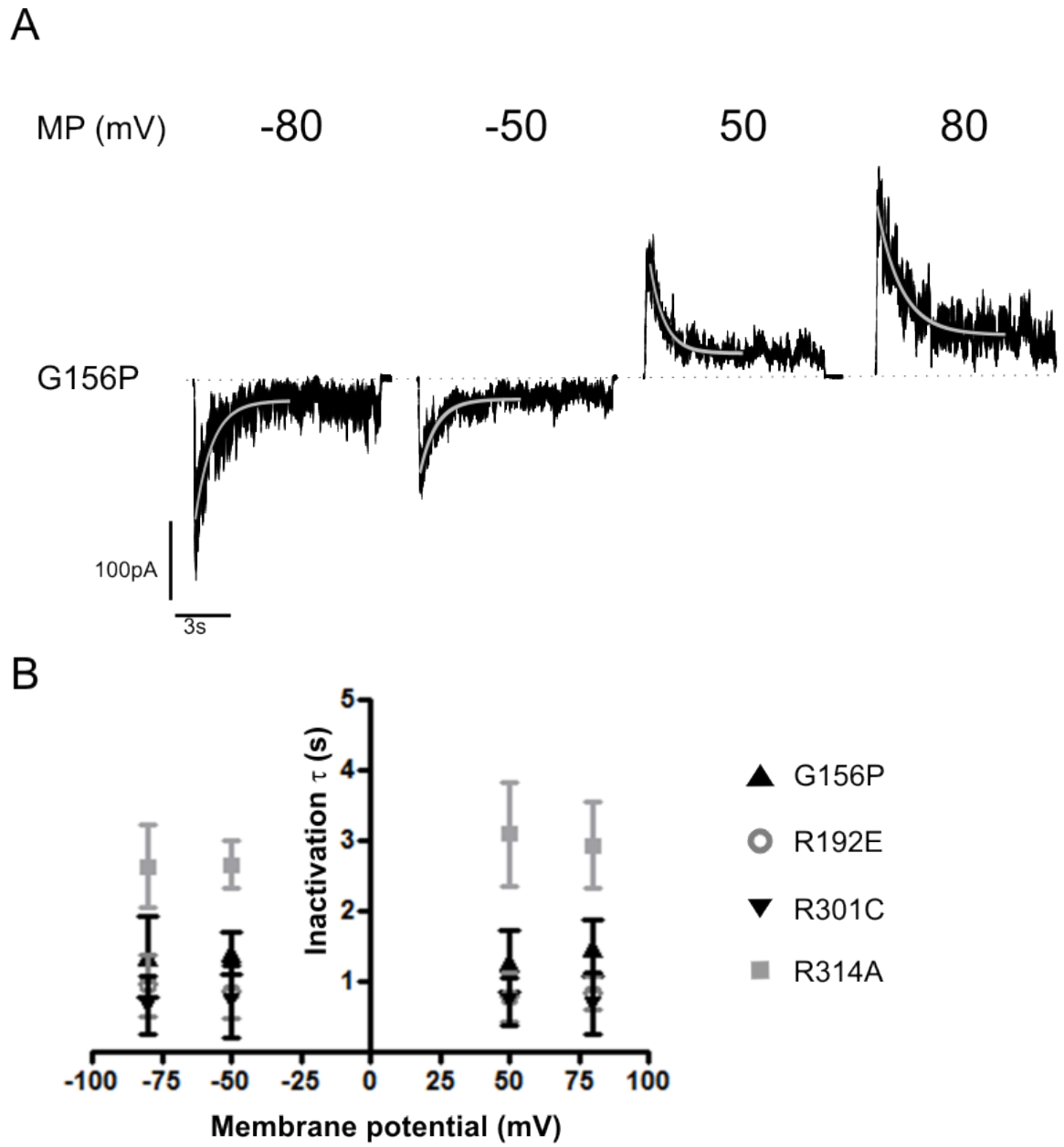
Figure 6. Cartoon Model of G156P Inactivation. From the closed state (top left), PIP₂ binding (in blue) to the Kir6.2 pore causes concomitant movements in the CTDs and TM2 segments that open the activation gate at the intracellular end of the membrane (top right). Increased PIP₂ levels can sustain channels in the open state. Proline mutation (yellow) causes a transition into an inactivated state (Bottom right); limited mobility in TM segments favor a closed “unbent” conformation and no longer functionally link to intact CTDs illustrated in red. ATP will bind at the interface of the CTDs and

induce a conformational change that recovers coupling at the TM-CTD interface (Bottom left). Removing ATP allows channels to revisit a state in which PIP₂ can readily re-bind to activate the channel. The black spheres next to each cartoon state show the status of the four subunit cytoplasmic domains.

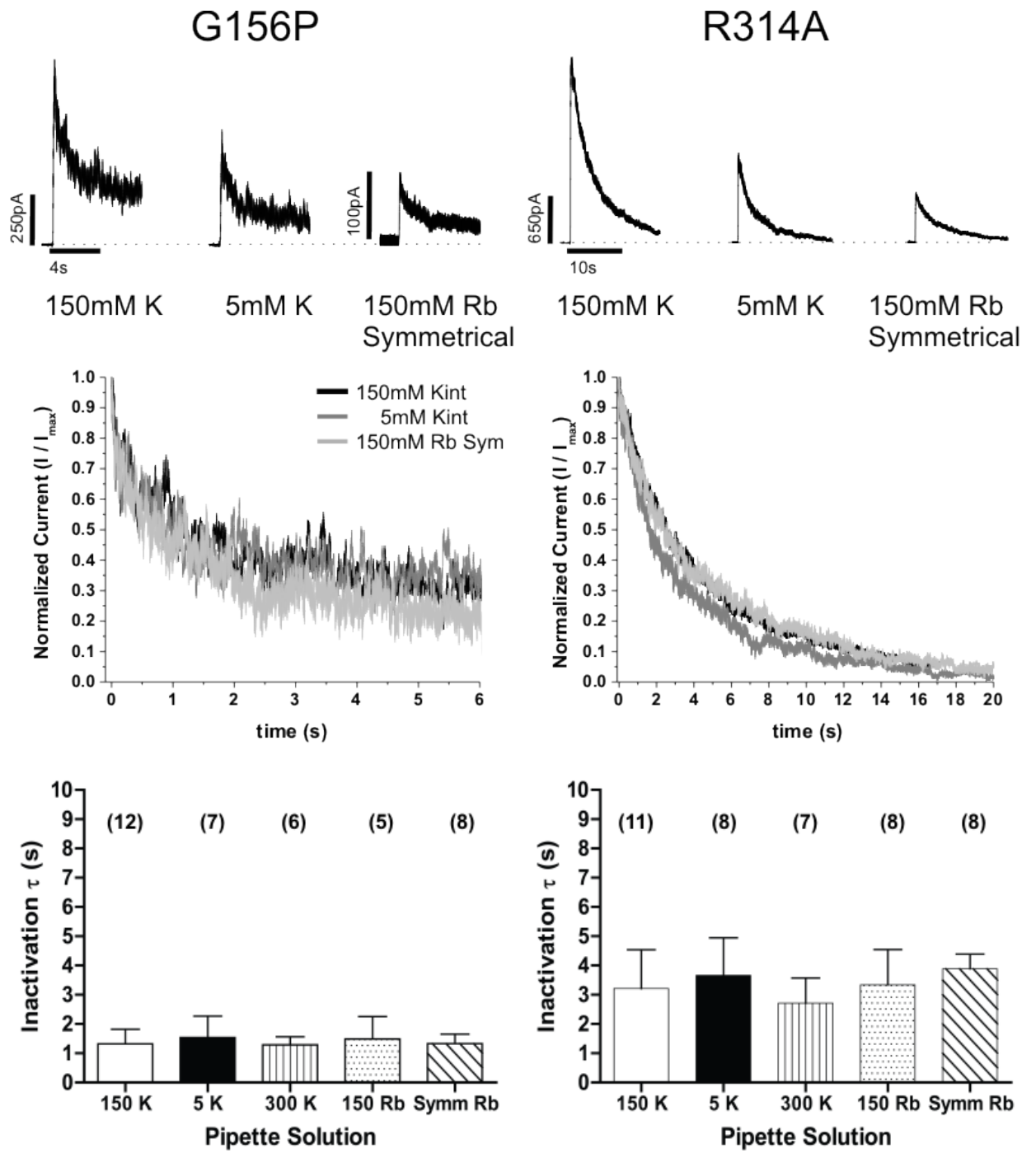
Supplementary Figure 1. Time-dependent recovery from inactivation. (A) Sample traces from the same patch of the paired pulse protocol. Between each pair, G156P channels were exposed to 5 mM ATP for 30 seconds. Then channels were activated to the first peak, and allowed to inactivate to reach a plateau, followed by a short interval of ATP exposure and removal to reach a second peak. Intervals were extended until the second peak reached near maximum. (B) Plot of re-activation time course for G156P and other inactivation mutations. Data for each mutation is from 3-4 patches. See methods for explanation of analysis.



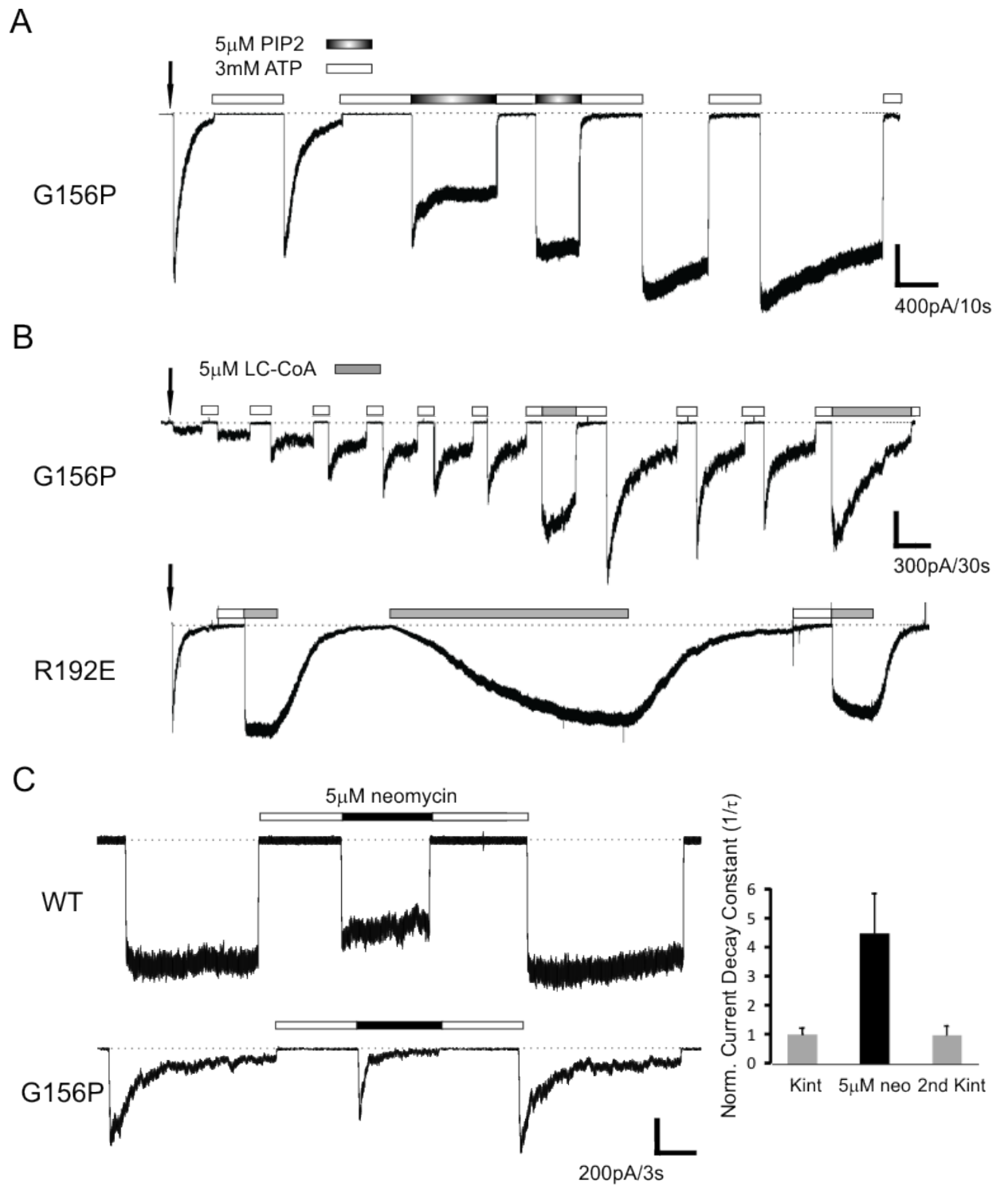
JDB Chapter 2 Figure 1



JDB Chapter 2 Figure 2

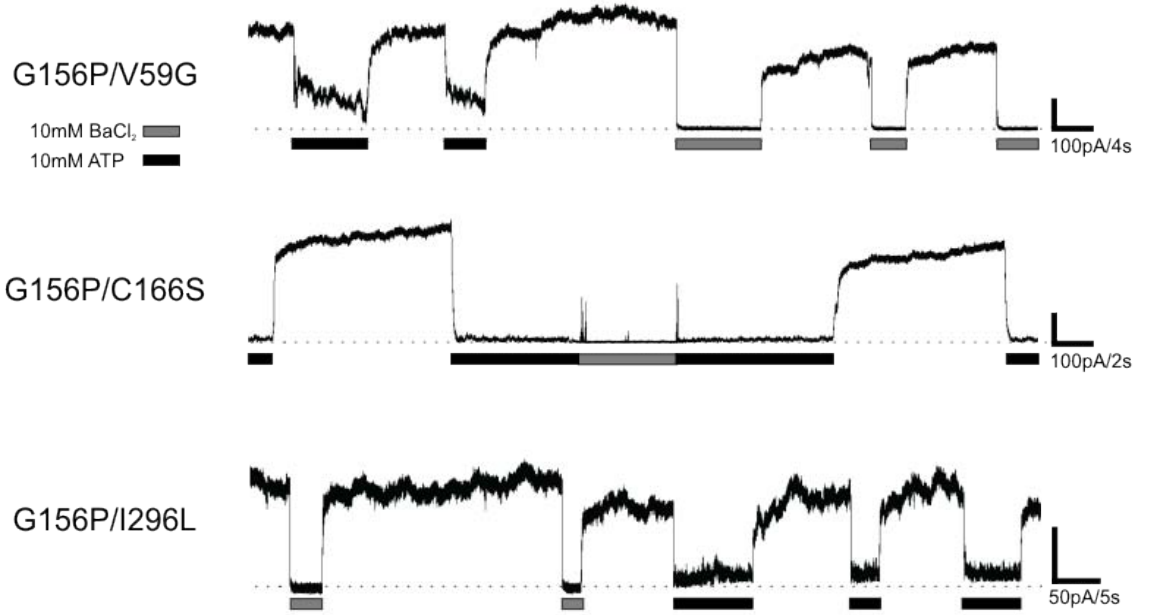


JDB Chapter 2 Figure 3

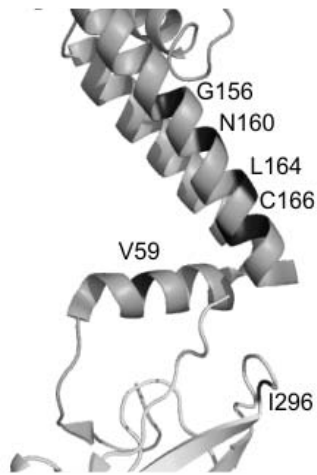


JDB Chapter 2 Figure 4

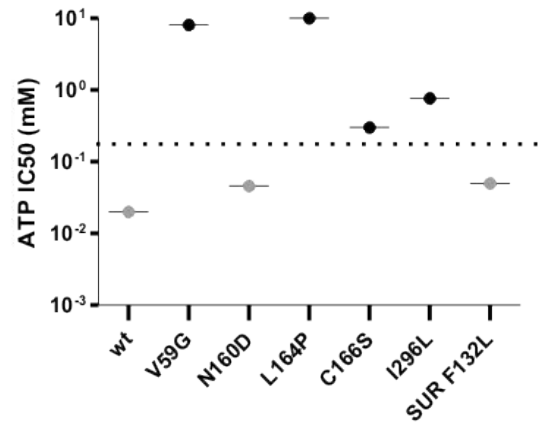
A



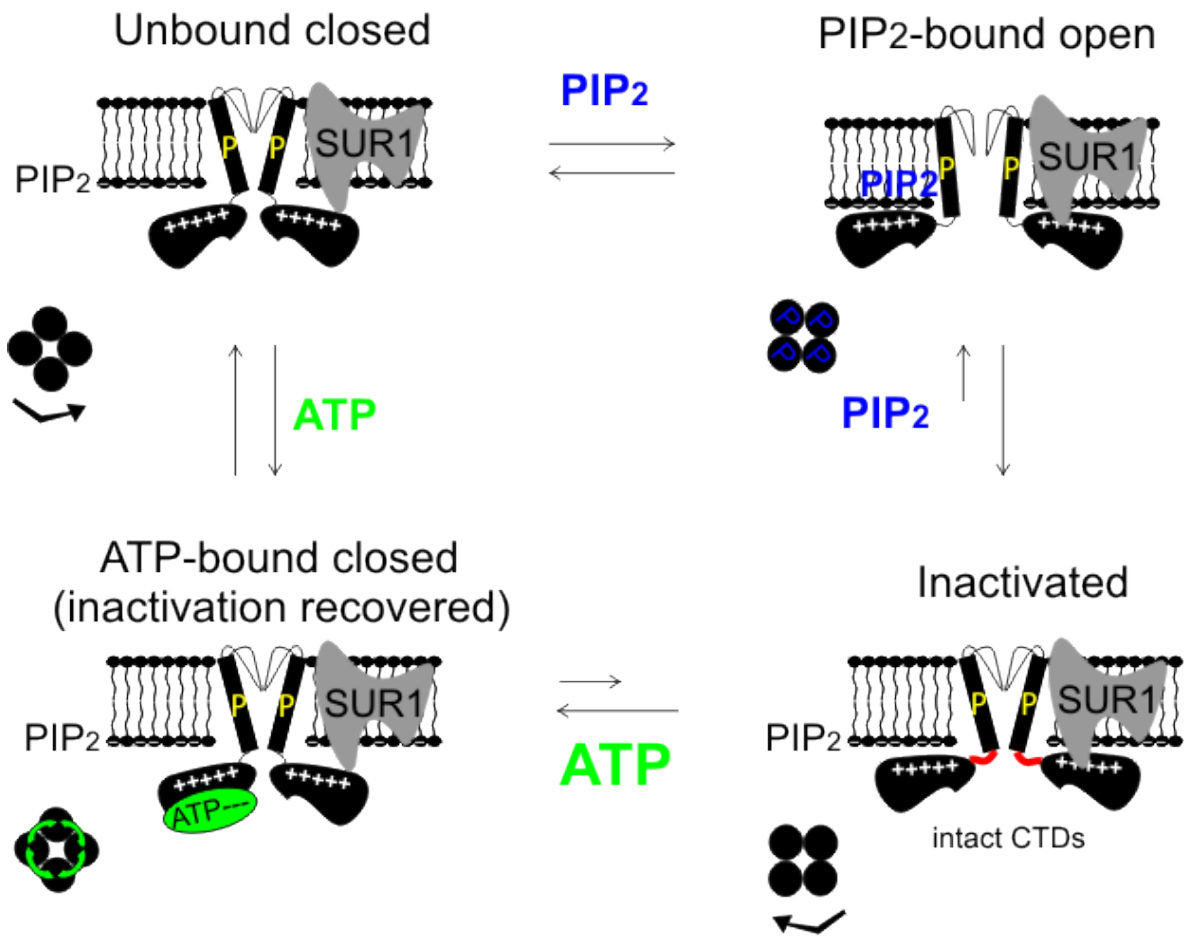
B



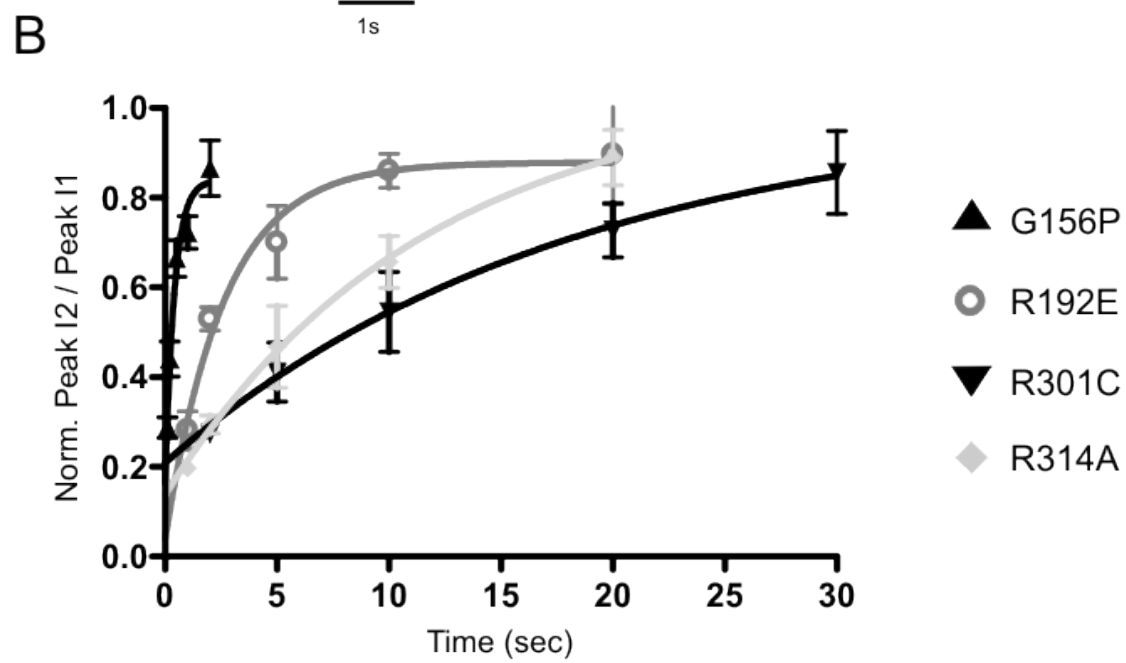
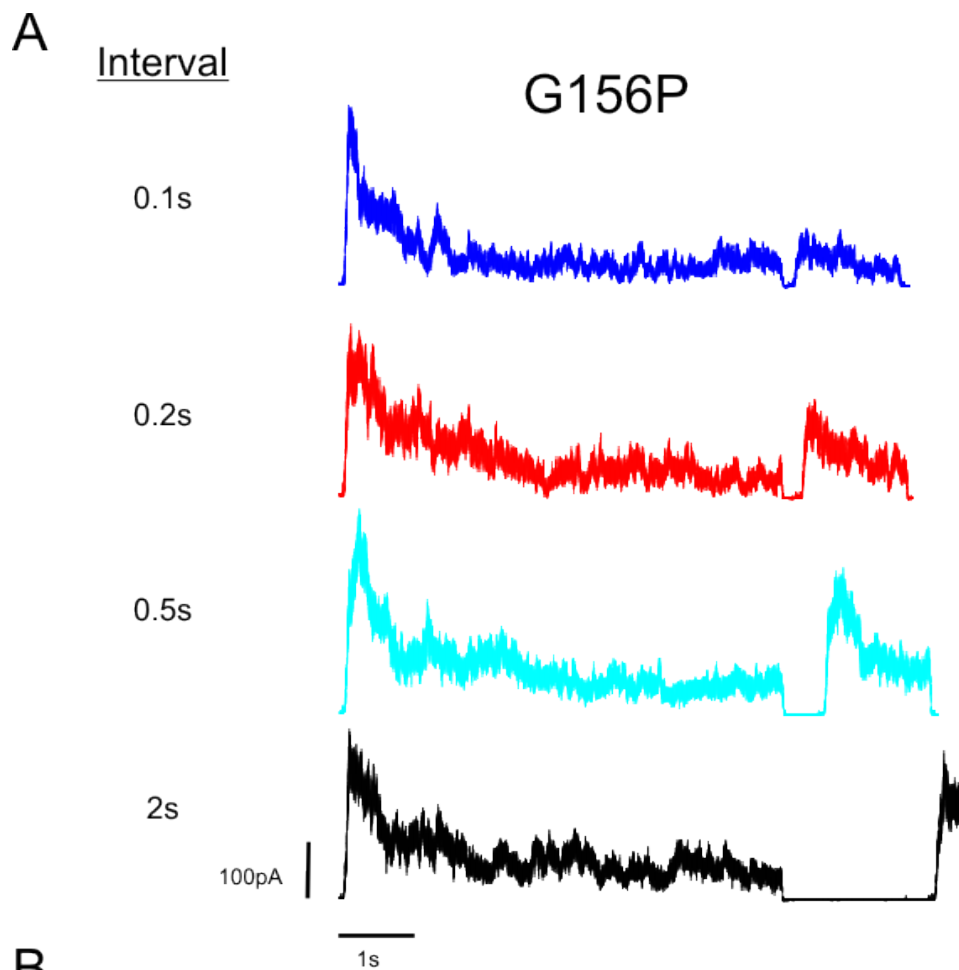
C



JDB Chapter 2 Figure 5



JDB Chapter 2 Figure 6



Supplemental Figure 1

CHAPTER 3

In Search of Flexibility in the TM2 Helices of Kir6.2

The data presented in this chapter is unpublished work. Most mutations generated, biochemistry, electrophysiology experiments and all of the writing were performed by JD Bushman with the following exceptions; roughly half of the proline scan mutations were made by Sara Haider, a chemiluminescence assay of the proline scan was performed by Joaquin Espinoza-Goodman, and the initial G165P mutation and its ATP sensitivity generated by Yu-Wen Lin, PhD.

Abstract

What is the mechanism by which the TM2 helices bend to open a gate? In Chapter 1, we concluded the upper glycine was unnecessary for flexibility in TM2 by replacing it with a salt bridge. In the current chapter introduction, I show and discuss preliminary evidence that the double mutant channels G156R/N160D and G156R/N160E have decreased mean open times and increased intraburst closed times consistent with altered gating at the selectivity filter. The result, in agreement with recent studies, reframes the double mutant “hinge” as a multi-point interaction between the salt bridge and the selectivity filter that balances interactions to produce WT-like nucleotide gating. Therefore, it remains a possibility that the upper glycine, which would not have side-chain interactions with the selectivity filter, is the principal position at which the TM2 helices bend in WT channels. Our study of a proline mutation in Chapter 2 was part of a proline scan to identify how introducing helix kinks in TM2 would interfere with gating by biasing channels towards open or closed states. We used a proline scan along the length of the inner cavity surrounding upper (residues 154-159) and lower (residues 163-167) glycines to search for ligand-sensitive effects due to gain-of-function or inactivation similar to G156P. Most of the positions tolerated substitution measured as ATP-sensitive currents from inside-out patches (not I167P), consistent with several other studies that scanned TM2 with other amino acids. L157P and L164P have reduced ATP sensitivity and L157P reduced LC-CoA activation suggesting enhanced open state stability. The irregular range of surface expression levels observed may be a confounding factor for other studies that solely use current amplitude as readout of change in flexibility. Interestingly, of the residues tested G156 was the only position to exhibit inactivation. This chapter further addresses more directly whether the upper and lower glycines confer flexible regions to the TM2 helices of Kir6.2 by testing a broader

spectrum of amino acid substitutions at the glycines. We replaced G156 with 15 of the remaining 16 natural amino acids (not G156F). Six substitutions produced measurable currents; two with low current amplitudes (G156T & N), two that showed an inactivation phenotype (G156P from Chapter 2 and G156C), and two with well-expressed WT-like current amplitudes (G156A & S). Initial measurements of single channel properties from excised patches of G156S with multiple single channels gave a mean open probability below WT, suggesting channel gating was reduced. I interpret these findings in favor of the upper glycine contributing to helix bending. Lastly, we consider flexibility at the lower glycine residue G165. Small non-polar substitutions did not produce any channel activity. Intriguingly, G165P channels were functional, and channel sensitivity to ATP was very weak. Single channels exhibit almost continuous burst behavior with a reduced conductance but WT-like intraburst properties. The results indicate a non-equivalent role for upper and lower glycines and implicate a lower glycine requirement for TM2. In the results and discussion, I posit a functional approach using single channel recording that would better validate or refute the glycine hinge hypothesis.

Introduction

A wealth of evidence from crystal structures supports the model that the TM2 helices bend and twist to open an intracellular gate in K⁺ channels. Comparison of the prokaryotic K⁺ channel homologue KcsA and MthK structures (presumably in closed and open states, respectively) shows the helix-bundle crossing (HBC) widens to open a 12 angstrom ion pathway from cytoplasm to selectivity filter (Doyle et al. 1998; Jiang et al. 2002). Several KcsA structures were published with a range of open conformations at the HBC (Cuello et al. 2010). Comparison of recent bacterial and eukaryotic Kir channel structures show closed HBCs and HBCs that appear to be opening with the short chain analogue C8-PIP₂ bound to a TM-CTD spanning site (Kuo et al. 2003; Nishida et al. 2007; Clark et al. 2010; Hansen et al. 2011). Analysis of ~500 K⁺-selective and related channel sequences (Jin et al. 2002) suggests the central glycine is well-conserved (>80%) and therefore bending at this glycine could be a common mechanism for these channels.

Currently, crystal structures analyzed for their hinge point offer a mixed view that the bend occurs at the central glycine (upper glycine in Kir). In the MthK open channel structure mentioned above, a bend in the TM2 helix occurs at the central glycine. Channel opening occurs by bending at the upper glycine in the Na⁺ and K⁺-conducting (or NaK) channel structures, whose TM architecture is similar overall to KcsA (Alam and Jiang, 2009; Shi et al., 2006). In contrast, a series of KcsA structures bend at different positions along TM2 in a 4-5 amino acid stretch containing the glycine, arguing the helix will flex in places other than the upper glycine hinge point even when the glycine is present (Cuello et al., 2010). It is unclear whether multi-point bending could be a general phenomenon, or whether it is an artifact of this particular truncation of KcsA

channel and a secondary effect of the selectivity filter which appears to close as the HBC opening widens. Nevertheless, the KcsA study casts doubt on the necessity of an upper glycine as a sole hinge point in TM2. Discussed in the thesis introduction (“Glycine Hinge Hypothesis” section) and consistent with double mutant channel data in Chapter 1, electrophysiological studies of mutations also find the upper glycine is not a requirement for gating in Kir channels.

Additional studies and consideration of the double mutations from Chapter 1 suggest the interpretation of non-essential is worth revisiting. N160D and N160E single mutations cause gain of function by increased open state stability, increasing channel P_o and decreasing ATP sensitivity (Shyng et al., 1997). When Arg and Asp interact in double mutants to reconstitute channel function, the gain of function from Asp may balance out a loss of function caused by Arg, depending on the structural cause of gain of function. How might Asp gain of function occur? The equivalent of N160 in KcsA channels (F103) was shown to interact with the selectivity filter, and links gate opening at the HBC to changes in filter gating (Cuello et al., 2010). When TM2 bends at the glycine, F103 side chains move toward the bottom of the filter close enough to interact. Gain of function in N160D K_{ATP} channels could occur by N160D hydrogen bonding with the side chain of T130 at the bottom of the filter and holding the TM helices open. Movement of side chains towards the filter could explain why swapping the positions of the two charges (ex. G156D/N160R in Chapter 1 Table 1) failed to recover currents; positive charges at N160 not fully compensated by the G156 Asp mutation would repel K^+ ions when the side chains approach the filter. Similarly, in G156R/N160D channels, the N160D-filter interaction might be partially intact when the salt bridge forms. Interestingly, we found a change in intraburst parameters during steady-state intrinsic gating in patches containing multiple G156R/N160D and G156R/N160E channels (Figure 1). Mean open times were

reduced and short intraburst closures were lengthened in double mutant channels compared to WT. This is consistent with the idea that the substitutions influence fast gating by local interactions with the filter either through side chain steric effects or electrostatically. Collectively, the data supports a model of balanced interactions between the substituted G156R/N160D side chains and the selectivity filter to generate WT-like nucleotide gating.

We now consider these ideas in the context of the glycine hinge hypothesis. The hinge hypothesis in part assumes that flexibility would be inherent to the TM2 alpha helix because glycine has no side chain and thus will not interact with the filter. Our conclusion that G156 is not essential can be understood to mean that in a minimal sense an artificial hinge can be introduced into TM2 and that recapitulates WT nucleotide gating. But the artificial hinge's interaction with structures outside of TM2 does not reflect an isolated test of TM2 flexibility, i.e. it is not a direct test of the glycine hinge hypothesis. We modify the conclusion from Chapter 1 that our findings do not exclude the upper glycine as a potential hinge in WT K_{ATP} channels.

An additional location for flexibility in TM2 of Kir channels arises from the presence of a second completely conserved "lower" glycine located roughly one helical turn above the HBC that could bend TM2 at a position closer to the gate (G165 in Kir6.2). Kir4.1/5.1 heteromeric channels had a profound reduction in channel activity when the lower glycine was substituted with alanine (Shang & Tucker, 2008). Similarly, Kir1.1 channels had a significant reduction in activation when the lower glycine was mutated, but changing both glycines to alanine did not eliminate channel currents (Sackin et al., 2006). The lower glycine residue corresponds by sequence position to the proline motif "PVP" in Kv channels, and an open state crystal structure shows this motif as the bend

point without any considerable change in the upper glycine (Bright et al. 2002; Long et al. 2005). A bend in the lower glycine has not been visible in current Kir crystal structures. A role in gating for the lower glycine remains unclear.

I began an investigation into the flexible nature of TM2 around the glycines by scanning with proline residues in order to introduce kinks in the helix that might lead to inactivation or gain-of-function phenotypes. I further examined the upper and lower glycines through mutagenesis and electrophysiology, including single channel recording of select mutations. Preliminary findings are discussed.

Results

Glycine has the highest conformational entropy in part due to lack of a beta-carbon (Feng Y et al. 2004). Proline can adopt only a few conformations and has the lowest conformational entropy (Trevino SR et al. 2007; Prajapati RS et al. 2007). Simply in terms of flexibility, it is likely that at the immediate location a protein segment will be less flexible when a proline is substituted for glycine. But prolines also have helix breaking properties, and can produce a bend and kink in a transmembrane helix that could impart increased flexibility in the structure adjacent to the proline. Thus despite the intriguing observations in Chapter 2 that replacing glycine with proline causes PIP₂-dependent inactivation, a molecular explanation of proline's effect on the helix is perhaps not immediately intuitive. The parsimonious explanation is proline increases rigidity where the glycine was located and introduces flexibility where it kinks the helix. If the glycines provide the most flexibility, then replacing the regions surrounding them with proline will likely reduce overall flexibility in TM2 and bias the pore towards the open or closed conformation without completely eliminating channel function.

Previous study showed that GIRK (Kir3.4) channels exhibit an alpha-helical periodicity for gain/loss-of-function effects on channel activation when residues in TM2 are mutated to proline, with little to no qualitative effect on channel surface expression (Jin et al., 2002). We performed a proline scan by replacing residues surrounding the upper and lower glycines along the cavity-lining portion of M2 (154-158,163-167). Several positions when mutated to proline in K_{ATP} appeared to decrease ATP sensitivity as expected for a gain-of-function phenotype (Figure 2). L157P mutation had decreased sensitivity to high concentration of ATP (1mM) and had little to no activation in response to a high concentration (5 μ M) of LC-CoA or an IC₅₀ concentration of tolbutamide suggesting increased open state stability; the effect is not likely due to direct interference with ATP binding in the CTD. The result is consistent with the equivalent S176P mutation in GIRK which renders a channel that is normally closed in the absence of Gbetagamma protein to become constitutively active (Sadja et al. 2001). Proline mutation near or at the lower glycine in K_{ATP} channels enhance channel activity and reduce ATP sensitivity, with at least one previously reported mutation (L164P) known to cause congenital diabetes, specifically PNDM (Tamarro F et al., 2008). Ensemble current amplitudes varied considerably between mutant channel patches (data not shown).

Large variation in mutant channel expression was observed in our measurements of proline mutant channel expression. Surface expression measured with chemiluminescence ranged as little as 10% to close to WT levels (Figure 3). In the GIRK channel proline scan mentioned above, images of GFP-tagged channels at the oocyte surface qualitatively show very little difference in intensity and Western blots of total cell lysates indicate similar channel expression, although considerable GFP is seen

within the cell not within the plasma membrane for some mutant channels (Jin et al. 2002). I am reluctant to posit that there is such a significant difference between factors that stabilize the pore architecture of different Kir channels without a more detailed study of expression (both overall protein and at the surface) in both channel types, especially since TM2 is unlikely to contact and thus interfere with SUR-Kir interactions that are necessary for channel expression. It should be noted that Kir6.2 L164P measurement was a single assay, and indirect indications from channel currents in a previous study using oocytes argue little to no reduction in expression (Tammaro et al. 2008). Also, endoplasmic reticulum quality control of channel folding and trafficking is likely to be different between oocytes and our mammalian expression system. Nevertheless, differences in mutant channel expression will complicate interpretations of mutant effects on ensemble channel activity if not properly accounted/normalized.

A rigorous test of flexibility would be to measure single channel fluctuations to evaluate gating parameters. If flexibility was decreased from loss of glycine, the rate constants of a kinetic scheme which represent the frequency of transitions between states would decrease, and we could measure the parameters specifically associated with slow gating. First, I measured ensemble currents from macroscopic inside-out patches to identify functional mutant channels. G156 was substituted for fourteen of the sixteen remaining amino acids (not G156F or G156E). G156E was shown to be marginally functional in a previous publication (Kurata et al., 2004). Currents were measured from 6 of 15 mutant Kir6.2 constructs coexpressed with SUR1 in COSm6 cells; the previously studied mutations are referenced for completeness (Figure 4 top). N and T mutations produced very small current amplitudes; at present it is unknown if this is a gating or an expression defect. It is tempting to suggest that gating is the cause since arginine, lysine and proline mutations (Chapters 2 & 3) had near WT expression, but expression

from G156V and G156L channels had significantly lower expression levels (Figure 4 bottom) indicating surface expression may vary significantly between mutations. It was quite interesting to see the cysteine mutation generate an inactivation phenotype. G156C construct was made and tested after the proline mutation had been partially characterized and was not further explored, but the phenotype substantiates inactivation as an effect of modifying the glycine rather than simply a grossly altered pore structure due to proline. Alanine (A) and serine (S) mutant channels generated robust ATP-sensitive current amplitudes. Hence, the last two mutations (G156A and G156S) produce readily functional K_{ATP} channels and make good candidates for detailed analysis of mutation effects, using single channel kinetics as the discriminator of flexibility. I note here that none of the mutations had an obvious effect on channel sensitivity to ATP, but more subtle yet significant changes are elucidated from concentration response profiles yet to be determined.

WT K_{ATP} single channel kinetics can be grouped into fast and slow processes. Fast gating refers to intraburst parameters including mean open time, short closed interval, and number of openings within a burst, while slow gating consists of burst lengths and interburst closed intervals. To test the glycine hinge hypothesis, I need to identify mutations with changes in slow gating parameters without affecting fast gating parameters (open times, fast closed times, number of closures per burst). If glycine flexibility is required, then kinetic parameters associated with slow gating (burst lengths, interburst intervals) will shift away from WT values in all cases even when fast gating is unaffected. In preliminary high resolution recordings, a single channel was rarely observed; G156S channel patches contained multiple amplitudes (Figure 5). Preliminary analysis of multi-channel patches shows a mean open probability of ~ 0.27 for G156S channels corresponding to overall reduced channel gating. Because burst and interburst

gating dominate changes in P_o , the finding for G156S is consistent with an effect on slow gating. I also observed a small decrease in the mean open time in G156S channels (Figure 5). Fast gating could be altered in G156S channels, although this seems less unlikely if the short closed time is not changed; the number of patches is too low for statistics. WT channel P_o measured using the methods to obtain high resolution recordings was lower than expected for the solution conditions used (~ 0.35 , Figure 5 versus 0.5-0.65 typically from our lab), although it is only slightly below average from previous studies (0.45, Enkvetchakul et al., 2000). Additional patches of isolated single channels are required for analysis of burst lengths and interburst intervals.

Lastly, we considered flexibility in the lower glycine. More subtle substitutions at G165 to alanine, serine, and valine did not produce channel currents (Figure 6); expression levels are currently unknown. However, G165P channels readily generated currents even in cell-attached configuration indicative of low sensitivity to ATP. Very high concentrations (5mM) of ATP only partially inhibited channel activity with full amplitudes determined by blocking outward currents with barium in inside-out excised patches. Single G165P channels have a reduced single channel conductance of approximately 40pS estimated from the current amplitude with a -80mV command potential but appear to be open in a near continuous burst mode (Figure 7). As seen in the increased time resolution trace, apparent interburst closures were observed suggesting the slow gate can briefly close. When 5mM ATP was bath applied, single channels decreased in P_o and exhibited shorter bursts and longer interburst intervals, an observation consistent with ATP's effects on WT channel slow gating parameters (Figure 7). As expected if only the slow gate was perturbed, fast gating intraburst properties were unaffected by the mutation (data not shown).

Discussion

Assigning flexibility for a particular residue such as the two glycines or a broader flexible region that functions as a hinge in TM2 has been actively studied to flush out channel components controlling gating motions in K⁺ channels. Limiting flexibility to a single position in the helix seems unlikely since initial results from the proline scan show several positions near the two glycines force the helix towards closed or open states. The only mutation that completely eliminated channel function was I167P, although the entire helix remains to be tested. Gain-of-function produced by the two leucine residue substitutions (L157P and L164P) adjacent to the glycines (G156 and G165) and the glycine-to-proline phenotypes suggest these regions may be gating-sensitive to significant structural changes in the helix.

Upper Glycine Hinge. If we assume flexibility is the principal requirement of a hinge, and glycine is the most flexible residue, then all mutations introduced at the glycine will impair channel gating. It has been a challenge to adequately attribute changes in measurements of channel activity solely to helix flexibility. Since the selectivity filter also can act as a gate, testing the hinge hypothesis requires a way to separate disruptive effects in the helix from an imbalance in pore electrostatics or changes in the selectivity filter. The glycine locates close to the selectivity filter and many if not most amino acids could interfere with the filter through direct interaction depending on side chain size (Jin et al., 2002). Local interactions between the upper glycine position and the pore helix could also be important for TM/selectivity filter communication in channels that do not contain a glycine as an alternative mechanism (Shang & Tucker 2008), so using these channels as a comparison may not be appropriate for testing the hinge hypothesis. Flexibility also implies bending in either direction, and a mutation could shift channel

equilibrium towards the closed state or the open state. In most cases a shift towards the closed state would be expected, as mutations that stabilize helix formation would decrease helix bending and thus decrease channel opening. I argue that in K_{ATP} channels two gates could be distinguished by analyzing the totality of single mutant channel kinetics and demonstrating the frequency of transitions correlated with slow gating are impaired while fast gating and other properties like selectivity and conductance are intact. To this end, most substitutions at G156 were useless because they eliminated channel currents completely (Figure 4). Channel expression at the surface still needs to be determined.

G156S and G156A channels were the best candidates to measure single channel kinetics, and the data from a limited number of patches of G156S mutant channels trends toward decreased channel gating. Ideally dwell times could be modeled with a reaction mechanism such as the tetrameric model (Enkvetchakul et al., 2000) that adequately describes intrinsic gating, with rate constants estimated from time constants globally constrained to fit the channel dwell time event distributions. At a minimum, patches containing current fluctuations from a single channel are necessary, and the high P_o from spontaneous intrinsic gating of K_{ATP} channels make it a good model system to determine the likelihood of a single channel present (Horn, 1991). The single open state and single conductance state modeled in K_{ATP} channels also make the analysis less complicated. Unfortunately, two or more current amplitudes were observed in most patch data collected here so the available data set falls short of the mark required for this analysis. If a G156 mutation was found that behaves exactly like WT, such as if G156A channels had no change in rate constants or conductance, the finding would convincingly argue against the glycine hinge hypothesis.

Lower Glycine Hinge. Lack of tolerance even for subtle mutations (alanine or serine) in K_{ATP} suggests G165 plays a critical role in the helix structure, but without measurable currents interpretations are limited. G165P channels have a fascinating but potentially complex phenotype for interpreting flexibility. Glycosylation mapping of transmembrane helices indicates prolines break the helix when they are inserted near the end (Nilsson et al., 1998), but breaking is unlikely since G165 is located several turns from the C-terminus of TM2. Natural prolines located near the center of protein transmembrane helices kink the helix placing an anisotropic hinge usually four residues N-terminal to the proline residue, at the residue that would normally hydrogen bond with the proline's location; proline residues closer to an end will favor a lower kink angle (Cordes et al., 2002). L164P markedly increased P_o with WT single channel conductance, and G165P increases P_o even closer to its maximum and reduces conductance. The difference in conductance argues that the proline kink changes the shape of the pore, increasing the energy barrier on a potassium ion fluxing through an open channel. This could happen several ways: by burying polar or charged amino acid side chains that attract ions into the pore; by decreasing the cavity size and decreasing entropy of water molecules hydrating the ion; by altering the efficiency or configuration of the selectivity filter; or by reducing the size of the open pore at the gates. Additional experiments could help eliminate some of these possibilities. Molecular dynamics simulations of a homology model with the introduced proline could offer clues to how the pore architecture was affected. Measuring permeability of other ions (Rb^+) with respect to K^+ would point to an effect on the selectivity filter or ion hydration.

Near maximum P_o and decreased sensitivity to ATP is consistent with a continuously open slow gate. A simple interpretation is that rigid proline locks the ATP-sensitive gate but kinks the helix to partially open it. If a proline kink also introduces flexibility to the

helix, why does the channel only exhibit the open state? Wouldn't the helix bend in a new position, or even bend at G156? A stuck gate could still be an effect from the anisotropic nature of a kink. A new helix trajectory could displace the HBC reducing efficiency of amino acid packing near the gate, and the gate settles into a partially open conformation that cannot bend in a direction that opens it further. It would be quite a novel finding then if G165P had normal neomycin sensitivity; this would argue that the near continuous burst and reduced conductance was a phenomenon of a displaced gate with physically restricted but energetically equivalent movements rather than increased open state stability and clearly demonstrate G165 does not act as a hinge. Most likely the channel will exhibit increased PIP₂ apparent affinity (decreased neomycin inhibition), similar to other Kir6.2 mutations that increase open state stability. Attempts also could be made to assess the opening at the HBC by measuring accessibility of the central cavity in G165P channels from the cytoplasmic side. Overall, the G165P phenotype clearly supports the HBC as the slow ligand- and PIP₂-sensitive gate.

The diametrically opposed phenotypes of the glycine to proline mutations – G156P loss of function with little to no effect on ATP inhibition (Chapter 2) versus G165P gain of function with significant loss of ATP sensitivity – point to non-equivalent roles for these two positions in Kir channel gating. I suggest a putative mechanical model to explain TM2 bending as a two step process: the lower glycine may be an initial flexure bearing where the helix loosens and contracts as the initial force transduction wave on the HBC arrives during activation causing the bottom portion to move outward first, followed by extension of the bottom of the helix as the upper half starts to pivot outwards bending near or at the upper glycine (Figure 8). This is analogous to a multiple gate zipper model where the helix opens like a series of poppers suggested by Proks & Ashcroft (2008). In this scenario a bend in the lower glycine would only be seen in a subset of

early intermediate structural conformations in the closed to open transition, but delegates the lower glycine as the initial hinge point. A bend at the lower glycine could be visible in Kir structures but none has been reported. The bend may be a minimal distortion difficult to observe without high resolution structures; current published structure resolutions are generally not below 2.5 angstrom. The upper glycine would be relegated to an auxiliary role as the second hinge point, but would be more likely seen as the bend point in structures of channels in a fully open state.

Methods

Molecular Biology, Chemiluminescence Assay, Electrophysiology – methods were identical to those described in Chapter 1. Important details reiterated in the figure legends.

Data Analysis – Data were analyzed and presented using Clampfit 9.0 and MS EXCEL. Histograms were plotted using log-linear graphs according to the method of Sigworth & Sine (Sigworth & Sine, 1987).

Figure Legends

Figure 1. Single channel bursts of G156R/N160D and G156R/N160E double mutant channels have altered intraburst kinetics. *Top*, Brief segments of single channel records show openings and closings during an isolated burst from steady-state spontaneous activity. Inside-out patch recordings at +80mV command potential (-80mV membrane) were sampled at 50 kHz and filtered using an analog 4-pole Bessel filter at 5 kHz. *Bottom*, histograms of the open and closed channel dwell time distributions for WT and G156R/N160D channels. Dwell times from burst periods randomly sampled were taken from patch recordings with multiple channel openings, and data were selected

only from regions with current amplitudes between baseline and the first conductance level. Fits to the distributions were mono-exponential probability density functions using the method of maximum likelihood in Clampfit 9.0.

Figure 2. Partial proline scan of TM2 surrounding the two glycine residues show changes in sensitivity to channel regulators. Patch recordings performed in the inside-out configuration; command potential was +50mV. N = 2-4 patches for mutant channels unless indicated.

Figure 3. Surface expression of TM2 proline mutations. Quantitative chemiluminescence corresponding to surface labeled channels shown as a percentage of WT (See Chapter 1 for methods). Number of experiments indicated above bars.

Figure 4. Patch recordings and expression of G156 mutations. (A), Representative traces are shown for channels that generated K⁺ currents with a +50mV potential. Channels were inhibited with 1mM ATP in all traces. Reference 1 was Kurata et al., 2004. (B), Surface expression of G156L and G156V mutations measured from 2 chemiluminescence assays.

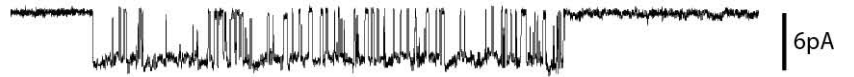
Figure 5. Single channel activity of WT and G156S from multi-channel patches. Top, example traces of inside-out patches containing multiple single channel amplitudes. 30-60 second segments were analyzed to determine channel open probability. Bottom, recording and analysis methods were same as in Figure 1, shown as bar plots. Po calculated from single channel idealization. Number of patches analyzed above bars.

Figure 6. Mutations at the lower glycine position. Conservative G165 mutant channels did not generate measurable K⁺ currents. Kir6.2 G165P + SUR1 & Kir6.2Δ36C G165P alone were expressed and K⁺ currents recorded at -50mV membrane potential. Number of patches tested in parentheses.

Figure 7. Single G165P channels have reduced conductance and show nearly continuous bursting. Representative traces from excised inside-out patches of single WT and G165P mutant channels recorded at -80mV membrane potential. Note the reduced current amplitude of G165P openings. Increased time resolution traces are from representative trace, and an example apparent interburst shut period was seen in the G165P trace. In the bottom two traces, channels were inhibited for a period with 5mM ATP. Time scales labeled respectively at the top apply to all traces. Data are from 2-3 patches.

Figure 8. Preliminary Two Hinge Model of Kir6.2 TM2 Gating. Cartoon diagram (*bottom images*) shows four possible functional states relevant to a three state kinetic model (*top*). First two functional states on the left represent two non-conducting states prior to an open bundle crossing in which TM2 initially bends at the lower glycine upon PIP2 binding to the cytoplasmic domain. Force propagating along TM2 pivots the helix at or near the upper glycine in order to widen the HBC enough to fully open the conduction pathway for hydrated K⁺ ions. While the HBC is open, the selectivity filter can briefly narrow and close the extracellular end of the pore (*bottom right*).

WT



Total time 50ms

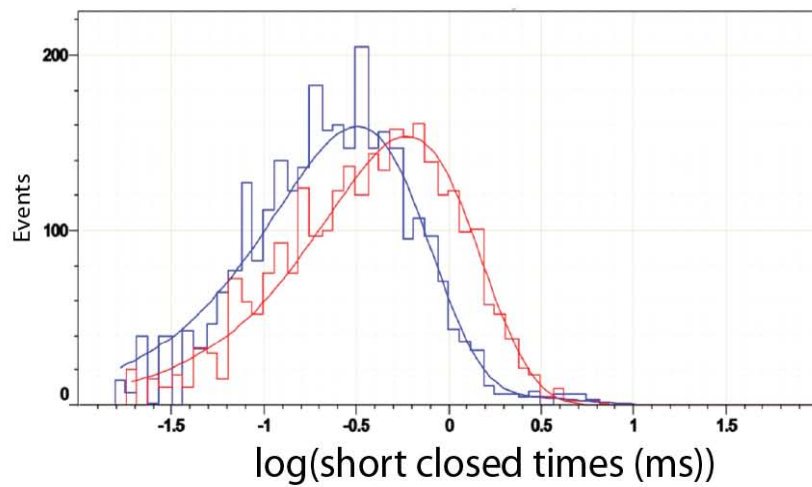
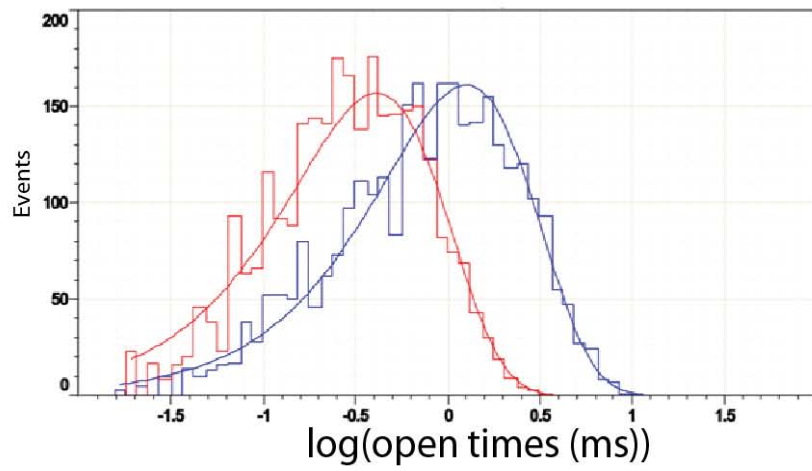
G156R/N160D



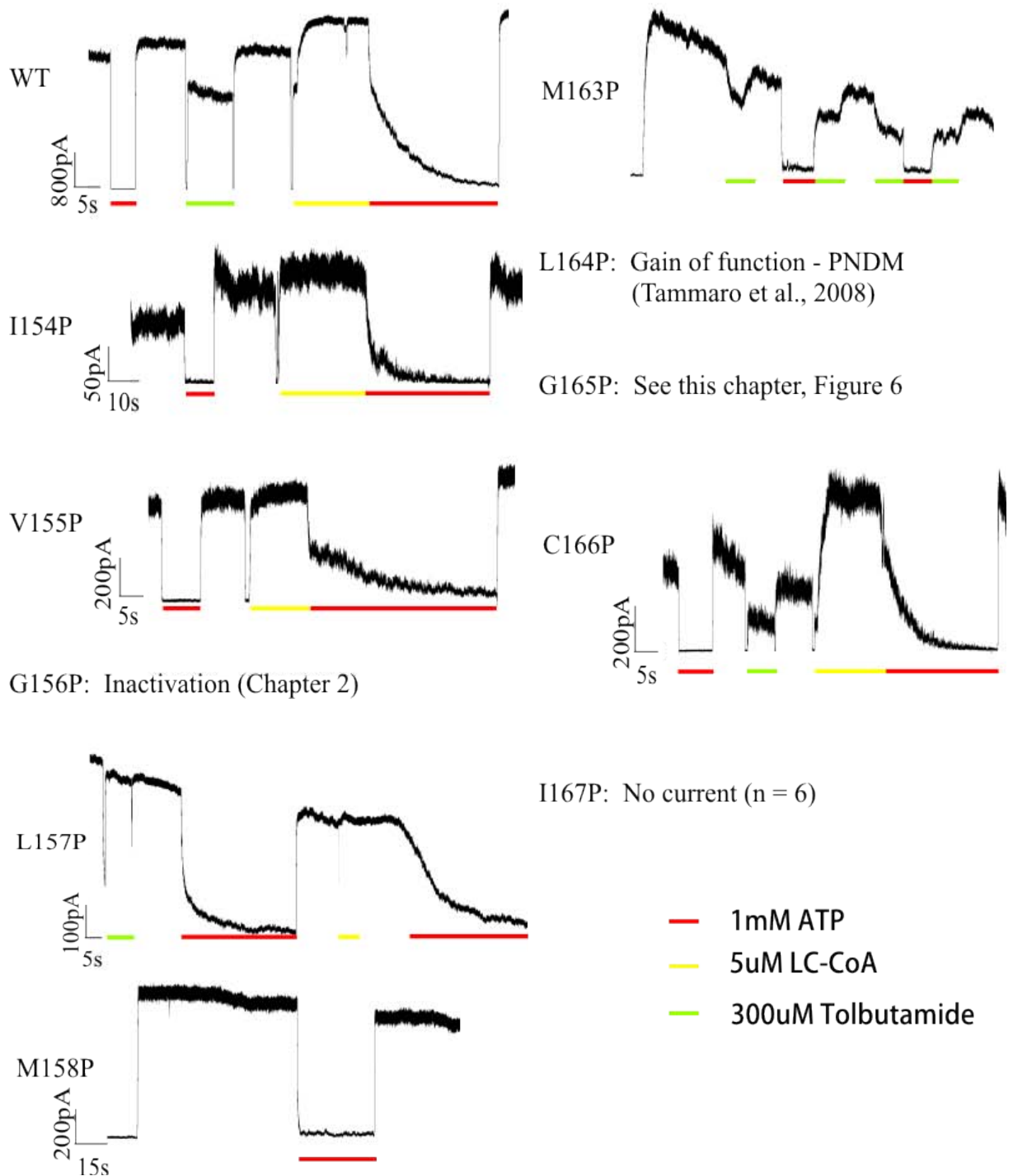
G156R/N160E



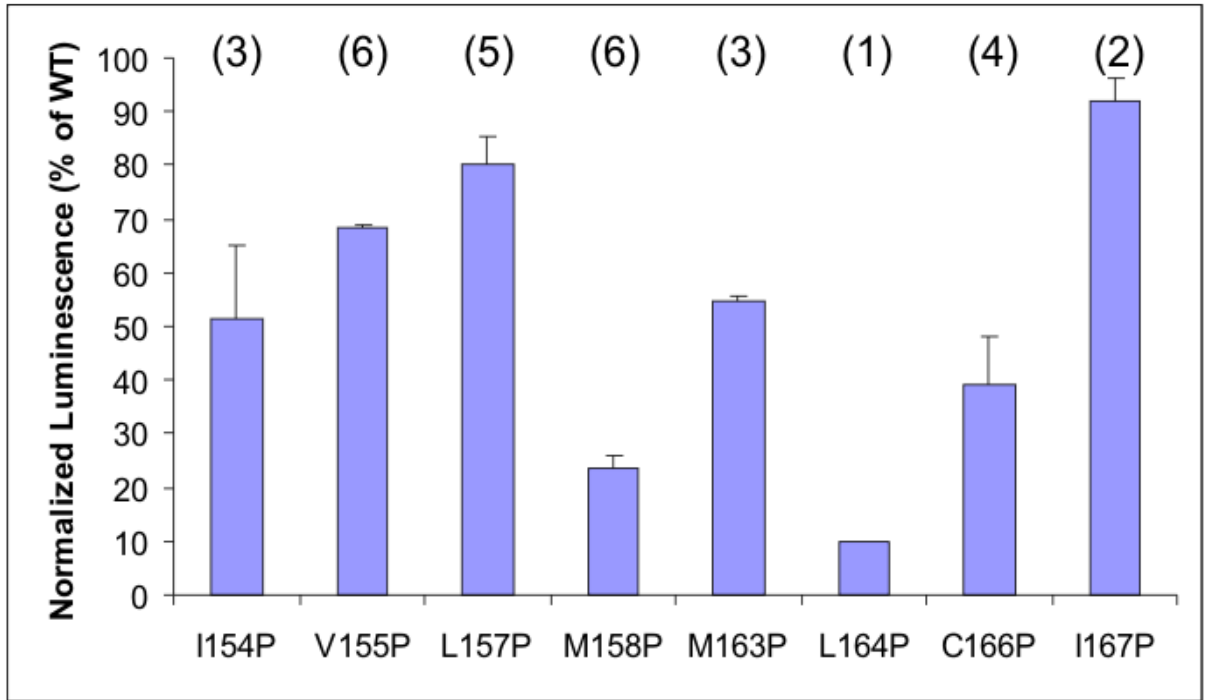
WT = blue
GR/ND = red



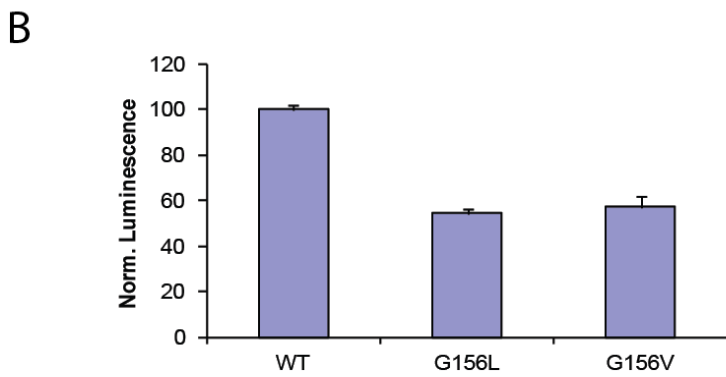
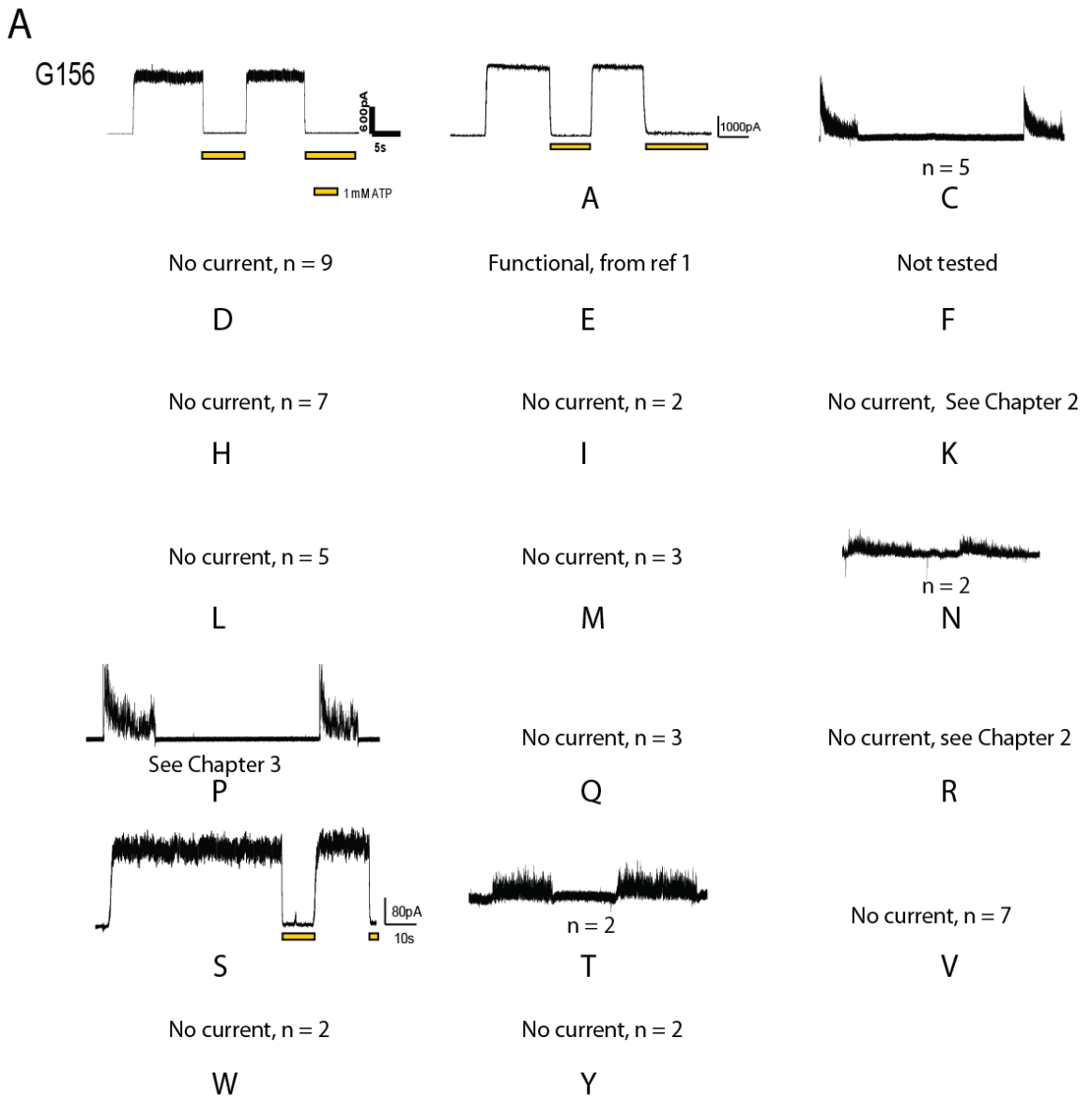
JDB Chapter 3 Figure 1



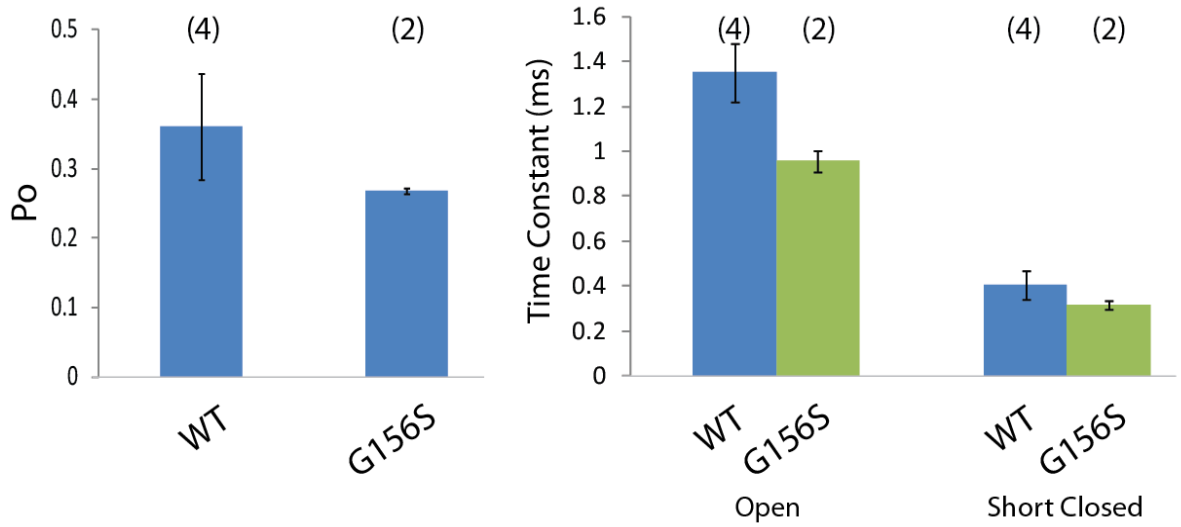
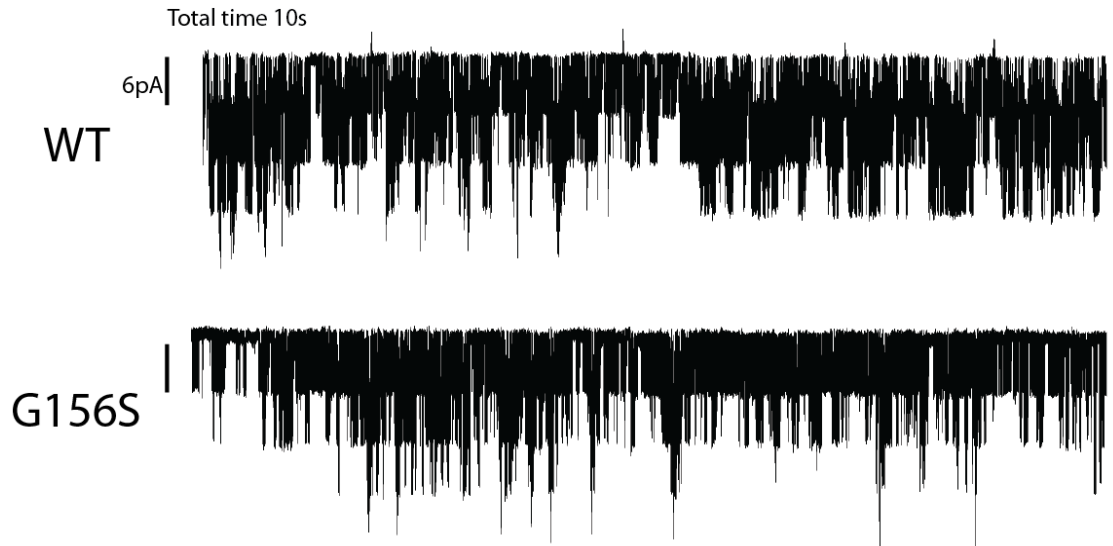
JDB Chapter 3 Figure 2



JDB Chapter 3 Figure 3



JDB Chapter 3 Figure 4



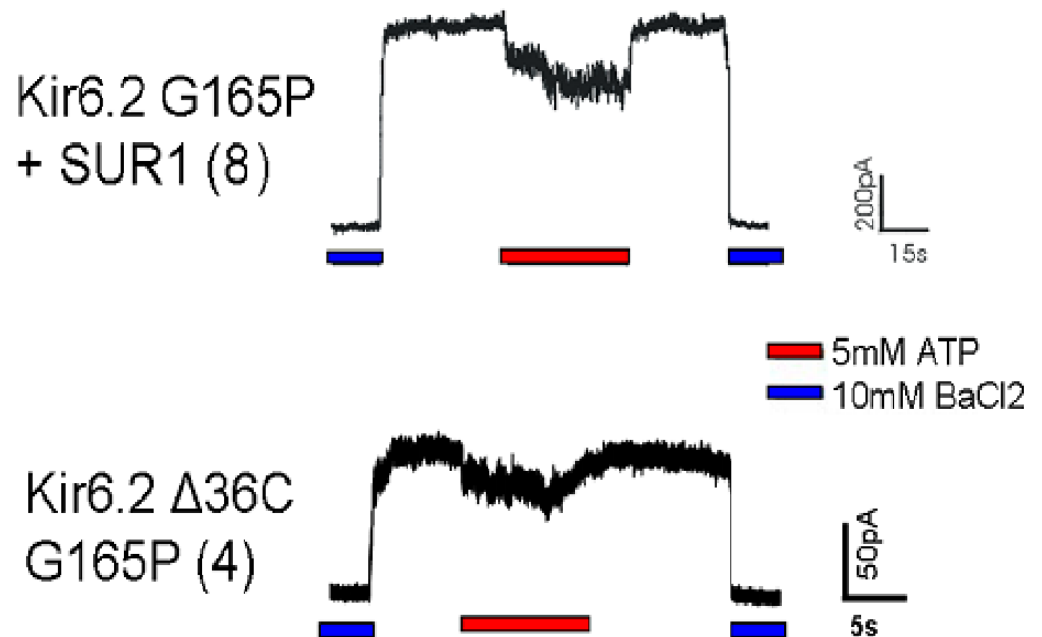
JDB Chapter 3 Figure 5

Kir6.2 G165A - no current (7 patches)

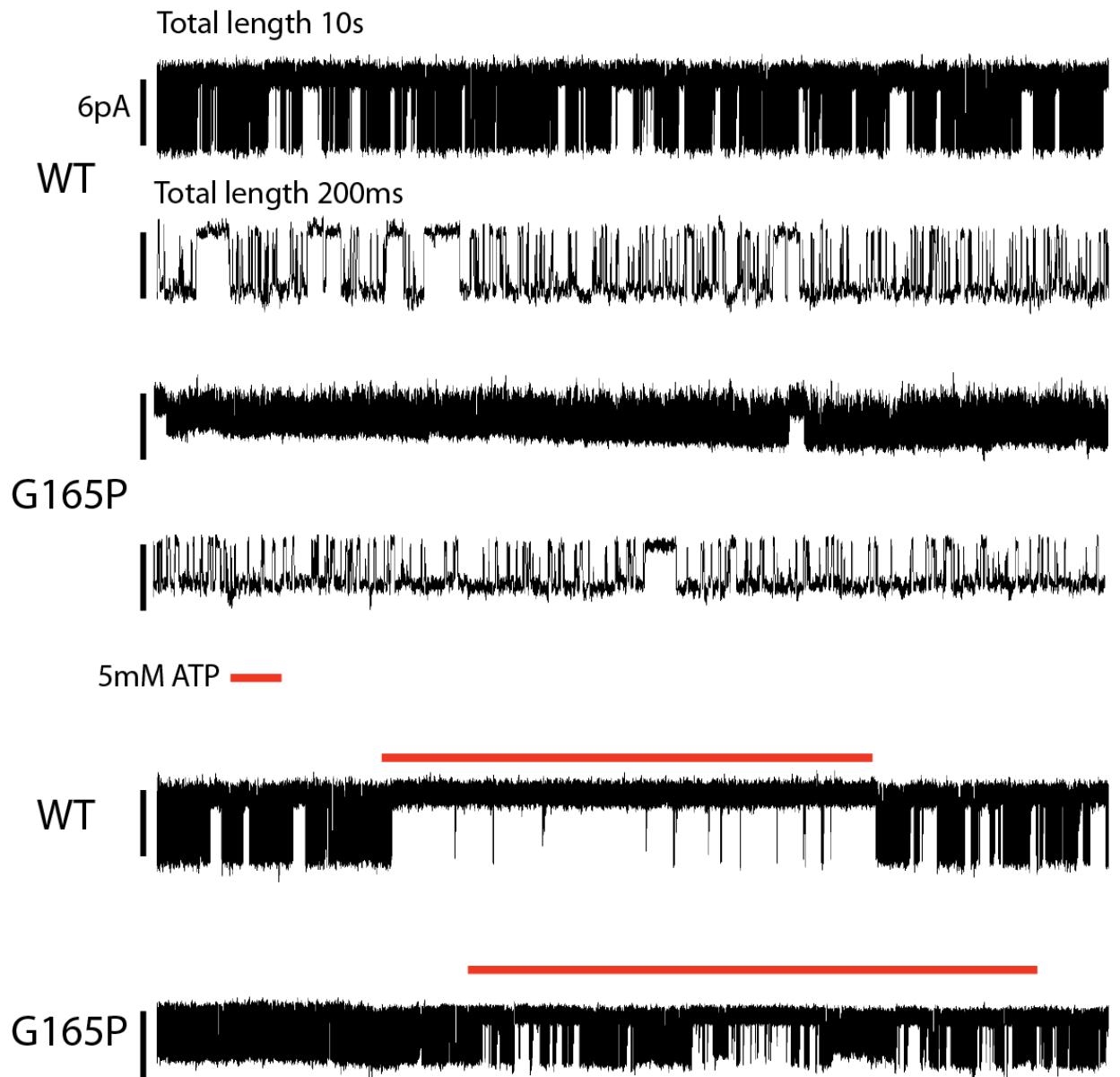
Kir6.2 G165S - no current (3 patches)

Kir6.2 G165V - no current (2 patches)

Kir6.2 G165C - no current (from Loussouarn G et al. JBC 2000)



JDB Chapter 3 Figure 6

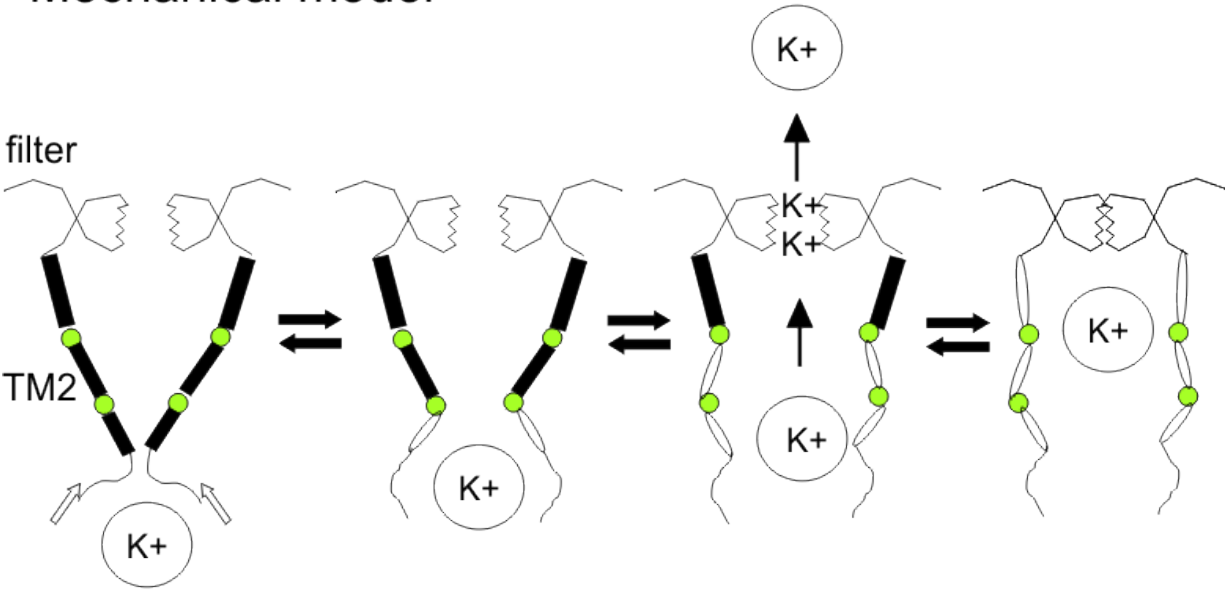





JDB Chapter 3 Figure 7

Kinetic model



Mechanical model



-  = water hydration shell
-  = activation signal
- K+ = potassium ion
-  = glycine hinge

JDB Chapter 3 Figure 8

Conclusions

The work of this dissertation enlightens the potassium channel field with fundamental knowledge of the pore through study of the upper (also called central) glycine in K_{ATP} channels. Our characterization of the G156R mutation contributes to the broader understanding of the mechanisms of human channelopathies. Numerous studies of other loss-of-function disease mutations identify structural defects that disrupt aspects of channel gating (Shyng et al., 2012). Our study asserts that the G156R phenotype does not arise from the putative role of this glycine as a hinge critical for channel gating; the mutation eliminates conduction by creating an unfavorable electrostatic environment in the pore. That heteromeric WT:G156R channels function *in vitro* in part explains the weak clinical presentation in the parent and milder phenotype and response to diazoxide in one of the siblings (Pinney et al. 2008). Future characterization of novel K_{ATP} channel disease mutations will help piece together aberrations in structure/function that bring about clinical manifestations and assist in identifying beneficial therapeutic methods.

From first principles, the interpretation drawn from placement of arginines into the channel lumen seems intuitive if not obvious. Positive charges in the low-dielectric environment of the inner cavity should strongly repel a cation conducting through the electric field of the membrane. A study published shortly after ours defies these expectations; mutation of the adjacent residue L157 to lysine in Kir6.2, with a side chain predicted by structural models to face directly toward the central axis of the conduction pathway, does not eliminate K^+ conduction (Kurata et al. 2010). The mutation N160R at the rectification controller one helical turn after L157 also eliminates K^+ currents (Shyng et al. 1997) illustrating the location of charges is a critical factor. The upper glycine occupies a small space next to the selectivity filter in all published K^+ channel structures

implying a larger side chain could sterically hinder or interact electrostatically with the filter. In Chapter 3, preliminary evidence from G156R/N160D single channels shows altered “fast gating” properties, suggesting the double mutant pair interferes with the filter (Chapter 3 Figure 1). The general conclusion of the arginine-to-glycine mutation remains unmitigated; altered pore electrostatics is the principal defect of G156R since conduction and ligand-gating were reconstituted when charge was compensated in the doubly mutant channels. Accumulated findings above highlight the complexity involved in functional study of the hinge hypothesis.

Further mutagenesis of G156 in Chapter 2 uncovered coupling between the cytoplasmic and transmembrane domains necessary for stable channel activation. The precise structural elements involved in coupling are unclear, but an initial consideration would be TM2 itself. Low intrinsic gating resulting in decreased PIP₂ sensitivity observed in G156P channels fits with a loss in TM2 flexibility through restriction of the polypeptide backbone. Perhaps it is a saving grace that proline kinks helices to create a new hinge point; otherwise the low conformational entropy of proline that replaces flexible glycine might eliminate channel function completely. The functional effect of a kink introduced by proline could be modified in a graded manner if the structural properties of proline were further expanded. Proline isomerization functions as a switch for opening/closing the gate in some cys-loop receptor ion channels (Lummis et al., 2005) and was explored through use of proline-like unnatural amino acids, and the unnatural amino acid technique has been previously developed for use in mammalian cell lines (Monahan et al., 2003). Unnatural amino acids placed at the upper glycine that mimic the low entropic effect of proline with preferences for the cis- or trans- isomer could be utilized to probe K_{ATP} gating and inactivation.

ATP recovery of G156P mutant channel activity in Chapter 2 was a surprising discovery. The appearance of inactivation from mutations throughout the channel structure could point to an unappreciated ability of ATP to induce conformational changes that are conducive to channel opening when ATP unbinds and perhaps needs further consideration when developing quantitative mechanisms that model channel gating kinetics. A single inactivated state added to a simple kinetic model could account for inactivation (Loechner 2011), but the connectivity of the inactivated state with other states will require kinetic model comparison with experimental kinetic data. Kinetic simulations could test how inactivation emerges from specific perturbations of a comprehensive reaction scheme. ATP interplay with PIP_2 may underlie channel re-activation, but PIP_2 currently is not incorporated into quantitative models of the K_{ATP} gating mechanism. Recent technical advancements to reliably purify and reconstitute Kir channels in an artificial lipid system lay a promising foundation for future quantitative study of PIP_2 -channel interactions (D'Avanzo et al., 2010). Removing SUR1 by expressing G156P Kir6.2 Δ C channels drastically reduced ATP re-activation, suggesting SUR1 may be involved. Sulphonylureas, which bind to SUR to inhibit channel gating, could be used to determine whether channel closure mediated through SUR also facilitates recovery from inactivation by inducing similar conformational changes as ATP.

Evidence from Chapter 2 also suggests the inactivation we observe does not proceed from collapse of the selectivity filter. A conserved Glu-Arg salt bridge in Kir channels supplants the hydrogen-bonding network seen in inactivating K^+ channels and may be critical to maintain the relatively stable conducting and K^+ -selective filter (Yang et al. 1997). When the hydrogen bond network was abolished in KcsA, a non-inactivating “flipped” conformation in the selectivity filter of KcsA E71A mutant channels permeates Na^+ at a higher rate and reduces K^+ selectivity (Cheng et al. 2011). The different

solution conditions used so far are only a small sample of potential tests on the selectivity filter conformation. Changes in filter conformation due to mutant K_{ATP} inactivation could be further investigated by testing ion selectivity and Na^+ permeability. In addition, changes in sensitivity of molecules that block K^+ conductance by binding at or near the selectivity filter such as barium and TEA could provide an additional functional readout.

Future Directions

Kir channel gating models have slowly incorporated structural locations that function as a gate in the permeation pathway. Briefly mentioned in the thesis introduction is a putative third gate formed by the G-loop in the cytoplasmic domain. Structural conformations in Kirbac1.1 and Kirbac3.1 show rearrangements of the N- and C-terminal CTDs, and the G-loop was noticeably different in diameter size between conformations (Clark et al. 2010). In more recent crystal structures of eukaryotic Kir channels, the G-loop diameter was dependent on ligand-bound factors or their simulated presence (Hansen et al., 2011; Whorton & MacKinnon, 2011). The intriguing possibility of a G-loop gate fits with a hypothesis that mutant K_{ATP} inactivation derives from changes in the equilibrium of cytoplasmic domain conformations. Inactivation mutations could decrease stability of CTD interactions, either inter-subunit or inter-domain in the case of G156P, important for CTD rearrangements that dynamically control the G-loop gate. Accessibility along the length of the pore above and below the G-loop could be tested if a rigorous approach were developed to fully control conformational changes in the CTDs. It may be possible to lock the N- and C-terminal CTDs into an open or closed conformation using cysteine cross-linking methods. A strategy was briefly employed using Kirbac1.1 homologous residues that show conformation-dependent interaction. N-

terminal domain D58C and C-terminal domain R206C mutations eliminate intrinsic K_{ATP} activity, and R206C was previously shown to express at the plasma membrane (Ribalet et al., 2003), but crosslinking in the double mutant channels was not observed. Limited knowledge of how the SUR subunit integrates with cytoplasmic domains of Kir6.2 complicates targeted strategies for crosslinking in this region of the channel complex. If two interacting cysteines were found, pore accessibility could be probed using inward rectification as the readout with single residues mutated to negatively-charged amino acids along the channel lumen above and below the G-loop.

If the Clarke et al. (2010) Kirbac structural study conclusions were extended to Kir6.2, in that CTD conformational changes correspond to changes in occupancy of the selectivity filter, then mutations in the CTDs that bias channel equilibrium towards the closed or open state could affect fast gating associated with the filter. The closed time constant associated with the selectivity filter is rarely rigorously analyzed in single channel recordings. The parameter expressed as a frequency (inverse of time constant) is typically close to or smaller than the low-pass filter cutoff frequency used in recordings leading to large errors in its measurement, but a diligent re-examination of currently available recordings at 5 kHz could provide an impetus for further study. The Kirbac study suggests an initial component of the structure to consider for mutagenesis is the Kir6.2 N-terminal region called the slide helix, which increased interactions with the C-terminal CTD in the low-occupancy filter structures.

Chapter 3 lays the foundations for future work to further test the glycine hinge hypothesis in K_{ATP} channels with mutagenesis, using the broad spectrum of natural amino acid properties and analyzing single channel kinetics to discern slow gating versus fast gating effects. To specifically test the hinge hypothesis, it is desirable to find amino acids that

do not interact with the selectivity filter. As discussed throughout this dissertation and specifically addressed in the Chapter 3 introduction, studying a mutation that interacts with the filter or studies from channels with amino acids other than glycine at this position does not directly test the glycine hinge hypothesis because side chain-filter interactions introduce a non-inherent property of glycine that confounds interpretation of helix flexibility. G156S and G156A mutant K_{ATP} currents were robust and channel activity was stable, inviting the possibility that small non-polar side chains other than glycine could also produce WT gating kinetics. Discovering mutant channels such as G156A are equivalent to WT channels in permeability, selectivity, conductance, and gating kinetics, together with the mutation placed into a homology model of the best available Kir structure showing absence of side chain interactions with the filter would nullify the glycine hinge hypothesis in K_{ATP} channels.

References

- Ader, C., R. Schneider, S. Hornig, P. Velisetty, E.M. Wilson, A. Lange, K. Giller, I. Ohmert, M.F. Martin-Eauclaire, D. Trauner, S. Becker, O. Pongs, and M. Baldus. 2008. A structural link between inactivation and block of a K⁺ channel. *Nat Struct Mol Biol.* 15: 605-612.
- Aguilar-Bryan, L., and J. Bryan. 1999. Molecular biology of adenosine triphosphate-sensitive potassium channels. *Endocr Rev.* 20:101-35.
- Aguilar-Bryan, L., J. Bryan, and M. Nakazaki. 2001. Of mice and men: K(ATP) channels and insulin secretion. *Recent Prog Horm Res.* 56:47-68.
- Aguilar-Bryan, L., J.P. Clement 4th, G. Gonzalez, K. Kunjilwar, A. Babenko, and J. Bryan. 1998. Toward understanding the assembly and structure of KATP channels. *Physiol Rev.* 78:227-45.
- Aguilar-Bryan, L., C.G. Nichols, S.W. Wechsler, J.P. Clement 4th, A.E. Boyd 3rd, G. González, H. Herrera-Sosa, K. Nguy, J. Bryan, and D.A. Nelson. 1995. Cloning of the beta cell high-affinity sulfonylurea receptor: a regulator of insulin secretion. *Science.* 268:423-6.
- Aittoniemi, J., C. Fotinou, T.J. Craig, H. de Wet, P. Proks, and F.M. Ashcroft. 2009. SUR1: a unique ATP-binding cassette protein that functions as an ion channel regulator. *Philos Trans R Soc Lond B Biol Sci.* 364:257-67.
- Alam, A., and Y. Jiang. 2009. High-resolution structure of the open NaK channel. *Nat Struct Mol Biol.* 16: 30-4.
- Alekseev, A.E., Brady, P.A., and A. Terzic. 1998. Ligand-insensitive state of cardiac ATP-sensitive K⁺ channels - basis for channel opening. *J. Gen. Physiol.* 111: 381-394.
- Antcliff, J.F., S. Haider, P. Proks, MS., Sansom, and F.M. Ashcroft. 2005. Functional analysis of a structural model of the ATP-binding site of the KATP channel Kir6.2 subunit. *EMBO J.* 24:229-39.
- Ashcroft FM. ATP-sensitive potassium channelopathies: focus on insulin secretion. 2005 *J Clin Invest.* 15:2047-58.
- Ashcroft, F.M. and F.M. Gribble. 1999. ATP-sensitive K⁺ channels and insulin secretion: their role in health and disease. *Diabetologia.* Aug;42(8):903-19.
- Ashcroft, F.M. and F.M. Gribble. 1998. Correlating structure and function in ATP-sensitive K⁺ channels. *Trends Neurosci.* 21:288-94.
- Ashcroft, F.M., D.E. Harrison, and S.J. Ashcroft. 1984. Glucose induces closure of single potassium channels in isolated rat pancreatic beta cells. *Nature.* 312:446-448.
- Babenko, A.P., and J. Bryan. 2003. SUR domains that associate with and gate KATP pores define a novel gatekeeper. *J Biol Chem.* 26:26.
- Baukowitz, T., U. Schulte, D. Oliver, S. Herlitze, T. Krauter, S.J. Tucker, J.P. Ruppertsberg, and B. Fakler. 1998. PIP2 and PIP as determinants for ATP inhibition of KATP channels. *Science.* 282:1141-4.
- Bichet, D., M. Grabe, Y.N. Jan, and L.Y. Jan. 2006. Electrostatic interactions in the channel cavity as an important determinant of potassium channel selectivity. *Proc Natl Acad Sci* 103:14355-60.
- Bichet, D., F.A. Haass, and L.Y. Jan. 2003. Merging functional studies with structures of inward-rectifier K⁺ channels. *Nat Rev Neurosci.* 4:957-67.
- Bienengraeber, M., A.E. Alekseev, M.R. Abraham, A.J. Carrasco, C. Moreau, M. Vivaudou, P.P. Dzeja, and A. Terzic. 2000. ATPase activity of the sulfonylurea

- receptor: a catalytic function for the KATP channel complex. *Faseb J.* 14:1943-1952.
- Blunk, R., J.F. Cordero-Morales, L.G. Cuello, E. Perozo, and F. Bezanilla. 2006 Detection of the Opening of the Bundle Crossing in KcsA with Fluorescence Lifetime Spectroscopy Reveals the Existence of Two Gates for Ion Conduction. *J. Gen. Physiol.* 128:569-581.
- Bright, J.N., I.H. Shrivastava, F.S. Cordes, and M.S. Sansom. 2002. Conformational dynamics of helix S6 from Shaker potassium channel: simulation studies. *Biopolymers* 64:303–313.
- Bushman, J.D., J.W. Gay, P. Tewson, C.A. Stanley, and S.L. Shyng. 2010 Characterization and functional restoration of a potassium channel Kir6.2 pore mutation identified in congenital hyperinsulinism. *J Biol Chem.* 285:6012-23.
- Capener, C.E., P. Proks, F.M. Ashcroft, and M.S. Sansom. 2003 Filter flexibility in a mammalian K⁺ channel: models and simulations of Kir6.2 mutants. *Biophys J.* 84:2345-56.
- Casamassima, M., M. C. D'Adamo, M. Pessia, and S. J. Tucker. 2003. Identification of a Heteromeric Interaction That Influences the Rectification, Gating, and pH Sensitivity of Kir4.1/Kir5.1 Potassium Channels. *J. Biol. Chem.* 278: 43533-43540.
- Chakrabarty, A., J.A. Schellman, and R.L. Baldwin. 1991 Large differences in the helix propensities of alanine and glycine. *Nature.* 351:586-8.
- Chan, K.W., H. Zhang, and D.E. Logothetis. 2003. N-terminal transmembrane domain of the SUR controls trafficking and gating of Kir6 channel subunits. *Embo J.* 22:3833-3843.
- Cheng, W.W., J.G. McCoy, A.N. Thompson, C.G. Nichols, and C.M. Nimigean. 2011. Mechanism for selectivity-inactivation coupling in KcsA potassium channels. *Proc. Natl. Acad. Sci.* 108:5272-7.
- Choi, K.L., R.W. Aldrich, and G. Yellen. 1991 Tetraethylammonium blockade distinguishes two inactivation mechanisms in voltage-activated K⁺ channels. *Proc Natl Acad Sci U S A.* 88:5092-5.
- Chutkow, W.A., M.C. Simon, M.M. Le Beau, and C.F. Burant. 1996. Cloning, tissue expression, and chromosomal localization of SUR2, the putative drug-binding subunit of cardiac, skeletal muscle, and vascular KATP channels. *Diabetes.* 45:1439-45.
- Clarke, O.B., A.T. Caputo, A.P. Hill, J.I. Vandenberg, B.J. Smith, and J.M. Gulbis. 2010. Domain reorientation and rotation of an intracellular assembly regulate conduction in Kir potassium channels. *Cell.* 141:1018-29.
- Clement, J.P., K. Kunjilwar, G. Gonzalez, M. Schwanstecher, U. Panten, L. Aguilar-Bryan, and J. Bryan. 1997. Association and stoichiometry of KATP channel subunits. *Neuron.* 18:827-838.
- Cook, D.L. and C.N. Hales. 1984. Intracellular ATP directly blocks K⁺ channels in pancreatic beta cells. *Nature.* 311:271-273.
- Cordes, F.S., J.N. Bright, and M.S. Sansom. 2002. Proline-induced distortions of transmembrane helices. *J. Mol. Biol.* 323: 951-60.
- Craig, T.J., F.M. Ashcroft, and P. Proks. 2008. How ATP inhibits the open KATP channel. *J Gen Physiol.* 132, 131-144.
- Cuello, L.G., V. Jogini, D.M. Cortes, A.C. Pan, D.G. Gagnon, O. Dalmas, J.F. Cordero-Morales, S. Chakrapani, B. Roux, and E. Perozo. 2010. Structural basis for the coupling between activation and inactivation gates in K⁺ channels. *Nature.* 466:272-5.

- Cuello, L.G., V. Jogini, D.M. Cortes, and E. Perozo. 2010 Structural mechanism of C-type inactivation in K⁺ channels. *Nature*. 466:203-8.
- Cukras, C.A., I. Jeliaskova, and C.G. Nichols. 2002(a). The role of NH₂-terminal positive charges in the activity of inward rectifier K(ATP) channels. *J Gen Physiol*. 120:437-446.
- Cukras, C.A., I. Jeliaskova, and C.G. Nichols. 2002(b). Structural and functional determinants of conserved lipid interaction domains of inward rectifying kir6.2 channels. *J Gen Physiol*. 119:581-591.
- D'Avanzo, N., W.W. Cheng, D.A. Doyle, and C.G. Nichols. 2010. Direct and specific activation of human inward rectifier K⁺ channels by membrane phosphatidylinositol 4,5-bisphosphate. *J Biol Chem*. 285:37129-32.
- Dean M. 2002. The Human ATP-Binding Cassette (ABC) Transporter Superfamily [Internet]. Bethesda (MD): National Center for Biotechnology Information (US).
- del Camino, D., and G. Yellen. 2001. Tight steric closure at the intracellular activation gate of a voltage-gated K⁺ channel. *Neuron* 32:649–656.
- Demo, S.D., and G. Yellen. 1992 Ion effects on gating of the Ca²⁺-activated K⁺ channel correlate with occupancy of the pore. *Biophys J*. 61:639-48.
- Ding, S., L. Ingleby, C.A. Ahern, and R. Horn. 2005. Investigating the putative glycine hinge in Shaker potassium channel. *J Gen Physiol*. 126:213-26.
- Domene, C., A. Grottesi, and M.S. Sansom. 2004. Filter flexibility and distortion in a bacterial inward rectifier K⁺ channel: simulation studies of KirBac1.1. *Biophys J*. 87:256-67.
- Doyle, D.A., J. Morais Cabral, R.A. Pfuetzner, A. Kuo, J.M. Gulbis, S.L. Cohen, B.T. Chait, and R. MacKinnon. 1998 The structure of the potassium channel: molecular basis of K⁺ conduction and selectivity. *Science*. 280:69-77.
- Drain, P., X. Geng, and L. Li. 2004. Concerted gating mechanism underlying KATP channel inhibition by ATP. *Biophys. J*. 86: 2101-2112.
- Drain, P., L. Li, and J. Wang. 1998. KATP channel inhibition by ATP requires distinct functional domains of the cytoplasmic C terminus of the pore-forming subunit. *Proc Natl Acad Sci U S A*. 95:13953-13958.
- Dunne, M.J., K.E. Cosgrove, R.M. Shepherd, A. Aynsley-Green, and K.J. Lindley. 2004. Hyperinsulinism in infancy: from basic science to clinical disease. *Physiol Rev*. 84:239-75.
- Durell, S.R. and H.R. Guy. 2001. A family of putative Kir potassium channels in prokaryotes. *BMC Evol Biol*. 1:14.
- Enkvetchakul, D., G. Loussouarn, E. Makhina, and C.G. Nichols. 2001. ATP interaction with the open state of the K(ATP) channel. *Biophys J*. 80:719-28.
- Enkvetchakul, D. and C.G. Nichols. 2003 Gating mechanism of KATP channels: function fits form. *J Gen Physiol*. 122:471-80.
- Fakler, B., U. Brändle, C. Bond, E. Glowatzki, C. König, J.P. Adelman, H.P. Zenner, and J.P. Ruppersberg. 1994. A structural determinant of differential sensitivity of cloned inward rectifier K⁺ channels to intracellular spermine. *FEBS Lett*. 356:199-203.
- Fan, Z., and J.C. Makielski. 1997. Anionic phospholipids activate ATP-sensitive potassium channels. *J Biol Chem*. 272:5388-95.
- Fan, Z. and J.C. Makielski. 1999. Phosphoinositides decrease ATP sensitivity of the cardiac ATP-sensitive K⁺ channel. A molecular probe for the mechanism of ATP-sensitive inhibition. *J Gen Physiol*. 114:251-69.

- Fang, K., L. Csanady, and K.W. Chan. 2006. The N-terminal transmembrane domain (TMD0) and a cytosolic linker (L0) of sulphonylurea receptor define the unique intrinsic gating of K_{ATP} channels. *Journal of Physiology (London)*. 576: 379-389.
- Feng, Y., S. Huang, W. Zhang, Z. Zeng, X. Zou, L. Zhong, J. Peng, and G. Jing. 2004. The effects of amino acid replacements of glycine 20 on conformational stability and catalysis of staphylococcal nuclease. *Biochimie*. 86: 893-901.
- Flagg, T.P., D. Enkvetchakul, J.C. Koster, and C.G. Nichols. 2010. Muscle K_{ATP} channels: recent insights to energy sensing and myoprotection. *Physiol Rev*. 90:799-829.
- Fox, J.E., J. Magga, W.R. Giles, and P.E. Light. 2003. Acyl coenzyme A esters differentially activate cardiac and beta-cell adenosine triphosphate-sensitive potassium channels in a side-chain length-specific manner. *Metabolism*. 52:1313-9.
- Glaser, B. 2000. Hyperinsulinism of the newborn. *Semin Perinatol*. 24:150-63.
- Haider, S., S. Khalid, S.J. Tucker, F.M. Ashcroft, and M.S. Sansom. 2007. Molecular dynamics simulations of inwardly rectifying (Kir) potassium channels: a comparative study. *Biochemistry*. 46:3643-52.
- Guo, L., and Y. Kubo. 1998. Comparison of the open-close kinetics of the cloned inward rectifier K^+ channel IRK1 and its point mutant (Q140E) in the pore region. *Receptors Channels*. 5:273-89.
- Haider, S., A.I. Tarasov, T.J. Craig, M.S. Sansom, and F.M. Ashcroft. 2007. Identification of the PIP2-binding site on Kir6.2 by molecular modelling and functional analysis. *EMBO J*. 26:3749-59.
- Hamill, O.P., A. Marty, E. Neher, B. Sakmann, and F.J. Sigworth. 1981. Pflugers Archiv : *European journal of physiology*. 391:85-100. (Reference for patch clamp)
- Hansen, S.B., X. Tao, and R. MacKinnon. Structural basis of PIP2 activation of the classical inward rectifier K^+ channel Kir2.2. *Nature*. 477:495-8.
- Hattersley, A.T., and F.M. Ashcroft. 2005. Activating mutations in Kir6.2 and neonatal diabetes: new clinical syndromes, new scientific insights, and new therapy. *Diabetes*. 54:2503-13.
- Heginbotham, L., Z. Lu, T. Abramson, R. MacKinnon. 1994. Mutations in the K^+ channel signature sequence. *Biophys J*. 66:1061-7.
- Hibino H, Inanobe A, Furutani K, Murakami S, Findlay I, Kurachi Y. 2010. Inwardly rectifying potassium channels: their structure, function, and physiological roles. *Physiol Rev*. 90: 291-366.
- Hilgemann DW. 2007. Local PIP2 signals: when, where, and how? *Pflugers Arch. - Eur. J. Physiol*. 455: 55-67.
- Hille B. 2001. Ion Channels of Excitable Membranes, 3rd Ed., pp. 150-154, 566-571, Sinauer Associates, Inc., Sunderland, MA.
- Hiriart, M., and L. Aguilar-Bryan. 2008. Channel regulation of glucose sensing in the pancreatic beta-cell. *Am J Physiol Endocrinol Metab*. 295:E1298-306.
- Hodgkin, A.L., and A.F. Huxley. 1952. A quantitative description of membrane current and its application to conduction and excitation in nerve. *J. Physiol*. 117: 500-544.
- Horn, R. 1991. Estimating the number of channels in patch recordings, *Biophys. J*. 55: 379-81.
- Hoshi, T., W.N. Zagotta, and R.W. Aldrich, 1990. Biophysical and molecular mechanisms of Shaker potassium channel inactivation. *Science*. 250, 533-538.
- Huopio, H., S.L. Shyng, T. Otonkoski, and C.G. Nichols. 2002. K_{ATP} channels and insulin secretion disorders. *Am J Physiol Endocrinol Metab*. 283: E207-16.

- Inagaki, N., T. Gonoi, J.P. Clement 4th, N. Namba, J. Inazawa, G. Gonzalez, L. Aguilar-Bryan, S. Seino, and J. Bryan. 1995. Reconstitution of IKATP: an inward rectifier subunit plus the sulfonylurea receptor. *Science*. 1995 Nov 17;270(5239): 1166-70.
- Inagaki, N., T. Gonoi, J.P. Clement 4th, C.Z. Wang, L. Aguilar-Bryan, J. Bryan, and S. Seino. 1996. A family of sulfonylurea receptors determines the pharmacological properties of ATP-sensitive K⁺ channels. *Neuron*. May;16(5): 1011-7.
- Inoue, I., H. Nagase, K. Kishi, and T. Higuti. 1991. ATP-sensitive K⁺ channel in the mitochondrial inner membrane. *Nature*. 352: 244-247.
- Jiang, Y., A. Lee, J. Chen, M. Cadene, B.T. Chait, and R. MacKinnon. 2002(a). The open pore conformation of potassium channels. *Nature*. 417: 523-6.
- Jiang, Y., A. Lee A, J. Chen, M. Cadene, B.T. Chait, and R. MacKinnon. 2002(b). Crystal structure and mechanism of a calcium-gated potassium channel. *Nature*. 417: 515-22.
- Jiang, Y., A. Lee, J. Chen, V. Ruta, M. Cadene, B.T. Chait, and R. MacKinnon. 2003. X-ray structure of a voltage-dependent K⁺ channel. *Nature*. 423: 33-41.
- Jin, T., L. Peng, T. Mirshahi, T. Rohacs, K.W. Chan, R. Sanchez, and D.E. Logothetis. 2002. The (beta)gamma subunits of G proteins gate a K⁺ channel by pivoted bending of a transmembrane segment. *Mol Cell*. 10: 469-81.
- Jones, P.A., S.J. Tucker, and F.M Ashcroft. 2001. Multiple sites of interaction between the intracellular domains of an inwardly rectifying potassium channel, Kir6.2. *FEBS Lett*. 508: 85-9.
- Kane, G.C., X.K. Liu, S. Yamada, T.M. Olson, and A. Terzic. 2005. Cardiac KATP channels in health and disease. *J Mol Cell Cardiol* 38: 937-943.
- Kiss, L., J. LoTurco, and S.J. Korn. 1999. Contribution of the selectivity filter to inactivation in potassium channels. *Biophys J*. 76: 253-63.
- Koster, J.C., Q. Sha, S. Shyng, and C.G. Nichols. 1999. ATP inhibition of KATP channels: control of nucleotide sensitivity by the N-terminal domain of the Kir6.2 subunit. *J Physiol*. 515: 19-30.
- Khurana, A., E.S. Shao, R.Y. Kim, Y.Y. Vilin, X. Huang, R. Yang, and H.T. Kurata. 2011. Forced gating motions by a substituted titratable side chain at the bundle crossing of a potassium channel. *J Biol Chem*. 286: 36686-93.
- Kuo, A., C. Domene, L.N. Johnson, D.A. Doyle, and C. Vénien-Bryan. 2005. Two different conformational states of the KirBac3.1 potassium channel revealed by electron crystallography. *Structure*. 13: 1463-72.
- Kuo, A., J.M. Gulbis, J.F. Antcliff, T. Rahman, E.D. Lowe, J. Zimmer, J. Cuthbertson, F.M. Ashcroft, T. Ezaki, and D.A. Doyle. 2003. Crystal structure of the potassium channel KirBac1.1 in the closed state. *Science*. 300: 1922-6.
- Kurata, H.T., and D. Fedida. 2006. A structural interpretation of voltage-gated potassium channel inactivation. *Prog Biophys Mol Biol*. 92: 185-208.
- Kurata, H.T., L.R. Phillips, T. Rose, G. Loussouarn, S. Herlitze, H. Fritzenschaft, D. Enkvetchakul, C.G. Nichols, and T. Baukrowitz. 2004. Molecular basis of inward rectification: polyamine interaction sites located by combined channel and ligand mutagenesis. *J. Gen. Physiol*. 124: 541-54.
- Kurata, H.T., M. Rapedius, M.J. Kleinman, T. Baukrowitz, and C.G. Nichols. 2010. Voltage-dependent gating in a "voltage sensor-less" ion channel. *PLoS Biol*. 8: e1000315.
- Leng, Q., G.G. MacGregor, K. Dong, G. Giebisch, and S.C. Hebert. 2006. Subunit-subunit interactions are critical for proton sensitivity of ROMK: Evidence in support of an intermolecular gating mechanism. *Proc. Natl. Acad. Sci*. 103: 1982-1987.

- Li, L., X. Geng, and P. Drain. 2002. Open state destabilization by ATP occupancy is mechanism speeding burst exit underlying KATP channel inhibition by ATP. *J. Gen. Physiol.* 119: 105-116.
- Li, L., J. Wang, and P. Drain. 2000. The I182 region of k(ir)6.2 is closely associated with ligand binding in K(ATP) channel inhibition by ATP. *Biophys J.* 79:841-852.
- Lin, C.W., Y.W. Lin, F.F. Yan, J. Casey, M. Kochhar, E.B. Pratt, and S.L. Shyng. 2006. Kir6.2 mutations associated with neonatal diabetes reduce expression of ATP-sensitive K⁺ channels: implications in disease mechanism and sulfonylurea therapy. *Diabetes.* 55: 1738-46.
- Lin, Y.W., J.D. Bushman, F.F. Yan, S. Haidar, C. MacMullen, A. Ganguly, C.A. Stanley, and S.L. Shyng. 2008. Destabilization of ATP-sensitive potassium channel activity by novel KCNJ11 mutations identified in congenital hyperinsulinism. *J Biol Chem.* 283: 9146-56.
- Lin, Y.W., C. MacMullen, A. Ganguly, C.A. Stanley, and S.L. Shyng. 2006. A novel KCNJ11 mutation associated with congenital hyperinsulinism reduces the intrinsic open probability of beta-cell ATP-sensitive potassium channels. *J Biol Chem.* 281: 3006-12.
- Lin, Y.W., T. Jia, A.M. Weinsoft, and S.L. Shyng. 2003. Stabilization of the activity of ATP-sensitive potassium channels by ion pairs formed between adjacent Kir6.2 subunits. *J Gen. Physiol.* 122: 225-37.
- Liu, Y., M. Holmgren, M.E. Jurman, and G. Yellen. 1997. Gated access to the pore of a voltage-dependent K⁺ channel. *Neuron.* 19: 175–184.
- Loechner, K.J., A. Akrouh, H.T. Kurata, C. Dionisi-Vici, A. Maiorana, M. Pizzoferro, V. Rufini, J. de Ville, J. de Goyet, C. Colombo, F. Barbetti, J.C. Koster, and C.G. Nichols. 2011. Congenital hyperinsulinism and glucose hypersensitivity in homozygous and heterozygous carriers of Kir6.2 (KCNJ11) mutation V290M mutation: K (ATP) channel inactivation mechanism and clinical management. *Diabetes.* 60:209-17.
- Long, S.B., E.B. Campbell, and R. Mackinnon. 2005. Crystal structure of a mammalian voltage-dependent Shaker family K⁺ channel. *Science.* 309:897–903.
- Lopatin, A.N., E.N. Makhina, and C.G. Nichols. 1994. Potassium channel block by cytoplasmic polyamines as the mechanism of intrinsic rectification. *Nature.* 372:366-9.
- López-Barneo, J., T. Hoshi, S.H. Heinemann, and R.W. Aldrich. 1993. Effects of external cations and mutations in the pore region on C-type inactivation of Shaker potassium channels. *Receptors Channels.* 1:61–71.
- Loussouarn, G., E.N. Makhina, T. Rose, and C.G. Nichols. 2000. Structure and dynamics of the pore of inwardly rectifying K_{ATP} channels. *J. Biol. Chem.* 275: 1137-44.
- Lu, T., L. Wu, J. Xiao, and J. Yang(a). 2001. Permeant ion-dependent changes in gating of Kir2.1 inward rectifier potassium channels. *J. Gen. Physiol.* 118, 509-522.
- Lu, T., A.Y. Ting, J. Mainland, L.Y. Jan, P.G. Schultz, and J. Yang(b). 2001. Probing ion permeation and gating in a K⁺ channel with backbone mutations in the selectivity filter. *Nat Neurosci.* 4:239-46.
- Lu Z, Klem AM, Ramu Y. 2001. Ion conduction pore is conserved among potassium channels. *Nature.* 413:809-13.
- Lu Z, MacKinnon R. 1994. Electrostatic tuning of Mg²⁺ affinity in an inward-rectifier K⁺ channel. *Nature.* 371:243-6.
- Lu Z, MacKinnon R. 1995. Probing a potassium channel pore with an engineered protonatable site. *Biochemistry.* 34:13133-8.

- Lummis, S.C., D.L. Beene, L.W. Lee, H.A. Lester, R.W. Broadhurst, and D.A. Dougherty. 2005. Cis-trans isomerization at a proline opens the pore of a neurotransmitter-gated ion channel. *Nature*. 438: 248-52.
- Ma, W., J. Berg, and G. Yellen. 2007. Ketogenic diet metabolites reduce firing in central neurons by opening K(ATP) channels. *J Neurosci*. 27:3618-25.
- Magidovich, E., and O. Yifrach. 2004. Conserved gating hinge in ligand- and voltage-dependent K⁺ channels. *Biochemistry*. 43:13242-7.
- Markworth, E., C. Schwanstecher, and M. Schwanstecher. 2000. ATP⁴⁻ mediates closure of pancreatic beta-cell ATP-sensitive potassium channels by interaction with 1 of 4 identical sites. *Diabetes*. 49:1413-1418.
- Matsuo, M., N. Kioka, T. Amachi, and K. Ueda. 1999. ATP binding properties of the nucleotide-binding folds of SUR1. *J Biol Chem*. 274:37479-37482.
- Meissner, T., E. Mayatepek. 2002. Clinical and genetic heterogeneity in congenital hyperinsulinism. *Eur J Pediatr*. 161:6-20.
- Mikhailov, M.V., J.D. Campbell, H. de Wet, K. Shimomura, B. Zadek, R.F. Collins, M.S. Sansom, R. C. Ford, and F.M. Ashcroft. 2005. 3-D structural and functional characterization of the purified KATP channel complex Kir6.2-SUR1. *EMBO J* 24:4166-4175.
- Monahan, S.L., H.A. Lester, and D.A. Dougherty. 2003. Site-specific incorporation of unnatural amino acids into receptors expressed in Mammalian cells. *Chem Biol*. 10: 573-80.
- Nagaoka, Y., L. Shang, A. Banerjee, H. Bayley, and S.J. Tucker. 2008. Peptide backbone mutagenesis of putative gating hinges in a potassium ion channel. *Chembiochem*. 9: 1725-8.
- Neusch, C., J.H. Weishaupt, and M. Bähr. 2003. Kir channels in the CNS: emerging new roles and implications for neurological diseases. *Cell Tissue Res*. 311: 131-8.
- Newman, E.A., D.A. Frambach, and L.L. Odette. 1984. Control of extracellular potassium levels by retinal glial cell K⁺ siphoning. *Science*. 225: 1174-5.
- Nichols, C.G., W.J. Lederer, and M.B. Cannell. 1991. ATP dependence of KATP channel kinetics in isolated membrane patches from rat ventricle. *Biophys. J*. 60: 1164-1177.
- Nichols, C.G., and A.N. Lopatin. 1997 Inward rectifier potassium channels. *Annu Rev Physiol*. 59: 171-91.
- Nichols, C.G. KATP channels as molecular sensors of cellular metabolism. 2006. *Nature*. 440: 470-6.
- Nichols, C.G., S.L. Shyng, A. Nestorowicz, B. Glaser, J.P. Clement 4th, G. Gonzalez, L. Aguilar-Bryan, M.A. Permutt, and J. Bryan. 1996. Adenosine diphosphate as an intracellular regulator of insulin secretion. *Science*. 272: 1785-7.
- Nilsson, I., A. Saaf, P. Whitley, G. Gafvelin, C. Waller, and G. von Heijne. 1998. Proline-induced disruption of a transmembrane alpha-helix in its natural environment. *J Mol Biol*. 284: 1165-75.
- Nishida, M., M. Cadene, B.T. Chait, and R. MacKinnon. 2007. Crystal structure of a Kir3.1-prokaryotic Kir channel chimera. *EMBO J*. 26: 4005-15.
- Nishida, M., and R. MacKinnon. 2002. Structural basis of inward rectification: cytoplasmic pore of the G protein-gated inward rectifier GIRK1 at 1.8 Å resolution. *Cell*. 111:957-965
- Noma, A. 1983. ATP-regulated K⁺ channels in cardiac muscle. *Nature*. 305: 147-148.
- Noskov, S.Y., and B. Roux. Ion selectivity in potassium channels. 2006. *Biophysical Chemistry*. 124: 279-291.

- Pegan, S., C. Arrabit, W. Zhou, W. Kwiatkowski, A. Collins, P.A. Slesinger, and S. Choe. 2005. Cytoplasmic domain structures of Kir2.1 and Kir3.1 show sites for modulating gating and rectification. *Nat Neurosci.* 8: 279-87.
- Perozo, E., M.D. Cortes, and L.G. Cuello. 1999. Structural rearrangements underlying K⁺-channel activation gating. *Science.* 285: 73-78.
- Phillips, L.R., D. Enkvetchakul, C.G. Nichols. 2003. Gating dependence of inner pore access in inward rectifier K⁺ channels. *Neuron.* 37: 953-62.
- Phillips, L.R., and C.G. Nichols. 2002. Cold draft through the teepee: MTSEA access to the inner vestibule of ATP closed Kir6.2 channels implies gating does not occur at the smokehole. *Biophys. J.* 82:590a.
- Pinney, S.E., C. MacMullen, S. Becker, L.Y. Lin, C. Hanna, P. Thornton, A. Ganguly, S.L. Shyng, and C.A. Stanley. 2008. Clinical characteristics and biochemical mechanisms of congenital hyperinsulinism associated with dominant KATP channel mutations. *J Clin Invest.* 118:2877-86.
- Prajapati, R.S., M. Das, S. Sreeramulu, M. Sirajuddin, S. Srinivasan, V. Krishnamurthy, R. Ranjani, C. Ramakrishnan, and R. Varadarajan. 2007. Thermodynamic effects of proline introduction on protein stability. *Proteins.* 66: 480-491.
- Pratt, E.B., P. Tewson, C.E. Bruederle, W.R. Skach, and S.L. Shyng. 2011. N-terminal transmembrane domain of SUR1 controls gating of Kir6.2 by modulating channel sensitivity to PIP₂. *J Gen Physiol.* 137:299-314.
- Proks, P., J.F. Antcliff, J. Lippiat, A.L. Gloyn, A.T. Hattersley, and F.M. Ashcroft. 2004. Molecular basis of Kir6.2 mutations associated with neonatal diabetes or neonatal diabetes plus neurological features. *Proc. Natl. Acad. Sci.* 101:17539-44.
- Proks, P., and F.M. Ashcroft. 2008. Modeling K(ATP) channel gating and its regulation. *Prog Biophys Mol Biol.* 99:7-19.
- Proks, P., C.E. Capener, P. Jones, and F.M. Ashcroft. 2001. Mutations within the P-loop of Kir6.2 modulate the intraburst kinetics of the ATP-sensitive potassium channel. *J Gen Physiol.* 118:341-53.
- Proks, P., C. Girard, S. Haider, A.L. Gloyn, A.T. Hattersley, M.S. Sansom, and F.M. Ashcroft. 2005. A gating mutation at the internal mouth of the Kir6.2 pore is associated with DEND syndrome. *EMBO Rep.* 6:470-5.
- Proks, P., K. Shimomura, T.J. Craig, C.A. Girard, and F.M. Ashcroft. 2007. Mechanism of action of a sulphonylurea receptor SUR1 mutation (F132L) that causes DEND syndrome. *Hum Mol Genet.* 16:2011-9.
- Qin, D., M. Takano, and A. Noma. 1989. Kinetics of ATP-sensitive K⁺ channel revealed with oil gate concentration jump method. *American Journal of Physiology* 257:H1624-H1633.
- Raja M. 2011 Diverse gating in K⁺ channels: differential role of the pore-helix glutamate in stabilizing the channel pore. *Biochem Biophys Res Commun.* 413:1-4.
- Rapedius, M., M. Soom, E. Shumilina, D. Schulze, R. Schönherr, C. Kirsch, F. Lang, S.J. Tucker, and T. Baukowitz. 2005. Long chain CoA esters as competitive antagonists of phosphatidylinositol 4,5-bisphosphate activation in Kir channels. *J Biol Chem.* 280:30760-7.
- Ribalet, B., S.A. John, and J.N. Weiss. 2000. Regulation of cloned ATP-sensitive K channels by phosphorylation, MgADP, and phosphatidylinositol bisphosphate (PIP₂): a study of channel rundown and reactivation. *J Gen Physiol.* 116: 391-410.
- Ribalet, B., S.A. John, and J.N. Weiss. 2003. Molecular basis for Kir6.2 channel inhibition by adenine nucleotides. *Biophys. J.* 84: 266-76.

- Ribalet, B., S.A. John, L.H. Xie, and J.N. Weiss. 2006. ATP-sensitive K⁺ channels: regulation of bursting by the sulphonylurea receptor, PIP₂ and regions of Kir6.2. *J. Physiol.* 571: 303-17.
- Robertson, J.L., L.G. Palmer, and B. Roux. 2008. Long-pore electrostatics in inward-rectifier potassium channels. *J. Gen. Physiol.* 132:613-32.
- Rosenhouse-Dantsker, A., and D.E. Logothetis. 2006. New roles for a key glycine and its neighboring residue in potassium channel gating. *Biophys. J.* 91:2860-73.
- Rosenhouse-Dantsker, A., and D.E. Logothetis. 2007. Potassium channel gating in the absence of the highly conserved glycine of the inner transmembrane helix. *Channels (Austin)*. 1: 189-97.
- Roux, B., and R. MacKinnon. 1999. The cavity and pore helices in the KcsA K⁺ channel: electrostatic stabilization of monovalent cations. *Science*. 285:100-2.
- Sackin, H., M. Nanazashvili, H. Li, L.G. Palmer, and D.E. Walters. 2009. An intersubunit salt bridge near the selectivity filter stabilizes the active state of Kir1.1. *Biophys. J.* 97:1058- 66.
- Sackin, H., M. Nanazashvili, L.G. Palmer, H. Li. 2006. Role of conserved glycines in pH gating of Kir1.1 (ROMK). *Biophys J.* 90:3582-9.
- Sadja, R., K. Smadja, N. Alagem, and E. Reuveny. 2001. Coupling Gβγ-dependent activation to channel opening via pore elements in inwardly rectifying potassium channels. *Neuron*. 29: 669-680.
- Schulze, D., M. Rapedius, T. Krauter, and T. Baukowitz. 2003. Long-chain acyl-CoA esters and phosphatidylinositol phosphates modulate ATP inhibition of KATP channels by the same mechanism. *J. Physiol.* 552:357-67.
- Seino, S., T. Miki. 2003. Physiological and pathophysiological roles of ATP-sensitive K⁺ channels. *Prog Biophys Mol Biol* 81:133–176
- Shang, L., and S.J. Tucker. 2008. Non-equivalent role of TM2 gating hinges in heteromeric Kir4.1/Kir5.1 potassium channels. *Eur. Biophys. J.* 37:165-71.
- Shi, N., S. Ye, A. Alam, L. Chen, and Y. Jiang. 2006. Atomic structure of a Na⁺- and K⁺-conducting channel. *Nature*. 440: 570-4.
- Shyng, S., T. Ferrigni, C.G. Nichols. 1997. Control of rectification and gating of cloned KATP channels by the Kir6.2 subunit. *J Gen Physiol.* 1997 110:141-53.
- Shyng, S., and C.G. Nichols. Octameric stoichiometry of the KATP channel complex. 1997. *J. Gen. Physiol.* 110:655-64.
- Shyng, S.L., J.D. Bushman, E.B. Pratt, and Q. Zhou. 2012. Monogenic Hyperinsulinemic Hypoglycemia Disorders, vol 21, pp. 30–42, Front Diabetes, Karger, Basel.
- Shyng, S.L., and C.G. Nichols. 1998. Membrane phospholipid control of nucleotide sensitivity of KATP channels. *Science*. 282:1138-41.
- Shyng, S.L., C.A. Cukras, J. Harwood, and C.G. Nichols. 2000. Structural determinants of PIP₂ regulation of inward rectifier K(ATP) channels. *J. Gen. Physiol.* 116:599-608.
- Sigworth, F.J., and S.M. Sine. 1987. Data transformations for improved display and fitting of single-channel dwell time histograms. *Biophys. J.* 52: 1047-54.
- Sivilotti LG. 2010. What single-channel analysis tells us of the activation mechanism of ligand-gated channels: the case of the glycine receptor. *J. Physiol.* 588:45-58.
- Stanley CA. 2002. Advances in diagnosis and treatment of hyperinsulinism in infants and children. *J. Clin. Endocrinol. Metab.* 87:4857-9.
- Suh BC, Hille B. 2008. PIP₂ is a necessary cofactor for ion channel function: how and why? *Annu. Rev. Biophys.* 37: 175-95.
- Swenson, R.P. Jr, and C.M. Armstrong. 1981. K⁺ channels close more slowly in the presence of external K⁺ and Rb⁺. *Nature*. 291: 427-9.

- Tammaro, P., S.E. Flanagan, B. Zadek, S. Srinivasan, H. Woodhead, S. Hameed, I. Klimes, A.T. Hattersley, S. Ellard, and F.M. Ashcroft. 2008. A Kir6.2 mutation causing severe functional effects in vitro produces neonatal diabetes without the expected neurological complications. *Diabetologia*. 51:802-10.
- Tanabe, K., S.J. Tucker, M. Matsuo, P. Proks, F.M. Ashcroft, S. Seino, T. Amachi, and K. Ueda. 1999. Direct photoaffinity labeling of the Kir6.2 subunit of the ATP-sensitive K⁺ channel by 8-azido-ATP. *J. Biol. Chem.* 274: 3931-3933.
- Taschenberger, G., A. Mougey, S. Shen, L.B. Lester, S. LaFranchi, and S.L. Shyng. 2002. Identification of a familial hyperinsulinism-causing mutation in the sulfonylurea receptor 1 that prevents normal trafficking and function of KATP channels. *J. Biol. Chem.* 277: 17139-46.
- Tieleman, D.P., I.H. Shrivastava, M.R. Ulmschneider, and M.S. Sansom. 2001. Proline-induced hinges in transmembrane helices: possible roles in ion channel gating. *Proteins*. 44: 63-72.
- Trevino, S.R., S. Schaefer, J.M. Scholtz, and C.N. Pace. 2007. Increasing protein conformational stability by optimizing beta-turn sequence. *J. Mol. Biol.* 373: 211-218.
- Tsuboi, T., J.D. Lippiat, F.M. Ashcroft, and G.A. Rutter. 2004. ATP-dependent interaction of the cytosolic domains of the inwardly rectifying K⁺ channel Kir6.2 revealed by fluorescence resonance energy transfer. *Proc. Natl. Acad. Sci.* 101:76-81.
- Tucker, S.J., F.M. Gribble, P. Proks, S. Trapp, T.J. Ryder, T. Haug, F. Reimann, and F.M. Ashcroft. 1998. Molecular determinants of KATP channel inhibition by ATP. *EMBO J.* 17:3290-6.
- Tucker, S.J., F.M. Gribble, C. Zhao, S. Trapp, and F.M. Ashcroft. 1997. Truncation of Kir6.2 produces ATP-sensitive K⁺ channels in the absence of the sulphonylurea receptor. *Nature*. 387:179-183.
- Venkatachalan, S.P., J.D. Bushman, J.L. Mercado, F. Sancar, K.R. Christopherson, and Boileau AJ. 2007. Optimized expression vector for ion channel studies in *Xenopus* oocytes and mammalian cells using alfalfa mosaic virus. *Pflugers. Arch.* 454:155-63.
- Whorton, M.R., and R. MacKinnon. 2011. Crystal structure of the mammalian GIRK2 K⁺ channel and gating regulation by G proteins, PIP2, and sodium. *Cell*. 147:199-208.
- Wang, C., K. Wang, W. Wang, Y. Cui, and Z. Fan. 2002. Compromised ATP binding as a mechanism of phosphoinositide modulation of ATP-sensitive K⁺ channels. *FEBS. Lett.* 532:177-182.
- Wible, B.A., M. Tagliatela, E. Ficker, and A.M. Brown. 1994. Gating of inwardly rectifying K⁺ channels localized to a single negatively charged residue. *Nature*. 371:246-9.
- Woolfson, D.N., R.J. Mortishire-Smith, and D.H. Williams. 1991. Conserved positioning of proline residues in membrane-spanning helices of ion-channel proteins. *Biochem Biophys Res Commun.* 175: 733-7.
- Xiao, J., X.G. Zhen, and J. Yang. 2003 Localization of PIP2 activation gate in inward rectifier K⁺ channels. *Nat Neurosci.* 6:811-8.
- Xie, L.H., M. Horie, M. Takano. 1999 Phospholipase C-linked receptors regulate the ATP-sensitive potassium channel by means of phosphatidylinositol 4,5-bisphosphate metabolism. *Proc Natl Acad Sci U S A.* 96:15292-7.
- Yang, J., Y.N. Jan, and L.Y. Jan. 1995. Control of rectification and permeation by residues in two distinct domains in an inward rectifier K⁺ channel. *Neuron*. 14:1047-54.

- Yang, J., M. Yu, Y.N. Jan, and LY Jan. 1997. Stabilization of ion selectivity filter by pore loop ion pairs in an inwardly rectifying potassium channel. *Proc. Natl. Acad. Sci.* 94: 1568-72.
- Yi, B.A., D.L. Minor Jr, Y.F. Lin, Y.N. Jan, and L.Y. Jan. 2001. Controlling potassium channel activities: Interplay between the membrane and intracellular factors. *Proc. Natl. Acad. Sci. U S A.* 98:11016-23.
- Zerangue, N., B. Schwappach, Y.N. Jan, and L.Y. Jan. 1999. A new ER trafficking signal regulates the subunit stoichiometry of plasma membrane K(ATP) channels. *Neuron.* 22:537-48.
- Zhou, M., J.H. Morais-Cabral, S. Mann, R. MacKinnon. 2001. Potassium channel receptor site for the inactivation gate and quaternary amine inhibitors. *Nature.* 411:657-61.